Advanced Fusion Fuel Cycles and Fusion Reaction Kinetics

G. Shuy

May 1980

UWFDM-357

Ph.D. thesis.

FUSION TECHNOLOGY INSTITUTE

UNIVERSITY OF WISCONSIN

MADISON WISCONSIN

Advanced Fusion Fuel Cycles and Fusion Reaction Kinetics

G. Shuy

Fusion Technology Institute
University of Wisconsin
1500 Engineering Drive
Madison, WI 53706

http://fti.neep.wisc.edu

May 1980

UWFDM-357

Ph.D. thesis.

ADVANCED FUSION FUEL CYCLES
AND
FUSION REACTION KINETICS

by

GEOFFREY WEN-TAI SHUY

A thesis submitted in partial fulfillment of the

requirements for the degree of

DOCTOR OF PHILOSOPHY
(Nuclear Engineering)

at the

University of Wisconsin-Madison

1980

ABSTRACT

ADVANCED FUSION FUEL CYCLES AND FUSION REACTION KINETICS

Geoffrey Wen-Tai Shuy

Under the Supervision of Professor Robert W. Conn

Three new effects in advanced fusion fuel cycle analysis—proper inclusion of large energy transfer collisions, propagating enhancements, and tail-tail interactions—are investigated and found to increase the reactivity, to alter energy balance calculations, and to affect predicted Q values and ignition conditions. For example, with the inclusion of these effects, the reactivity of the catalyzed d-d plasma at T_i = 75 keV can be increased from 21% at T_e = 50 keV to 53% at 100 keV relative to the reactivity neglecting these effects. The fraction of energy given to the electrons is likewise influenced. As an example, the fraction of a 14.5 MeV proton's energy given to the electrons at 100 keV decreases from 85% when only coulomb scattering is assumed to 51% when nuclear scattering is added to the calculation, and decreases further to 38% when coulomb plus nuclear scattering and tail-tail interactions are properly included.

Charged particle cross sections required for an advanced fusion fuel cycle calculation are discussed. Reactions important for the d-d, d-^{3}He, d-^{6}Li, p-^{6}Li and p-^{11}B cycles are described. The inclusion of nuclear elastic scattering is found to be essentail. Important fusion cross sections and energy ranges where data is required are identified.

The kinetic equations to describe the velocity distribution functions for a reacting fusion plasma are studied, and a linearized model is formualted. A slowing down theory to treat the small energy transfer range by a continuous theory and to treat the large energy transfer range by a discrete multigroup energy technique is developed. Formulae for the power density in propagating reaction cycles, the fusion probability for an energetic particle reacting to the background ions, the energy distribution of reaction products, and the power balance equations including injection power, ash removal and the relativistically corrected electron-ion rethermalization and bremsstrahlung radiation are derived.

Computer codes including the appropriate kinetic equations, the fast fusion reactions, and nuclear elastic scattering have been developed, implemented and are presented along with results. Steady state analyses on catalyzed d-d, d-^{3}He and p-^{11}B are completed. It is found that the p-^{11}B cycle can ignite if the losses are due solely to bremsstrahlung and ash removal. The reactivity for the catalyzed d-d cycle is enhanced by 20% - 40%. Assuming perfect ion energy confinement, the minimum electron $n\tau_E$ value required for ignition is decreased from 9×10^{14} to 1.5×10^{14} with the inclusion of these effects. The reactivity for the d-^{3}He cycle is enhanced by 35% - 75%. Assuming perfect ion energy confinement, the minimum electron $n\tau_E$ requirement for ignition is reduced from 9×10^{14} to 1.01×10^{14}. Based on this research, suggestions for important areas requiring additional research are presented.

Date: 5/19/80 Approved: Robert W. Conn

Robert W. Conn

Professor of

Nuclear Engineering

ACKNOWLEDGEMENTS

It is on this page that tradition requires homage to those who have played a role in my program of graduate study. To associate this work with the abettors could add little credit to already illustrious credentials while to identify any detractors would accomplish even less.

I must however express my sincere appreciation to Professor R. W. Conn whose dedication, encouragement, and support made this work possible. His example and friendship will forever remain among the most notable of my memories.

I am also indebted to Professor K. W. McVoy, who was able to demonstrate the utility of the esoteric, for much valuable guidance in my nuclear physics graduate study; and to Professors H. H. Barschall, D. W. Kerst, and G. A. Moses with whom any association can only lead to enrichment.

My fellow graduates also provided additional insight and support, especially Michael Gordinier. The aid of R. Israel in portions of the computer programming is also gratefully acknowledged.

No amount of prose could give proper credit to my most ardent supporter, my wife Margaret. Her patience, love, and understanding have provided endurance during a period of tribulation. My daughter Christina is also to be credited for tolerating periods of regrettable negligence.

This work is dedicated to my parents for their life time sacrifices which have made a poor boy's dream come true.

This research has been supported by a contract with TRW, Inc. and the Electric Power Research Institute.

TABLE OF CONTENTS

Page

Abstract ii

Acknowledgements v

List of Tables x

List of Figures xi

Chapter I

INTRODUCTION 1

I-1. Background 2

I-2. Scope of The Analysis 5

Table and Figures 11

References 20

Chapter II

CHARGED PARTICLE CROSS SECTION REQUIREMENTS
FOR ADVANCED FUSION FUEL CYCLE ANALYSIS 22

II-1. Required Nuclear Data 23

II-2. Status of Nuclear Data for Advanced
Fusion Fuel Cycle Analysis 27

Table and Figures 33

References 40

Chapter III

FUSION REACTION KINETICS 53

III-1. Kinetic Equations for a Fusion
Reacting Plasma 54

III-2. Simplified Model Used in This Analysis. . . . 56

III-3. Slowing Down Theory 57

III-4. Reactions While Slowing Down 61

III-5. The Reactivity of a Propagating Reaction 62

III-6. Doppler Broadening and Energy Distribution of Products from Nuclear Reaction 65

III-7. Power Balance Calculation. 70

Figures 72

Reference 74

Chapter IV

THE STEADY STATE SIMULATION CODE FOR ADVANCED FUSION FUEL CYCLE BURN KINETICS 75

Table and Figure 76

References 85

Chapter V

THE TIME DEPENDENT SIMULATION CODE FOR ADVANCED FUSION FUEL CYCLE BURN KINETICS 86

V-1. Computer Code Survey 87

V-2. Physics Features and Subtle Issues 88

V-3. Basic Equations of the BAFCO code 93

V-4. Time Step 96

V-5. Nuclear Inelastic Scattering 100

V-6. Energy Distribution from Nuclear Reaction Products 100

Figure 101

References 102

Chapter VI

ADVANCED FUSION FUEL CYCLE ANALYSES 103

VI-1. New Effects Investigated 104

VI-2. The d-^{3}He Cycle 106

VI-3. The Catalyzed d-d Cycle 108

VI-4. The p-^{11}B Cycle 110

Table and Figures 112

References 124

Chapter VII

SUMMARY AND FUTURE DIRECTION 125

VII-1. Summary 126

VII-2. Discussions 128

VII-3. Future Direction 132

References 134

Appendix

BRIEF ELABORATION ON THE EXPANSION OF THE
BOLTZMANN EQUATION IN A COMPLETE SET 135

Reference 140

LIST OF TABLES

Table No.		Page
I-1	Potential Advantages of Proton-Based Fusion Reactors	11
II-1	Summary of the Status of Nuclear Data for Nuclei A<12	33
II-2	Summary of the Status of Nuclear Data for Nuclei A<12	34
II-3	Summary of the Status of Nuclear Data for Nuclei A<12	35
II-4	Parameters for p-^{11}B Resonances	39
IV-1	Comparisons of The d-t Fast Fusion Probabilities due to Large Energy Transfer Collisions in 50-50 d-t Plasma . . .	83
VI-1	Power Balance for p-^{11}B Cycle	123

LIST OF FIGURES

Figure No. | Page

I-1. The proton-deuterium nuclear elastic scattering cross section after subtraction of the coulomb cross section. 12

I-2. Fraction of energy transferred from 3 and 4 MeV α's to produce deuterons with energy > 1 MeV in a pure d plasma. 13

I-3a. Fraction of energy transferred from 3 MeV proton to produce deuterons with energy > 1 MeV in a pure d plasma. 14

I-3b. Fraction of energy transferred from 14.5 MeV proton to produce deutrons with energy > 1 MeV. in pure d plasma. 15

I-4. Relative reactivity for catalyzed d-d fuel cycle as a function of electron temperature. 16

I-5. Fraction of energy transferred from 4 MeV α to electrons in pure d plasma, as a function of electron temperature.. 17

I-6. Fraction of energy transferred from 3 MeV protons to electrons in a pure d plasma, as a function of electron temperature. . . 18

I-7. Fraction of energy transferred from 14.5 MeV protons to electrons in a pure d

	plasma, as a function of electron temperature.	19
II-1.	Cross section data and recommend values for $D(d,n)^3He$ reaction as a function of deuteron energy..	36
II-2.	Cross section data and recommend values for $T(p,n)^3He$ reaction as a function of proton energy..	37
II-3.	Cross section data for $^6Li(p,^3He)^4He$ reaction as a function of proton energy..	38
III-1.	Angular distribution of the $p+^6Li$ reaction cross section.	72
III-2.	Power balance calculation for advanced fusion fuel cycles.	73
IV-1.	Block diagram showing calculation sequence of the BAFSS computer code.	84
V-1.	Block diagram showing physics features of the BAFCO computer code..	101
VI-1.	Stripped distribution of protrons as a function of energy for $p-^{11}B$ reacting plasma.	112
VI-2.	Energy transferred to electrons by 14.5 MeV protons as a function of electron temperature in a catalyzed d-d reacting plasma.	113

VI-3. Neutron production and power density for d-^{3}He fuel cycle as a function of ^{3}He/d density ratio. 114

VI-4. Neutron energy and power density for d-^{3}He fuel cycle as a function of ^{3}He/d density ratio. 115

VI-5. Minimum $n\tau_E$ required for ignition, assuming perfect ion energy confinement, for d-^{3}He cycle in different ion temperatures. 116

VI-6. Relative reactivity for d-^{3}He fuel cycle at different electron temperatures.. . . . 117

VI-7. Minimum required $n\tau_E$ for different ion temperatures for the d-^{3}He fuel cycle. . . 118

VI-8. Enhanced reactivity at T_i=75 KeV for different electron temperatures, cat. d-d fuel cycle. 119

VI-9. Minimum $n\tau_E$ requirement for ignition for cat. d-d fuel cycle, as a function of ion temperature. 120

VI-10. Enhanced reactivity at diferent electron temperatures for p-^{11}B fuel cycle. 121

VI-11. Increase in <σv> relative to the Maxwllian averaged value for the p-^{11}B fuel cycle, as a function of ion temperature. . 122

CHAPTER I

INTRODUCTION

CHAPTER I

INTRODUCTION

I-1. Background

Energy is the lifeblood of modern economic systems. Controlled fusion has the potential to be one of the truly long term sources of that energy. Since there appears to be only a few long term solutions to energy needs, the development of fusion power is clearly imperative. Based on a pedagogical approach, self-consitent conceptual reactor designs have been studied by several interdisciplinary groups[1-5]. The fusion cycle proposed in these studies is the d-t cycle. Since ^{6}Li and ^{7}Li are used in the tritium breeding process, this cycle is also referred to as the d-t-Li cycle. Nevertheless, a large number of light elements will also fuse if the temperature of the mixture is sufficiently high. The potential fusion fuel cycles can be classified as deuterium based, proton based and helium-3 based. The deuterium based fuel cycles include d-t, d-d, d-^{3}He and d-^{6}Li. The proton based fuel cycles include p-^{11}B and p-^{6}Li. The d-t cycle has the highest reaction rate for ion temperatures below 100 keV. Ignition based on the d-t cycle will be the easiest to achieve, but it also produces high energy neutrons and a high level of induced radioactivity. There are fusion reactions such as p+^{11}B and d+^{3}He which hold the promise for lower levels of neutron production. The neutrons produced in these cycles are governed by low probability side reactions. Since the burn scenarios based on these cycles would be quite difficult to achieve, they are referred to as advanced fuel cycles.[6]

Fusion devices utilizing the d-t-Li cycle will certainly be the first to demonstrate energy breakeven and also very likely will be the first cycle for commercial fusion reactors. Nevertheless, fusion reactors with tritium fuel should be viewed as an intermediate step in fusion power development. The ultimate goal is to achieve a reactor based on either hydrogen or deuterium to insure both an inexhaustible fuel supply and systems with minimum radioactivity. To preserve this potential, it is essential to maintain efforts to develop advanced fuel cycle fusion power based on d-d, d-^{3}He, d-^{6}Li or proton based cycles such as p-^{11}B and p-^{6}Li. Minimizing the plasma deuterium content is a key to a minimum neutron producing reactor.

The potential advantages of a proton based fusion reactor are summarized in Table I-1. First, both fuels in p-^{11}B or p-^{6}Li are abundant. Secondly, there is little gaseous radioactivity and no need to breed tritium. The elimination of tritium breeding and fueling minimizes problems of tritium management and eliminates in many cases the need for an intermediate loop in the power cycle. Thirdly, the neutron level is so low that bulk radiation damage to materials is not an issue. This will have a favorable impact on reactor design by permitting improved maintainability, availability and reliability. Some neutron induced radioactivity will result from deuteron reactions but this depends on branching ratios. Together with the absence of gaseous radioactivity, this low radioactivity and tritium level provides particular environmental advantages that will affect costs, licensing and siting. Fourthly, although the plasma power density is likely to be lower than that in a d-t reactor with the same β value (defined as the ratio of plasma presure to magnetic field pressure), the minimum neutron advanced fuel cycle allows the magnets to be closer to the reaction chamber, offsetting the need for somewhat higher fields. Since the energy is released primarily in charged particles and electromagnetic radiation, the blanket is no more than the first wall itself. In short, a proton based fusion reactor would be the fusion analog of a coal fired boiler. Cost advantages can be gained by reducing the shielding of nuclear qualified equipment and by eliminating systems such as intermediate heat exchangers, tritium extraction, tritium cleanup, radioactive waste control and remote handling. Potential environmental advantages can minimize licensing and siting issues. These savings can be used to a degree to offset disadvantages such as lower plasma power density.

Driven by the desire to achieve a reactor design which incorporates the advantages stated above, Maxwellian averaged reactivity calculations[6-8] for advanced fuels and preliminary studies[9-11] for advanced fuel cycle fusion reactor designs have been carried out in the last decade. The reactivity is a function of the product of the distribution functions of the reacting species and the reaction cross section. The reactivity is sensitive to the tail population, since the cross section is peaked for energies consistent with the tail of the distribution. A typical fusion plasma temperature is in the tens to hundreds of keV range, while the reaction products are in the MeV to tens of MeV range. Large energy transfer collisions of energetic fusion products with background ions will increase the ion tail population. Using a continuous slowing down theory for the relaxation of the reaction products (which treats large energy transfer collision as multiple small energy transfer collision), could result in an underestimated reactivity. Therefore the proper inclusion of the large energy transfer collision is essential. Since the coulomb scattering cross section is inversly proportional to the square of the relative energy of the colliding particles, a charged particle will transfer its energy via coulomb scattering preferentially to the species with comparable speed. Given a large tail population, a charged particle with medium energy will receive energy from higher energy charged particles preferentially. Neglecting the rethermalization process between tail ions results in an overestimated energy loss rate. This rethermalization process between various tail ions will be referred to as a "tail-tail interaction" throughout this thesis.

I-2. Scope of The Analysis

The proper determination of the potential of an advanced fuel cycle requires a relatively thorough literature survey on basic nuclear data and a study of fusion reaction kinetics, including subtle effects like fast fusion, nuclear elastic and inelastic scattering, Doppler broadening of the energy distribution of reaction products, and the fraction of slowing down energy given separately to the ions and electrons.

There are three new effects in the analysis of advanced fuel cycles which have been investigated[12-14] and found to increase the reactivity of the cycles, to alter energy balance calculations and to affect predicted Q values or ignition conditions. The first effect is the propagation in the cycles such as p-^{6}Li. ^{3}He, the energetic p+^{6}Li reaction product, reacts with ^{6}Li and produces an energetic proton before slowing down; these protons can undergo fast fusion again and propagate the reaction further. The second effect is the enhanced fast fusion reactivity due to nuclear elastic scattering. Nuclear elastic scattering of the background fuel ions by the energetic fusion products produces additional energetic particles which can undergo fast fusion and further propagate the reaction. The third effect is the enhanced fast fusion reactivity due to tail-tail interactions which make the tail fast fuel ions stay longer in the more reactive energy region; resulting in higher reaction probabilities.

The proton-deuterium nuclear elastic scattering cross section is shown in Fig. I-1 as a function of proton energy. The coulomb scattering cross section has been subtracted prior to plotting the result. The nuclear elastic scattering cross section is typically 1 barn or greater when the incident energy is in the range 1 to 15 MeV.

The average energy transfer per collision is large. For example, counting only collisions which transfer 1 MeV or more, a 3 MeV proton in a deuterium plasma with a 75 keV ion temperature is found to transfer ~30% of its energy to the energetic deuterons when the electron temperature is 60 keV. This fraction increases to ~50% when T_e is 100 keV. The fast fuel ions produced from the process undergo fusion while slowing down, thereby enhancing the reactivity and the propagation of the reaction. Figs. I -2 and I -3 show the fraction of energy transferred from fast alphas and fast protons to produce energetic deuterons with an energy greater than 1 MeV. The effect for alphas at 3 to 4 MeV is smaller than for protons at either 3 MeV because of the larger coulomb cross section for alphas.

The catalyzed d-d fuel cycle can be used to elaborate the role of nuclear elastic scattering, tail-tial interactions and propagation enhancement. The major reactions for this cycle are:

$$d + d \rightarrow n\ (2.45\ \text{MeV}) + {}^3\bar{\text{He}}\ (.87\ \text{MeV}) \qquad \text{(I-1)}$$

$$\rightarrow \bar{p}\ (3.01\ \text{MeV}) + \bar{t}\ (1.\ \text{MeV}) \qquad \text{(I-2)}$$

$$d + t \rightarrow n\ (14.06\ \text{MeV}) + \bar{\alpha}\ (3.5\ \text{MeV}) \qquad \text{(I-3)}$$

$$d + {}^3\text{He} \rightarrow \bar{p}\ (14.68\ \text{MeV}) + \bar{\alpha}\ (3.67\ \text{MeV}) \qquad \text{(I-4)}$$

The overbars denote fast charged particles. Nuclear elastic events such as

$$\bar{p} + d \rightarrow p + \bar{d} \qquad \text{(I-5)}$$

$$\bar{\alpha} + d \rightarrow \alpha + \bar{d} \qquad \text{(I-6)}$$

$$\vdots$$

promote fast deuterons from the background Maxwellian distribution. A few of the propagating sequences in this cycle are:

$$\left\{ \begin{array}{l} d + d \rightarrow \bar{p} + \bar{t} \\ \bar{p} + d \rightarrow \bar{d} + p \\ \bar{d} + d \rightarrow \bar{p} + \bar{t} \end{array} \right\} \quad \text{(I-7)} \qquad \left\{ \begin{array}{l} d + d \rightarrow {}^3\bar{He} + n \\ {}^3\bar{He} + d \rightarrow \bar{p} + \bar{\alpha} \\ \bar{p} + d \rightarrow \bar{d} + p \\ \bar{d} + d \rightarrow {}^3\bar{He} + n \end{array} \right\} \quad \text{(I-8)}$$

$$\vdots \qquad\qquad \vdots$$

$$\left\{ \begin{array}{l} d + d \rightarrow \bar{t} + \bar{p} \\ \bar{t} + d \rightarrow \bar{\alpha} + n \\ \bar{\alpha} + d \rightarrow \bar{d} + \alpha \\ \bar{d} + d \rightarrow \bar{t} + \bar{p} \end{array} \right\} \quad \text{(I-9)} \qquad \left\{ \begin{array}{l} d + d \rightarrow {}^3\bar{He} + n \\ {}^3\bar{He} + d \rightarrow \bar{\alpha} + \bar{p} \\ \bar{\alpha} + d \rightarrow \bar{d} + \alpha \\ \bar{d} + d \rightarrow {}^3\bar{He} + n \end{array} \right\} \quad \text{(I-10)}$$

$$\vdots \qquad\qquad \vdots$$

As an example, the propagating sequence indicated in set (I-7) produces fast protons. The fast proton promotes the deuterons out of the thermal bath; the energetic deuteron then reacts before slowing down, producing a fast proton, and so on.

The tail-tail interactions which alter slowing down, make the tail fast fuel ions stay longer in the more reactive energy region, therefore enhancing the reactivity. The inclusion of these effects increase the reactivity of the catalyzed d-d cycle at T_i = 75 keV by 21% when T_e is 50 keV and by 53% when T_e is 100 keV. The results are shown as the dashed curve in Fig.I-4. These increases are measured relative to a standard calculation in which nuclear elastic scattering and propagating reactions are neglected. The solid curve in Fig. I-4 is the result where the tail-tail interactions are neglected.

Nuclear knock-on events and tail-tail interactions also alter the fraction of energy given to electrons and ions by energetic fusion products. The energy transferred to electrons by various fast particles (a 4 MeV alpha, a 3 MeV proton, and a 14.5 MeV proton) is shown in Figs. I-5, I-6 and I-7 as a function of electron temperature. The dashed curve in each figure is the fraction of the initial energy received by electrons when only the coulomb interaction is assumed. The dash-dot curves in each figure give the analogous result when both coulomb and nuclear elastic scattering are included. Finally, the solid curve properly includes the effect of fast ion production by nuclear scattering and the subsequent slowing down of those ions with background ions and electrons. The background plasma in all cases is composed of electrons and deuterium ions. The ion termperature is fixed at 75 keV. While the inclusion of the nuclear knock-on effect results in small changes for the 4 MeV alpha particle, a substantial effect is seen for both the 3 MeV and 14.5 MeV protons. The effect becomes more important as the electron temperature is increased. Accounting for both nuclear elastic scattering and subsequent slowing down of knock-on ions, a 14.5 MeV proton in a 75 keV ion temperature deuterium plasma will transfer 79% of its energy to 50 keV electrons compared to 93% when only coulomb scattering is assumed. At an electron temperature of 100 keV, the percentage of energy transferred to the electrons decreases to 51% compared to 85% with coulomb interactions only. The tail-tail interactions enhance energy transferred to ions even more, which will be reported in Chapter VI. The effect is clearly important in a plasma energy balance calculation. Overall, the net result is that lower $n\tau_E$ values are required to meet either the Lawson or ignition condition for the catalyzed d-d cycle, and will be detailed in Chapter VI.

In Chapter II a summary of the literature survey on the basic nuclear data for nuclei with atomic mass numbers less than 12 is reported. A detailed study of the fusion reaction theory, including the appropriate kinetic equations, slowing down theory, reactions while slowing down, the reactivity of a propagating reaction, Doppler broadening the energy distribution from nuclear reactions is presented in Chapter III. The self-consistent iteration method used to evaluate the equilibrium density of various species in a steady state advanced fuel burning plasma is detailed in Chapter IV. In Chapter V a computer code developed for advanced fuel cycle calculations is described and compared with existing codes. In chapter VI, advanced fusion fuel cycle analyses for the steady state burn catalyzed d-d, d-^{3}He and p-^{11}B cycles are reported. Summary and suggestions for future work in this area are made in Chapter VII.

TABLE I-1

Potential Advantages of Proton-Based Fusion Reactors

1. Fuels are essentially inexhaustible.
2. No gaseous radioactivity.
3. No fuel breeding requirement.
4. Simple blanket design - blanket is now just a first wall.
5. No radiation damage to structural materials.
6. Safety aspects more similar to coal plants than to nuclear power.
7. Improved system maintainability and thus, potentially, improved reliability and availability.
8. Very low levels of induced radioactivity.
9. Potentially low environmental impact on air pollution, mining, and long term solid waste disposal.
10. Potential for good system economics.
    - A. Balance of plant costs should be similar to coal plant. Nuclear oriented subsystems are minimized.
    - B. Fuel costs will be less than for nuclear.
    - C. Fusion island costs can be greater than for nuclear.
    - D. No intermediate loop required for safety.

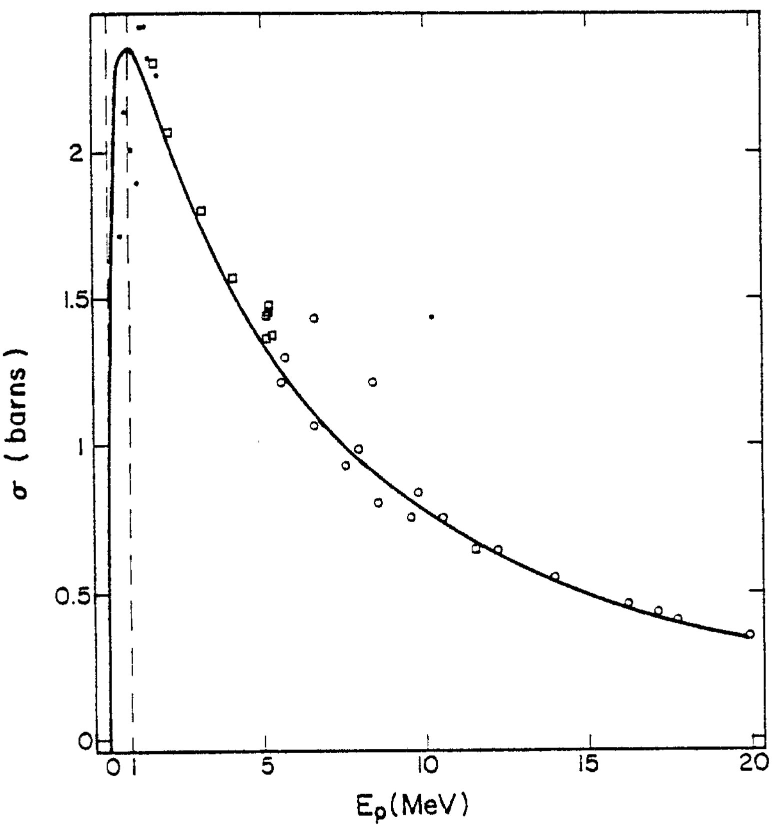

Fig. I-1. The proton-deuterium nuclear elastic scattering cross section after subtraction of the coulomb cross section.

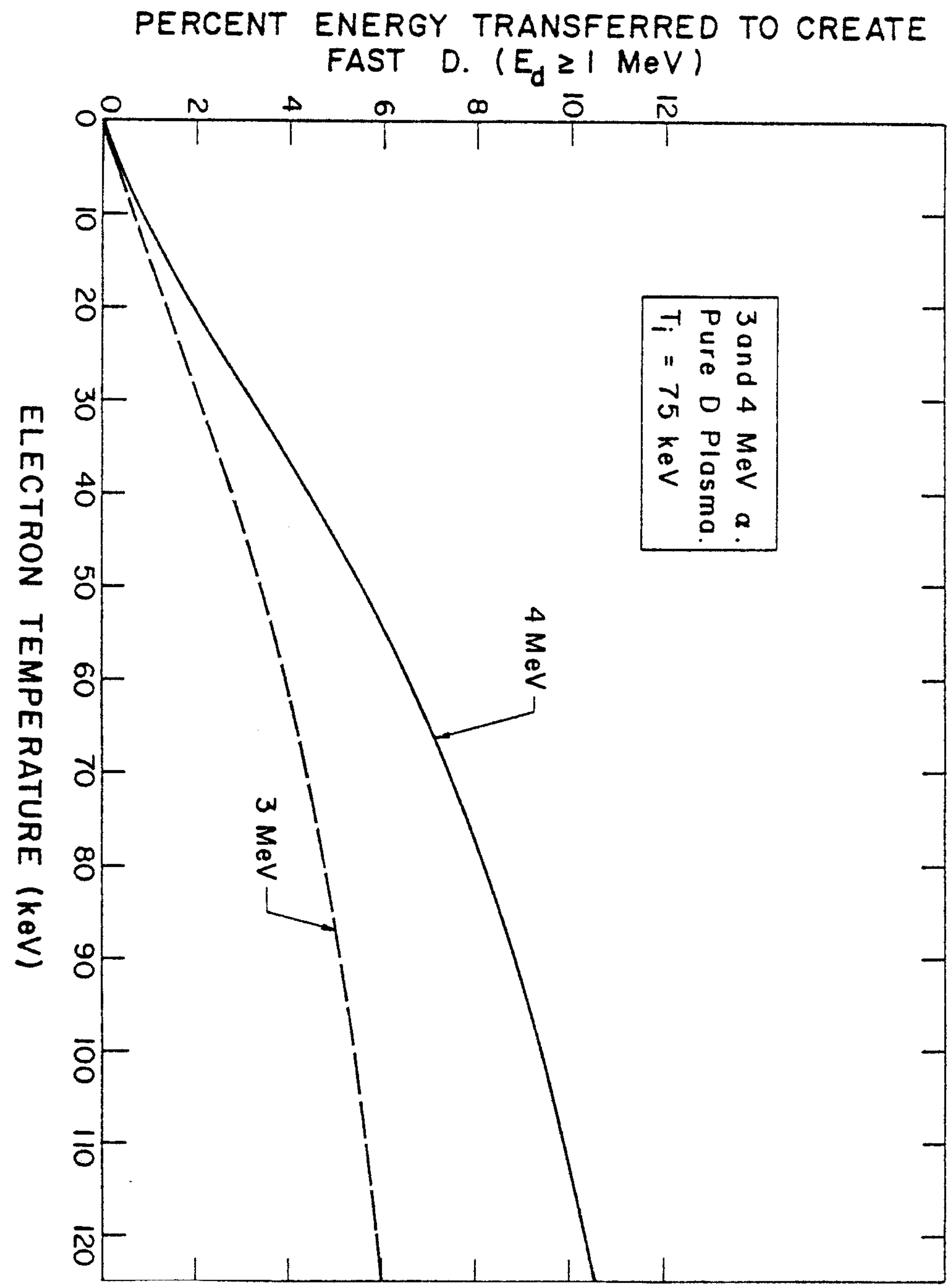

Fig. I-2. Fraction of energy transferred from 3 and 4 MeV α's to produce deutrons with energy > 1 MeV in a pure deuterium plasma.

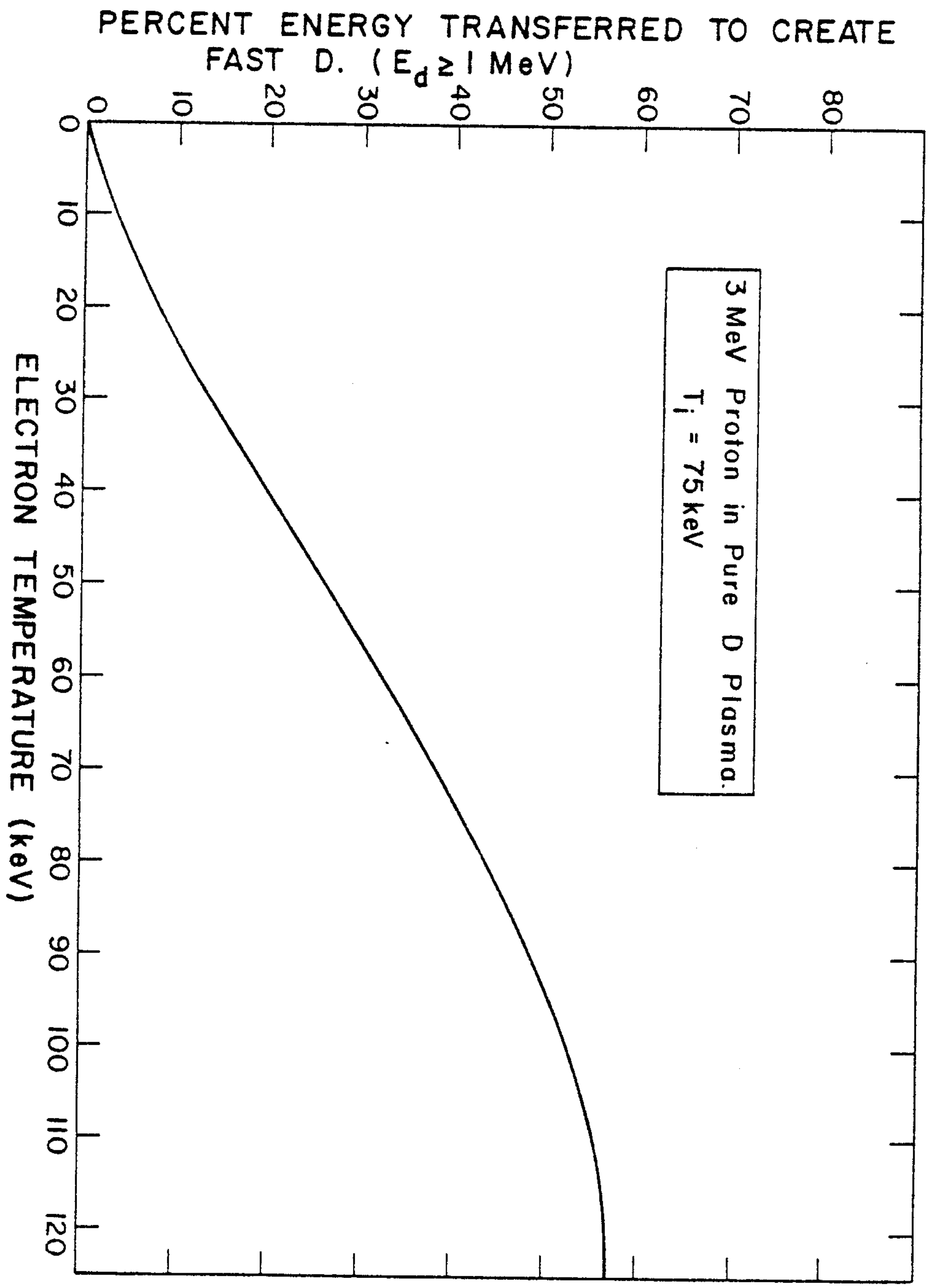

Fig. I-3a. Fraction of energy transferred from 3 MeV proton to produce deutrons with energy > 1 MeV in a pure deuterium plasma.

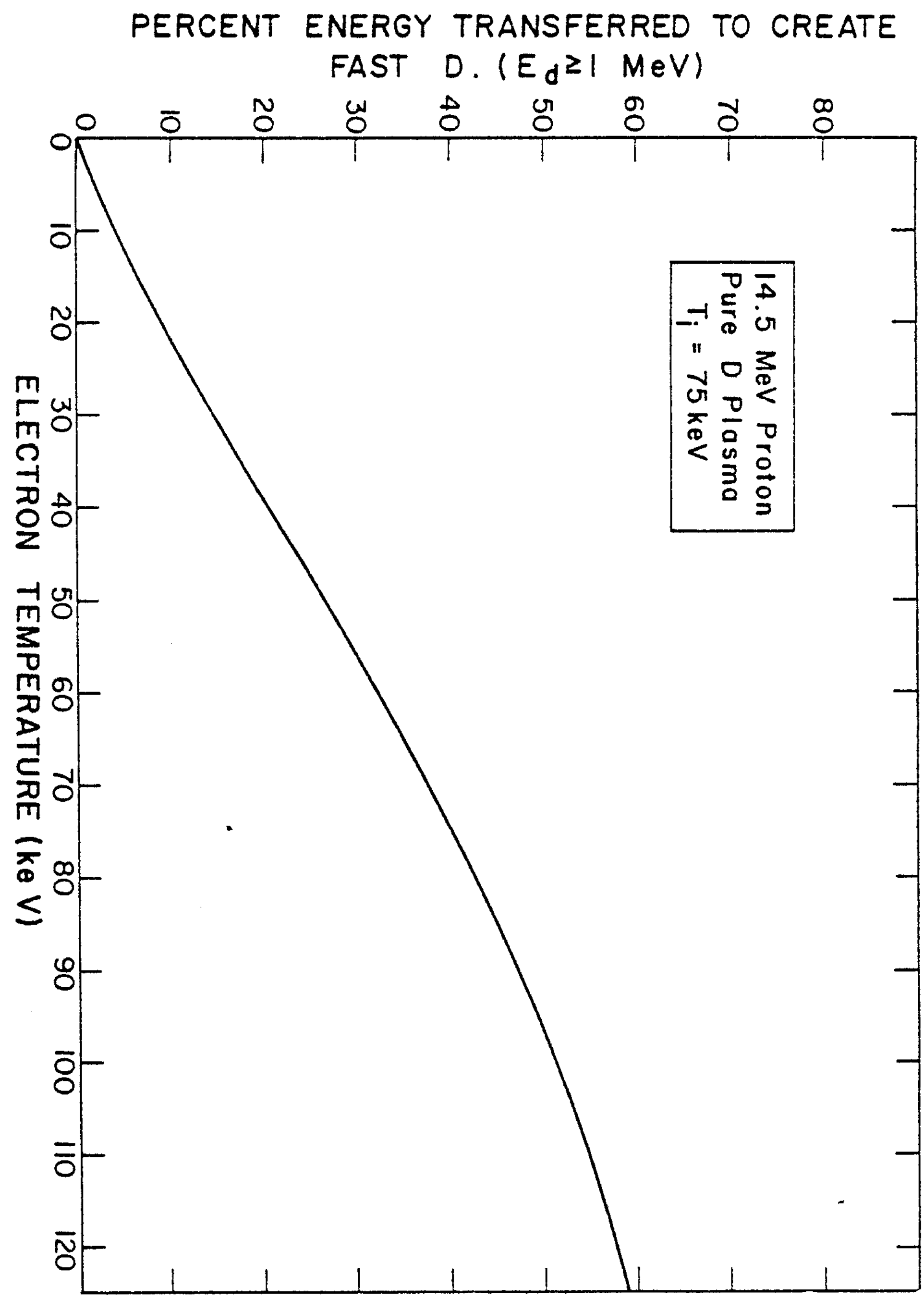

Fig. I-3b. Fraction of energy transferred from 14.5 MeV proton to produce deutron with energy > 1 MeV in a pure deuterium plasma.

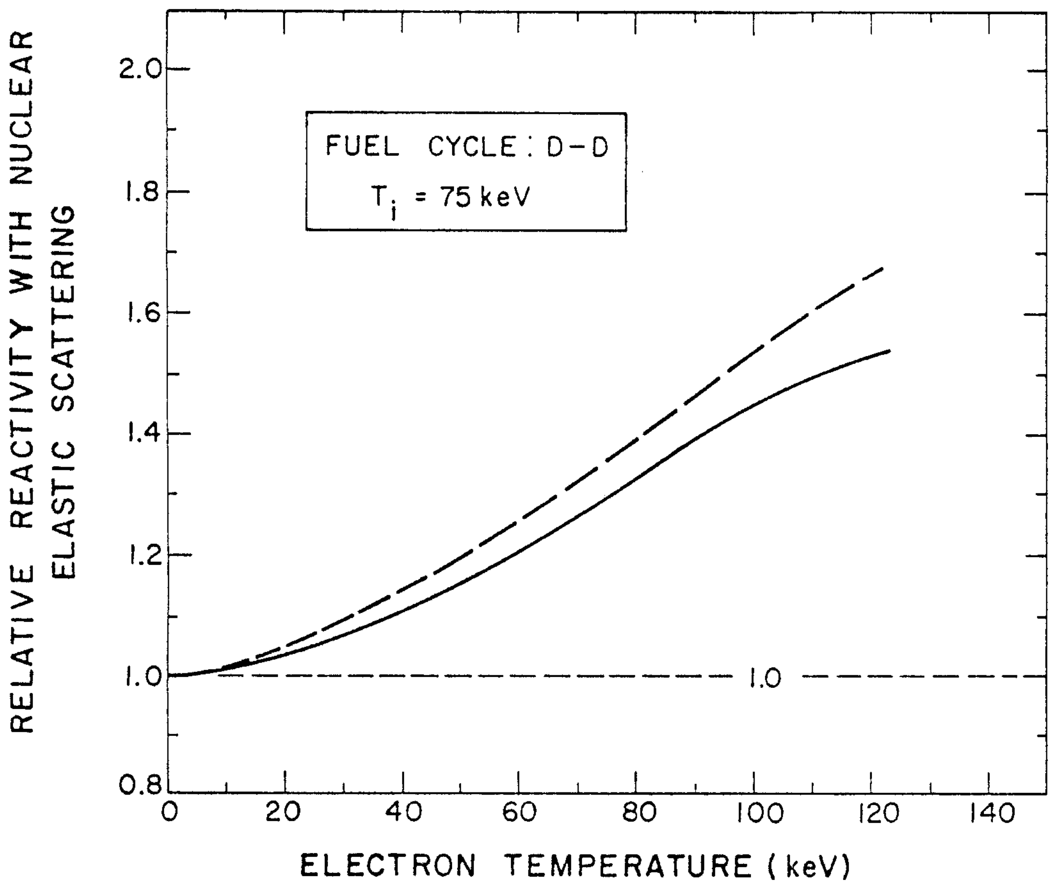

Fig. I-4. Relative reactivity for catalyzed d-d fuel cycle as a function of electron temperature.

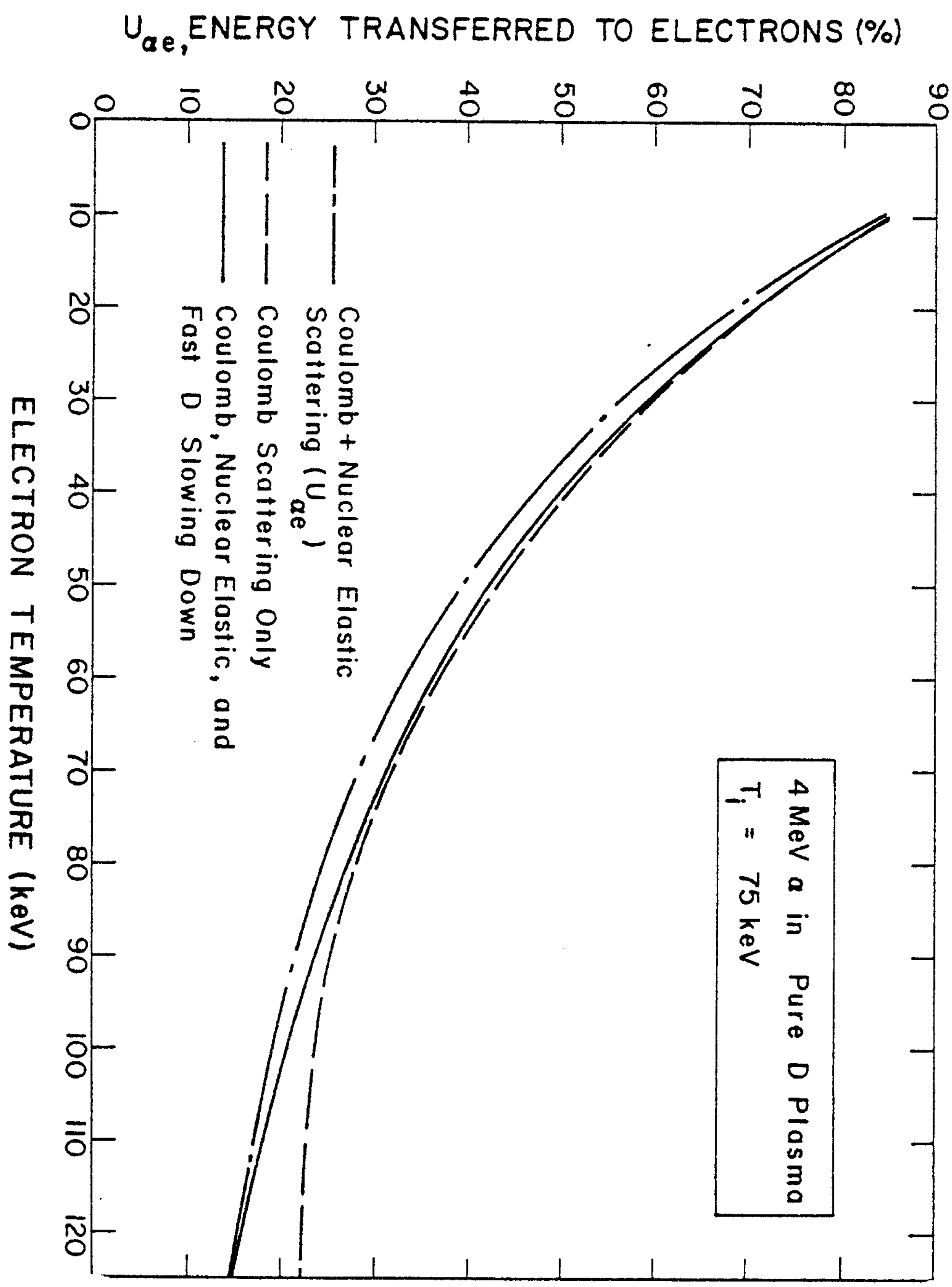

Fig. I-5. Fraction of energy transfered from 4 MeV α to electrons in a pure deuterium plasma, as a function of electron temperature.

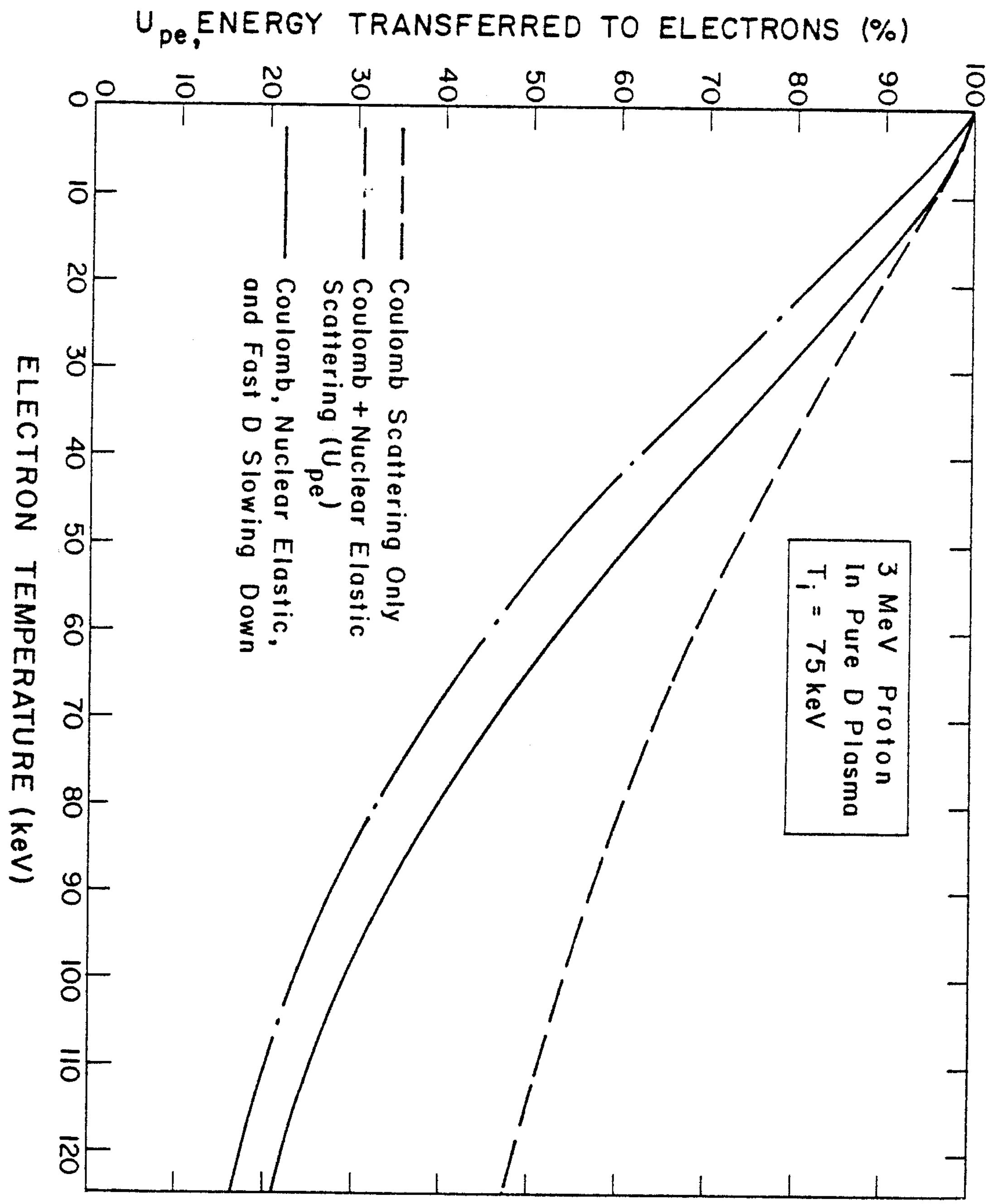

Fig. I-6. Fraction of energy transferred from 3 MeV protons to electrons in a pure deuterium plasma, as a function of electron temperature.

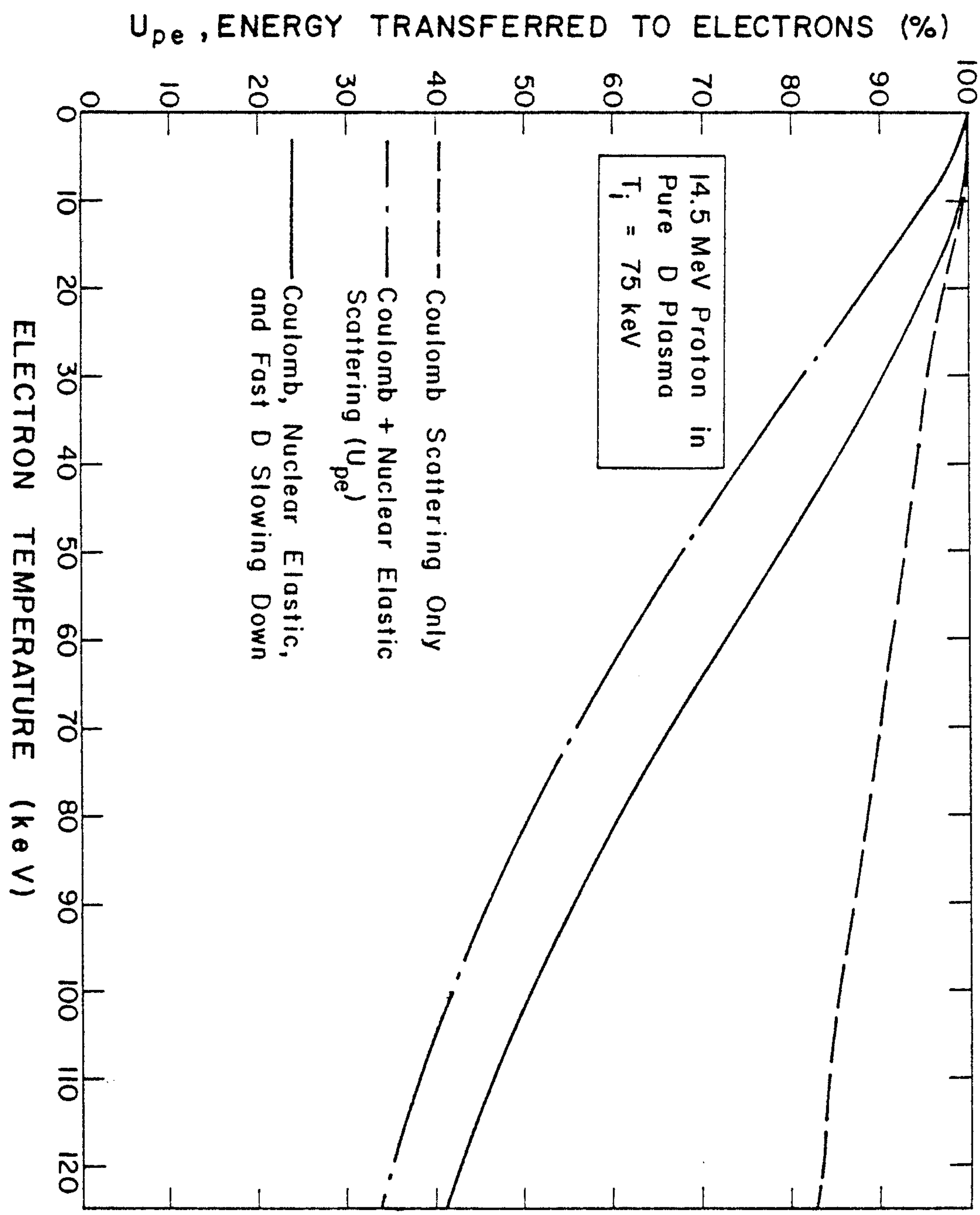

Fig. I-7. Fraction of energy transferred from 14.5 MeV protons to electrons in a pure deuterium plasma, as a function of electron temperature.

CHAPTER I

REFERENCES

1. B. Badger, et. al., UWMAK-I, A Wisconsin Toroidal Fusion Reactor Design, UWFDM-68 ('74).
2. R. G. Mills, editor, A Fusion Power Plant, Princeton Plasma Physics Lab. MATT-1050 ('74).
3. An Engineering Design Study of a Reference Theta-Pinch Reactor (RTPR), LA-5336 or ANL-8019, Joint Report by LASL and ANL ('74).
4. R. W. Werner, et. al., Progress Report No. 2 in the Design Considerations of a low Power Experimental Mirror Fusion Reactor, UCRL-7405 4-2 ('74).
5. E. Bertolini, et. al., Preliminary Design of a Minimum Size Technical Feasibility Tokamak Fusion Reactor, Proc. of 1st Top. Mtg. on the Tech of Controlled Thermonuclear Fusion, CONF 740402-P1, USAEC San Diago ('74).
6. J. R. McNally, Jr., Nucl Fus 11(71) 187.
7. J. M. Dawson, UCLA Plasma Group Report, PPG-273 (Aug. 1976).
8. J. G. Cordey, lecture 2. Course on Theory of Magnetically Confined Plasma (Varenna, Italy) Sept. 1977.
9. R. W. Conn, et. al., "Aspects of Octopoles as Advanced Cycle Fusion Reactors" in Fusion Reactor Design Problems, IAEA (Vienna) 1978.
10. J. R. Mcnally, Jr., R. D. Sharp, R. H. Fowler, J. F. Clarke, Reactivity of Closed Fusion Reactor System for Advanced Fuels, Nucl Fusion 14('74)579.

11. G. H. Miley, et. al., Advanced-Fuel Fusion systems. The D-^{3}He Satellite Approach. (The ILB Reactors), IAEA, Fusion Design Concepts. Madison, WI. U.S.A., p. 709, 1978.

12. Geoffrey W. Shuy, Advanced Fusion Fuel Cycles and Fusion Reaction Kinetics (Preliminary Proposal), UWFDM-335, Dec 79.

13. Geoffrey W. Shuy and Robert W. Conn, The p-^{6}Li Propagating Reaction Cycle, Transaction, ANS Winter Conference, San Francisco, Oct. 79.

14. R. W. Conn and G. W. Shuy, Advanced Fuel Cycles and Propagating p-^{6}Li Cycle, UWFDM-262, Sept. 78.

CHAPTER II

CHARGED PARTICLE CROSS SECTION REQUIREMENTS

FOR

ADVANCED FUSION FUEL CYCLE ANALYSIS

CHAPTER II

CHARGED PARTICLE CROSS SECTION REQUIREMENTS FOR ADVANCED FUSION FUEL CYCLE ANALYSIS

II-1. Required Nuclear Data

In order to properly determine the potential of each fusion fuel cycle, the basic nuclear data for nuclei with atomic mass numbers less than 12 must be known accurately. The nuclear data required to analyze advanced fuels include fusion reaction cross sections, reaction rate parameters such as $\langle\sigma v\rangle$, reaction probabilities for fast fusion products to react with various elements in the background plasma, and nuclear elastic and inelastic cross sections to determine the energy transfer from the energetic fusion products to the background ions and electrons. The reaction rate, R, for two reacting species, a and b, is:

$$R = \int d\bar{v}_a \int d\bar{v}_b \; f_a(\bar{v}_a) \; f_b(\bar{v}_b) \; \sigma(u) \; u \qquad \text{(II-1)}$$

where R is the number of reactions per unit volume per unit time, f_a and f_b are the distribution functions, σ is the reaction cross section, and u is the relative velocity, $u = |\bar{v}_a - \bar{v}_b|$. It is convenient to write R as $n_a n_b \langle\sigma v\rangle$, where the density of species a and b (n_a and n_b) are found from

$$n_i = \int f_i \; (\bar{v}_i) \; d\bar{v}_i \qquad (i=a,b). \qquad \text{(II-2)}$$

The reaction rate parameter, $<\sigma v>$, depends on the form of the normalized distribution functions $\hat{f}_i\ (\bar{v}_i) = \frac{1}{n_i}\ f_i\ (\bar{v}_i)$:

$$<\sigma v> = \int d\bar{v}_a \int d\bar{v}_b\ \hat{f}_a\ (\bar{v}_a)\ \hat{f}_b\ (\bar{v}_b)\ \sigma(u)\ u. \qquad \text{(II-3)}$$

If $\hat{f}_i(\bar{v}_i)$ is the Maxwellian distribution,

$$\hat{f}_i(\bar{v}_i) = \left(\frac{m_i}{2\pi kT}\right)^{3/2} \exp\ (-m_i v_i^2/2kT), \qquad \text{(II-4)}$$

the integral in Eqn. (II-3) can be expressed as:

$$<\sigma v> = 4\pi \int_0^\infty u^2\ du\ \left(\frac{\mu}{2\pi kT}\right)^{3/2} \exp\ \left(\frac{-\mu u}{2kT}\right)^2 \sigma(u) u, \qquad \text{(II-5)}$$

where μ is the reduced mass. Using $E = 1/2\mu u^2$, Eqn. (II-5) becomes

$$<\sigma v> = \sqrt{\frac{8}{\pi\mu}}\ \left(\frac{1}{kT}\right)^{3/2} \int_0^\infty E\ \sigma(E)\ \exp\ (-E/kT)\ dE. \qquad \text{(II-6)}$$

The ion temperature in an advanced fuel cycle fusion plasma may reach 500 keV. One clearly would like to know the reaction cross section, $\sigma(E)$, up to an energy at least 4 kT (or 2 MeV in the most extreme case) to analyze fusion reactions among species with a Maxwellian distribution. In addition, nuclear scattering events between energetic products and the background Maxwellian can transfer significant energy (> 1 MeV) to the struck particle thereby promoting it to higher energy where it is typically more reactive. In short, cross sections are required not just to an energy of 4-5 kT but to the energy of fusion reaction products. The p-^{6}Li cycle is particularly useful to demonstrate this requirement.

The primary reactions of this fuel cycle are:

$$p + {}^6Li \rightarrow {}^3He\ (2.3\ MeV) + {}^4He\ (1.7\ MeV) \qquad (II\text{-}7)$$

$$^3He + {}^6Li \rightarrow p\ (11.3\ MeV) + 2\ {}^4He\ (2.81\ MeV) \qquad (II\text{-}8a)$$

$$\rightarrow p + {}^8Be\ (\text{various nuclear levels}) \qquad (II\text{-}8b)$$

$$\rightarrow d\ (.088\ MeV) + {}^7Be\ (.026\ MeV) \qquad (II\text{-}8c)$$

Secondary and tertiary reactions include:

$$d + {}^6Li \rightarrow n + {}^7Be\ (.42\ MeV) \qquad (II\text{-}9a)$$

$$d + {}^6Li \rightarrow p\ (4.4\ MeV) + {}^7Li\ (.63\ MeV) \qquad (II\text{-}9b)$$

$$d + {}^6Li \rightarrow p\ (1.6\ MeV) + t + {}^4He \qquad (II\text{-}9c)$$

$$d + {}^6Li \rightarrow n + {}^3He + {}^4He \qquad (II\text{-}9d)$$

$$d + {}^6Li \rightarrow 2\ {}^4He\ (11.2\ MeV) \qquad (II\text{-}9e)$$

$$d + {}^3He \rightarrow p\ (14.6\ MeV) + {}^4He\ (4.7\ MeV) \qquad (II\text{-}10)$$

$$d + d \rightarrow n + {}^3He\ (.82\ MeV) \qquad (II\text{-}11a)$$

$$d + d \rightarrow p\ (3\ MeV) + t\ (1.01\ MeV) \qquad (II\text{-}11b)$$

$$d + {}^7Be \rightarrow p\ (11.2\ MeV) + 2\ {}^4He\ (2.8\ MeV) \qquad (II\text{-}12)$$

$$d + t \rightarrow n + {}^4He\ (3.5\ MeV) \qquad (II\text{-}13)$$

$$t + {}^3He \rightarrow d\ (9.6\ MeV) + {}^4He\ (4.8\ MeV) \qquad (II\text{-}14a)$$

$$t + {}^3He \rightarrow p + n + {}^4He \qquad (II\text{-}14b)$$

$$^3He + {}^3He \rightarrow 2p\ (5.7\ MeV) + {}^4He\ (1.4\ MeV) \qquad (II\text{-}15)$$

$$^3He + {}^7Be \rightarrow 2p\ (4.5\ MeV) + 2\ {}^4He\ (1.1\ MeV) \qquad (II\text{-}16)$$

$$t + {}^7Be \rightarrow p\ (4.2\ MeV) + 2\ {}^4He \qquad (II\text{-}17)$$

$$d + {}^{7}Li \rightarrow n + 2d \; (2.52 \text{ MeV}) \qquad \text{(II-18)}$$

In addition there are at least thirty side reactions and thirteen ${}^{6}Li + {}^{6}Li$ exothermic reactions which produce elements from H to ${}^{12}C$ and neutrons. Many of the fusion reaction products are energetic and may react with elements in the background plasma prior to completely slowing down (fast fusion or two-component fusion events). Including these fast fusion events is crucial, particularly for cycles that are propagating. Some important propagating fusion reaction sequences in the p-${}^{6}Li$ cycle (the fast particle has a bar over the element's designation) include:

$$\left\{\begin{array}{l} \bar{p} + {}^{6}Li \rightarrow \overline{{}^{3}He} + \alpha \\ \overline{{}^{3}He} + {}^{6}Li \rightarrow \bar{p} + 2\alpha \\ \bar{p} + {}^{6}Li \rightarrow \overline{{}^{3}He} + \alpha \end{array}\right\} \text{(II-19)} \qquad \left\{\begin{array}{l} \bar{p} + {}^{6}Li \rightarrow \overline{{}^{3}He} + \alpha \\ \overline{{}^{3}He} + d \rightarrow \bar{p} + \alpha \\ \bar{p} + {}^{6}Li \rightarrow \overline{{}^{3}He} + \alpha \end{array}\right\} \text{(II-20)}$$

$$\vdots \qquad\qquad \vdots$$

$$\left\{\begin{array}{l} \bar{p} + {}^{6}Li \rightarrow \overline{{}^{3}He} + \alpha \\ \overline{{}^{3}He} + {}^{6}Li \rightarrow \bar{d} + {}^{7}Be \\ \bar{d} + {}^{6}Li \rightarrow \bar{p} + {}^{7}Li \\ \bar{p} + {}^{6}Li \rightarrow \overline{{}^{3}He} + \alpha \end{array}\right\} \text{(II-21)} \qquad \left\{\begin{array}{l} \bar{p} + {}^{6}Li \rightarrow \overline{{}^{3}He} + \alpha \\ \overline{{}^{3}He} + {}^{6}Li \rightarrow \bar{d} + {}^{7}Be \\ \bar{d} + {}^{7}Be \rightarrow \bar{p} + 2\alpha \\ \bar{p} + {}^{6}Li \rightarrow \overline{{}^{3}He} + \alpha \end{array}\right\} \text{(II-12)}$$

$$\vdots \qquad\qquad \vdots$$

and there are others. See Eqns. (II-7) through (II-18) for the energies of the reaction products.

Nuclear elastic scattering of the energetic products with the background plasma produces additional energetic particles which can undergo fast fusion and further propagate the reaction. Therefore, the reaction cross section for the various channels and nuclear elastic scattering cross sections are required up to about 20 MeV.

II-2. Status of Nuclear Data for Advanced Fusion Fuel Cycle Analysis

The literature has been examined through October 1979. All data for a given reaction were examined for consistency. In general the uncertainties or inconsistencies ranged from 10% to as much as an order of magnitude. Cross sections for some of the reaction branches have either been partially measured or not measured at all. In the reactions ^{3}He-^{6}Li and d-^{7}Be, for example, recent measurements at ANL indicate that the total reaction cross section may be 10 to 50 times larger than previously reported values. For other reactions, such as ^{3}He with ^{7}Be, the data are nonexistent.

The status of nuclear data is summarized in matrix form in Tables II-1, II-2 and II-3 except p-p, p-^{4}He and ^{4}He-^{4}He elastic scattering data which are well known. The references are listed in (58, 59, 466-500). The asterisk (*) indicates the reaction is important for fusion fuel cycle analysis; the check (✓) indicates the data for that reaction are reasonably consistent; While the cross (X) indicates the existing data are highly inconsistent or have large error bars. References are given in the parentheses. The numbers followed by MeV give the energy range over which data have been measured. A literature search for nuclear inelastic cross sections is in progress.

The data for several of the major fusion reactions will now be examined in greater detail.

(1) The d+d Reactions

$$d + d \rightarrow n + {}^3He \qquad Q = 3.269 \text{ MeV} \qquad \text{(II-23)}$$

$$d + d \rightarrow p + t \qquad Q = 4.033 \text{ MeV} \qquad \text{(II-24)}$$

Liskien and Paulsen[461] have summarized and evaluated the cross section measurements for E_d = .013 - 10 MeV. The data and evaluation are shown in Fig. II-1. This is adequate for fusion fuel cycle analysis.

(2) The p+t Reaction

$$t + p \rightarrow n + {}^3He \qquad Q = -.764 \text{ MeV} \qquad \text{(II-25)}$$

Cross section measurements have been evaluated by Liskien and Paulsen.[462] The angular distribution measurements are inconsistent with one another. Most of the integrated cross section measurements are within 15% of the recommended values. Experimental values for E_p = 1.0 - 10 MeV are shown in Fig. II-2. This data is adequate for fusion fuel cycle analysis.

(3) The d+t Reactions

$$t + d \rightarrow n + \alpha \qquad Q = 17.590 \text{ MeV} \qquad \text{(II-26)}$$

There has been only one measurement since 1960. The cross section measurements have been evaluated[463] and indications are that a number of reported angular distributions are not satisfactory at energies above 5 MeV. Most of the integrated cross section measurements are within 10% of the recommended values. In general, the data is adequate for fusion fuel cycle analysis.

(4) The d+^{3}He Reaction

$$^3He + d \rightarrow p + \alpha \qquad Q = 18.35\ MeV \qquad (II-27)$$

There have been no measurements since 1960. A pronounced resonance occurs at E_d = 430 keV with $\Gamma \simeq$ 450 keV. The experimental data disagree in the neighborhood of this resonance (~25%). However, analysis by Hale[464] suggests that the recommended values are very good. Thus, the cross sections are adequate for fusion fuel cycle analysis.

(5) The ^{3}He+^{3}He Reactions

$$^3He + {}^3He \rightarrow p + {}^5Li \qquad Q = 10.890\ MeV \qquad (II-28)$$
$$\quad {}^5Li \rightarrow p + \alpha$$

$$^3He + {}^3He \rightarrow 2p + \alpha \qquad Q = 12.86\ MeV \qquad (II-29)$$

A study of the proton spectrum indicates that the reaction proceeds mainly via a direct mechanism and the ^{5}Li channel. However, the branching ratio is not firmly established, particularly at low energy.

(6) The p+^{6}Li Reaction

$$^6Li + p \rightarrow {}^3He + \alpha \qquad Q = 4.023\ MeV \qquad (II-30)$$

The cross section measurements for E_p = .14-3 MeV by Elwyn et al.[197] appear to be definitive. The earlier measurements are inconsistent with one another as shown in Fig. II-3. Cross section measurements for E_p = 3 to 12 MeV have been made recently by Gould et al.[198] The measurements for E_p = 62 to 188 keV deviate from an S-wave Gamow plot above ~130 keV.

(7) The $d+{}^6Li$ Reactions

$$d + {}^6Li \rightarrow n + {}^7Be \qquad Q = 3.380 \text{ MeV} \qquad (II-31)$$

$$\rightarrow p + {}^7Li \qquad Q = 4.026 \text{ MeV} \qquad (II-32)$$

$$\rightarrow p + t + \alpha \qquad Q = 2.561 \text{ MeV} \qquad (II-33)$$

$$\rightarrow n + {}^3He + \alpha \qquad Q = 1.796 \text{ MeV} \qquad (II-34)$$

$$\rightarrow 2\alpha \qquad Q = 22.374 \text{ MeV} \qquad (II-35)$$

The recent measurements for E_d = .1 - 1 MeV by Elwyn et al.[214] are definitive. Other measurements differ sharply with one another, even in recent experiments.[218] Cross section measurements for E_d > 1 MeV are needed for a complete analysis.

(8) The ${}^3He+{}^6Li$ Reactions

$$ {}^6Li + {}^3He \rightarrow p + {}^8Be(g.s.) \rightarrow 2\alpha \qquad Q = 16.787 \text{ MeV} \qquad (II-36)$$

$$\rightarrow p + {}^8Be(2.94) \rightarrow 2\alpha \qquad Q = 13.847 \text{ MeV} \qquad (II-37)$$

$$\rightarrow p + {}^8Be(11.4) \rightarrow 2\alpha \qquad Q = 5.387 \text{ MeV} \qquad (II-38)$$

$$\rightarrow p + {}^8Be(16.63) \rightarrow 2\alpha \qquad Q = .157 \text{ MeV} \qquad (II-39)$$

$$\rightarrow p + {}^8Be(16.92) \rightarrow 2\alpha \qquad Q = -.1325 \text{ MeV} \qquad (II-40)$$

$$\rightarrow p + {}^8Be(17.64) \qquad Q = -.853 \text{ MeV} \qquad (II-41)$$

$$\rightarrow p + 2\alpha \qquad Q = 16.88 \text{ MeV} \qquad (II-42)$$

$$\rightarrow \alpha + {}^5Li \rightarrow p + \alpha \qquad Q = 14.91 \text{ MeV} \qquad (II-43)$$

$\rightarrow d + {}^{7}Be$ $\quad Q = .1126$ MeV (II-44)

$\rightarrow d + {}^{7}Be(.43)$ $\quad Q = -.31$ MeV (II-45)

$\rightarrow 2p + {}^{7}Li$ $\quad Q = -.468$ MeV (II-46)

A measurement is in progress by A. Elwyn et al., at the Argonne National Laboratory.[465] The earlier measurements are not complete. At least 5 nuclear levels in ${}^{8}Be$ can be excited. It is expected that the reaction cross section to all branches will be at least a factor of 10 larger than those now known. For example, at $E_{{}^{3}He} = 3.5$ MeV, Gould et al.[245] measured $\sigma_r \simeq$ 10-12 mb for the ${}^{8}Be$ (g.s.) branch, $\sigma_r \simeq$ 55 mb for the ${}^{8}Be$(2.94 MeV) branch and estimated $\sigma_r \simeq$ 42 mb for the continuum breakup reaction, Elwyn et al., indicate values could be $\sigma_r \simeq$ 30-50 mb for the ${}^{8}Be$(16.63 MeV) branch, $\sigma_r \simeq$ 20-40 mb for the ${}^{8}Be$ (16.9 MeV) branch and $\sigma_r \simeq$ 400 mb for the $d + {}^{7}Be$ branch.

(9) The $d+{}^{7}Be$ Reactions

There have been no measurements since 1960, since ${}^{7}Be$ does not exist. $d + {}^{7}Be$ reacts via the same compound nucleus as ${}^{3}He + {}^{6}Li$. Therefore, it will have the same reaction channels as ${}^{3}He + {}^{6}Li$ except for eqns. (II-44) and (II-45). Since the existing data are only for the eqn. (II-36) and (II-37) branches, measurements for each branch stated above are required. However, in lieu of an experimental determination of σ, a standard 9-nucleon R-matrix calculation can give good estimated values, provided that the cross sections of each branch of ${}^{3}He + {}^{6}Li$ reaction are given.

(10) The $p+{}^{11}B$ Reaction

$${}^{11}B + p \rightarrow \alpha + {}^{8}Be \qquad Q = 8.590 \text{ MeV} \qquad \text{(II-47)}$$

$${}^{11}B + p \rightarrow 3\alpha \qquad Q = 8.682 \text{ MeV} \qquad \text{(II-48)}$$

The most recent cross section measurements for E_p = 0.08 - 1.4 MeV by Davidson et al.(434) appear to be definitive. There are 7 pronounced resonances in the range, E_p = .1 - 5 MeV. The energy of the resonances, the cross sections at each resonance peak, and the width of each resonance are summarized in Table II-4. The cross sections are uncertain above 2 MeV and should be measured again.

TABLE 1

	p	d	t	^3He	^4He
d	ELASTIC (1 - 20) σ (E, θ) 0.2 - 30. MeV * ✓ REACTION (——) ——	ELASTIC (46 - 67) σ (E, θ) 2. - 20. MeV * ✓ REACTION (60-90) σ (E) or σ (E, θ) 0.013 - 14. MeV	S	S	ELASTIC (164 - 178) σ (E, θ) 0.3 - 20. MeV * ✓ REACTION (——) ——
t	ELASTIC (21 - 30) σ (E, θ) 0.05 - 8.3 MeV * ✓ REACTION (31 - 45) σ (E) or σ (E, θ) 1.0 - 10. MeV	ELASTIC (91 - 93) σ (E, θ) 0.013 - 10. MeV * ✓ REACTION (94 - 112) σ (E) or σ (E, θ) 0.01 - 15. MeV	ELASTIC (141 - 142) σ (E, θ) 1.58 - 2. MeV X REACTION (143 - 146) σ (E) or σ (E, θ) 0.04 - 2.2 MeV	S	ELASTIC (179 - 182) σ (E, θ) 1.2 - 18.2 MeV * X REACTION (——) ——
^3He	ELASTIC (126 - 140) σ (E, θ) 0.1 - 20. MeV * ✓ REACTION (——) ——	ELASTIC 113 - 116 σ (E, θ) 0.38 - 20. MeV * ✓ REACTION (117 - 125) σ (E) or σ (E, θ) 0.25 - 15. MeV	ELASTIC (147 - 148) σ (E, θ) 5. - 19. MeV X REACTION 149 - 154 σ (E) or σ (E, θ) .15 - 1.9 MeV	ELASTIC (155 - 158) σ (E, θ) 5. - 20. MeV * ✓ REACTION (159 - 163) σ (E) or σ (E, θ) 0.06 - 2.2 MeV	ELASTIC (183 - 190) σ (E, θ) 1.72 - 20. MeV * X REACTION (——) ——

TABLE 2

	p	d	t	^{3}He	^{4}He
^{6}Li	ELASTIC (191 - 196) $\sigma(E, \theta)$ 0.5 - 16. MeV * ✓ REACTION (197 - 210) $\sigma(E, \theta)$ 0.14 - 12. MeV	ELASTIC (211 - 213) $\sigma(E, \theta)$ 2. - 7. MeV * ✓ REACTION (213 - 225) $\sigma(E, \theta)$ 0.1 - 1. MeV	ELASTIC (———) No measurement X REACTION (226 - 230) $\sigma(E, \theta)$ 0.3 - 20. MeV	ELASTIC (231) $\sigma(E, \theta)$ 8. - 20. MeV * X REACTION 232 - 245 $\sigma(E, \theta)$ or $\sigma(E)$ 1.2 - 4.2 MeV	ELASTIC (246 - 250) $\sigma(E, \theta)$ 2. - 7.5 MeV REACTION (———) ———
^{7}Li	ELASTIC (251 - 254) $\sigma(E, \theta)$ 0.4 - 20. MeV X REACTION (255 - 285) $\sigma(E, \theta)$ or $\sigma(E)$ 0.8 - 15. MeV	ELASTIC (286) $\sigma(E, \theta)$ 0.4 - 1.8 MeV X REACTION (287 - 300) $\sigma(E)$ or $\sigma(E, \theta)$ 0.6 - 2.6 MeV	ELASTIC (———) No measurement X REACTION (301 - 310) $\sigma(E, \theta)$ 0.23 - 2.5 MeV	ELASTIC (311) $\sigma(\theta)$ 11. MeV X REACTION (312 - 325) $\sigma(E, \theta)$ 0.8 - 6. MeV	ELASTIC (326 - 330) $\sigma(E, \theta)$ 1.6 - 20. MeV REACTION (———) ———
^{7}Be	ELASTIC (———) No measurement X REACTION (———) ———	ELASTIC (———) No measurement * X REACTION (331-332) $\sigma(E, \theta)$ 0.8 - 1.7 MeV	ELASTIC (———) No measurement X REACTION (306) No measurement $<\sigma V>$ Estimated	ELASTIC (———) No measurement * X REACTION (306) No measurement $<\sigma V>$ Estimated	ELASTIC (———) No measurement REACTION (———) ———

TABLE 3

	p	d	t	^3He	^4He
^9Be	ELASTIC (333 - 340) $\sigma(E, \theta)$ 0.2 - 10. MeV ✓ REACTION (341 - 345) $\sigma(E, \theta)$ 0.028 - 2.0 MeV	ELASTIC (346 - 350) $\sigma(E, 90^0)$ 0.4 - 7. MeV ✓ REACTION (351 -370) $\sigma(E)$ or $\sigma(E, \theta)$ 0.15 - 19. MeV	ELASTIC (371, 372) $\sigma(E, \theta)$ 0.6 - 2.1 MeV ✓ REACTION (371, 372) $\sigma(E, \theta)$ 0.52 - 2.1 MeV	ELASTIC (373 - 375) $\sigma(E, 45^0)$ or $\sigma(E, 90^0)$ 1.2 - 20. MeV X REACTION (376 - 380) $\sigma(E, \theta)$ 1.6 - 20. MeV	ELASTIC (381 - 384) $\sigma(E, \theta)$ 1.4 - 20. MeV REACTION (———) ———
^{10}B	ELASTIC (385 - 387) $\sigma(E, \theta)$ 0.15 - 10.5 MeV X REACTION (388 - 390) $\sigma(E, \theta)$ 0.06 - 6.3 MeV	ELASTIC (391 - 393) $\sigma(E, \theta)$ 1. - 16. MeV X REACTION (394 - 415) $\sigma(E)$ or $\sigma(E, \theta)$ 0.14 - 12 MeV	ELASTIC (416 - 418) $\sigma(E, \theta)$ 1.5 - 3.3 MeV X REACTION (418) $\sigma(E)$ 0.8 - 2.0 MeV	ELASTIC (419 - 423) $\sigma(E, \theta)$ 4. - 20. MeV X REACTION (424 - 430) Excitation function 2. - 19. MeV	ELASTIC (431 - 433) Excitation function 2. - 20. MeV REACTION (———) ———
^{11}B	ELASTIC (———) No data reported * X REACTION (434 - 440) $\sigma(E)$ or $\sigma(E, \theta)$ 0.17 - 10. MeV	ELASTIC (———) No data reported X REACTION (441 - 453) $\sigma(E)$ or $\sigma(E, \theta)$ 0.3 - 10. MeV	ELASTIC (———) No data reported X REACTION 454, 455 $\sigma(E, \theta)$ 1.0 - 2.1 MeV	ELASTIC (———) No data reported X REACTION (456 - 460) Excitation function or $\sigma(E)$ 0.9 - 18. MeV	ELASTIC (———) No data measured below 27. MeV REACTION (———) ———

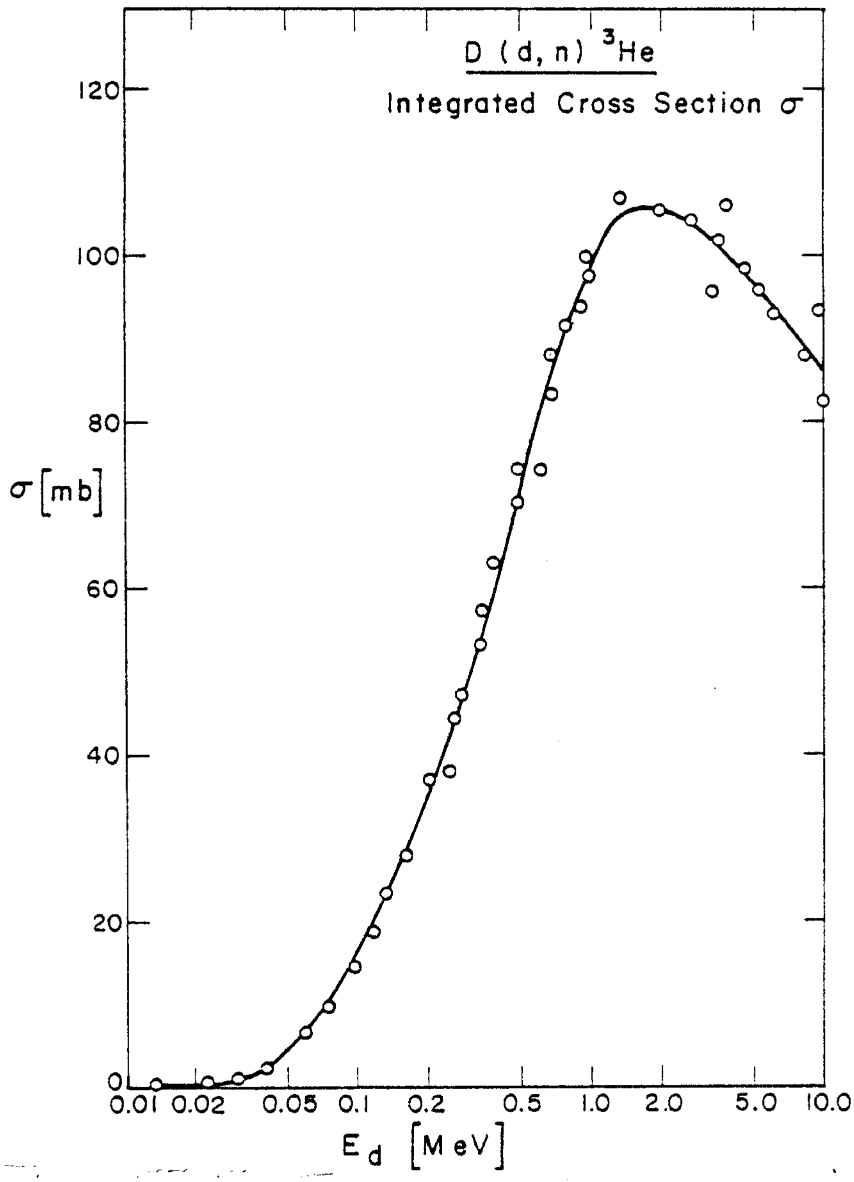

Fig. II-1. Cross section data and recommend values for $D(d,n)^3He$ reaction as a function of detron energy.

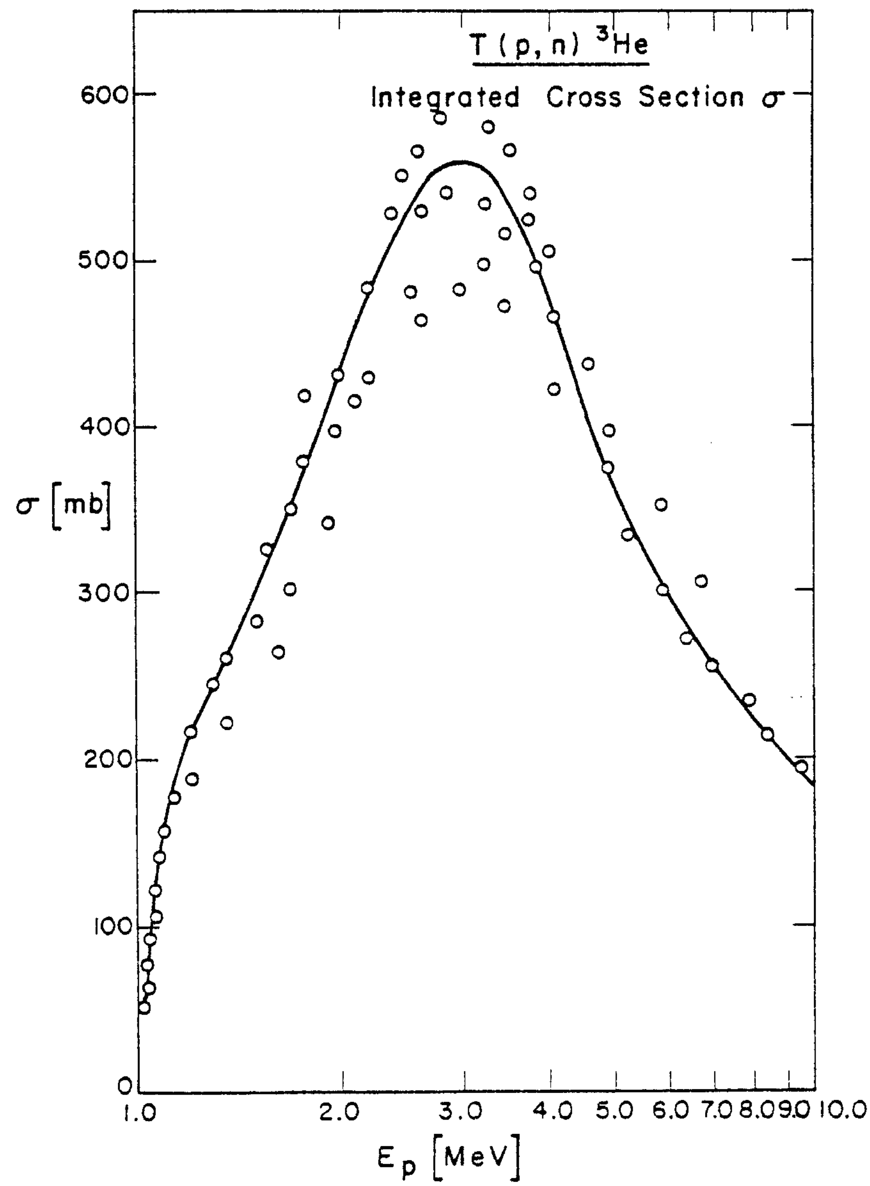

Fig. II-2. Cross section data and recommend values for $T(p,n)^3He$ reaction as a function of proton energy.

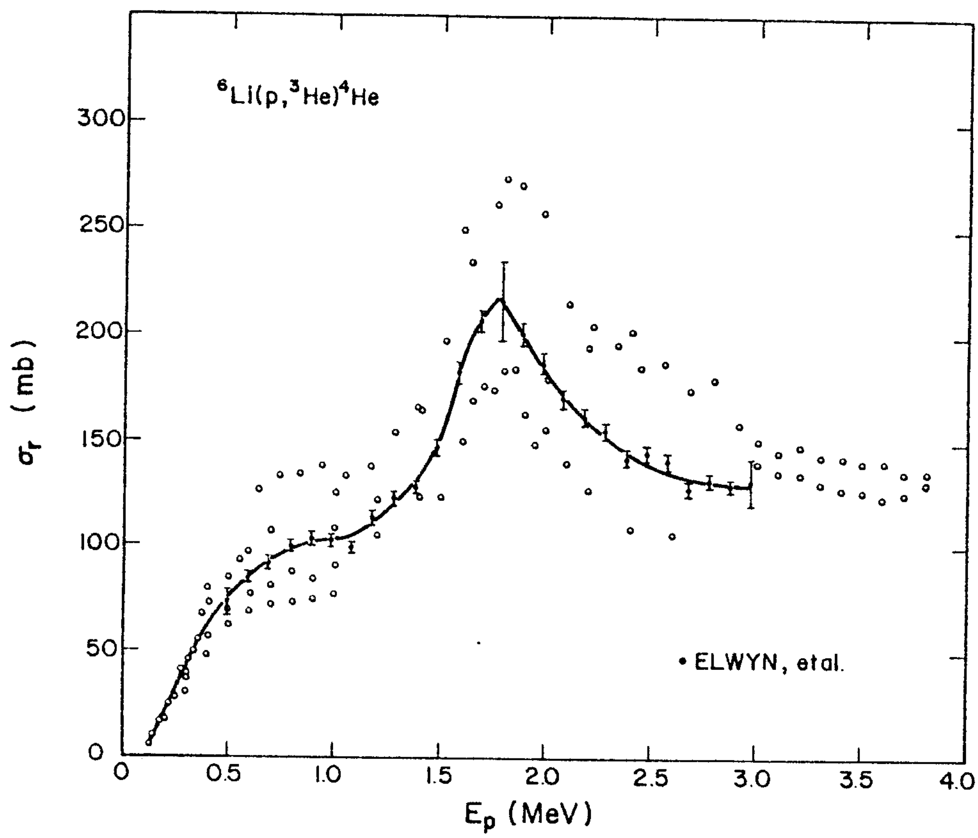

Fig. II-3. Cross Section data shown for $^6Li(p,^3He)^4He$ reaction as a function of proton energy.

Table II-4

Parameters for p-^{11}B Resonances

Resonance Energy E_p (MeV)	Cross Section at Resonance Peak (mb)	Resonance Width Γ (keV)
.172	28	10
.64	800	300
1.39	180	1160
1.98	133 - 132	100
2.62	200 - 347	320
3.75	200 - 348	1100
4.93	130 - 210	180

CHAPTER II

REFERENCES

1. Taschek, Phys. Rev. 61 (42) 13.
2. Sherr et al., Phys. Rev 72 (47) 662.
3. Kocher and Clegg, Nucl. Phys. A132 (69) 455.
4. Wilson et al., Nucl. Phys. A130 (69) 624.
5. Kikuchi et al., J. Phys. Soc. Japan 15 (60) 9.
6. Kerman, Phys. Rev. 107 (57) 200.
7. Kiceleva et al., Ukr. Fiz. Zh. 4 (71) 83.
8. Cahill et al., Phys. Rev C4 (71) 83.
9. Cadlwell and Richardson, Phys. Rev. 98 (55) 28.
10. Allred and Rosen, Phys. Rev. 79 (50) 227.
11. Karr et al., Phys. Rev. 81 (51) 37, 78 (50) 292.
12. Allred et al., Phys. Rev. 88 (52) 433.
13. Simpson, Thesis, Rice Univ., Houston (65).
14. Grötzschel et al., Nucl. Phys. A176 (71) 261.
15. Brolley Jr. et al., Phys. Rev. 117 (60) 1307.
16. Mather, Phys. Rev. 88 (52) 1408.
17. Heither et al., Proc. Roy. Soc. A190 (47) 180.
18. Brown et al., Phys. Rev. 88 (52) 253.
19. Tuve et al., Phys. Rev. 50 (36) 806.
20. Bunker et al., Nucl. Phys. A113 (68) 461.
21. Balashko et al., Zh. eksp. Teor. Fiz. 36 (59) 1937, JETP (soviet Physics) 9 (59) 1378.
22. Baumann, J. Phys. Rad. 18 (57) 337.
23. Jarmie et al., Phys. Rev. 130 (63) 1987.
24. Balashko et al., JETP 19 (64) 1281.
25. Kurepin, Trudy of the Lebedev Phys. Inst., Vol. 33 (65) p.1 (Transl. by Consultant Bureau, N.Y. 66).
26. Jarmie and Allen, Phys. Rev. 114 (59) 176.
27. Hemmendinger et al., Phys. Rev. 79 (49) 1137.
28. Ennis and Hemmendinger, Phys. Rev. 95 (54) 772.
29. Brolley et al., Phys. Rev. 117 (60) 1307.
30. Classen et al., Phys. Rev. 82 (51) 589.
31. Seagrave, Proc. Conf. on Nuclear Forces and the Few Nuclear Problem, London (59) Vol. II, p.583.
32. Macklin and Gibbons, EANDC-50-S, Vol. I (65).
33. Willard et al., Phys. Rev. 90 (53) 865.
34. Jarmie and Seagrave LA-2014 (56).
35. Gibbons and Macklin, Phys. Rev. 114 (59) 571.
36. Batchelor et al., Rev. Sci. Instr. 26 (55) 1037.
37. Costello et al., Nucl. Sci. Eng. 39 (70) 409.
38. Vlasov et al., JETP 1 (55) 500.
39. Coon, Phys. Rev. 80 (50) 488.
40. Sayres et al., Phys. REv. 122 (61) 1853.

41. Seagrave et al., Phys. Rev. 119 (60) 1981.
42. Bogdandov et al., JETP 9 (59) 440.
43. Stewart et al., Bull. Am. Phys. Soc. 1 (56) 93.
44. Wilson et al., Nucl. Phys. 27 (61) 421.
45. Goldberg et al., Phys. Rev. 122 (61) 1510.
46. Theus et al., Nucl. Phys. 80 (66) 273.
47. Bacher and Tombrello, Nucl. Phys. a113 (68) 557.
48. Wilson et al., Nucl. Phys. A126 (69) 193.
49. Cahill et al., CEN-Saclay Annual Report CEA-N 844 (67) 121.
50. Rosen and Allred, Phys. Rev. 88 (52) 431.
51. Brolley et al., Phys. Rev. 117 (60) 1307.
52. Jarmie and Jett, Phys. Rev. C10 (74) 54.
53. Burrows et al., Proc. Roy. Soc. 209 (51) 489.
54. Marlinghaus and Genz, Nucl. Phys. 255 (75) 13.
55. Allred et al., Phys. Rev. 76 (49) 1430.
56. Blair et al., Phys. Rev. 74 (48) 1594.
57. Rosen et al., Phys. Rev. 76 (49) 1283.
58. Jarmie and Jett, Phys. Rev. C10 (74) 54.
59. Jarmie and Jett, Phys. Rev. C13 (76) 2554.
60. Goldberg, Progress in Fast Neutron Physics (U. of Chicago Press 63).
61. Arnold et al., Phys. Rev. 93 (54) 483.
62. Booth et al., Proc. Phys. Soc. (london) A69 (56) 265.
63. McNeill and Keyser, Phys. Rev. 81 (51) 602.
64. Ganeev et al., Atomnaya Energiya Suppl. 5 (57) 21.
65. Preston, et al., Proc. Roy. Soc. (london) A226 (54) 206.
66. Chagnon and Owen, Phys. Rev. 101 (56) 798.
67. Hunter and Richards, Phys. Rev. 76 (49) 1445.
68. Ref. 40
69. Brolley et al., Phys. Rev. 107 (57) 820.
70. Blair et al., Phys. Rev. 74 (48) 1599.
71. Schulte et al., Nucl. Phys. A192 (72) 609.
72. Goldberg et al., Phys. Rev. 119 (60) 1992.
73. Thornton, Nucl. Phys. A139 (69) 25.
74. Brolley et al., Phys. Rev. 107 (57) 820.
75. Eliot et al., Proc. Roy. Soc. (London) 216 (53) 57.
76. Ref. 46
77. Kane, Nucl. Phys. 10 (59) 429.
78. Fuller et al., Phys. Rev. 108 (57) 91.
79. Volkov et al., Stomnaya Energiya Suppl. 5 (57) 13.
80. Milone and Ricamo, Nuovo Cim. 22 (61) 116.

81. Cranberg et al., Phys. Rev. 104 (56) 1639.
82. Kerr and Anderson, Bull. Am. Phys. Soc. 13 (68) 564.
83. Daehnick and Fowler, Phys. Rev. 111 (58) 1309.
84. Ref. 43
85. Wilson et al., Bull. Am. Phys. Soc. 5 (60) 410.
86. Brill et al., Atomnaya Energiya 16 (64) 141.
87. Bame et al., Rev. Sci. Instr. 28 (57) 997.
88. Fowler and Brolley, Rev. Mod. Phys. 28 (56) 103.
89. Ref. 34
90. Defacio, Proc. 3rd Int. Symp. on Polarization Phenomena in Nuclear Reactions (71) 534 (U. of Wisconsin Press).
91. Stratton et al., Phys. Rev. 88 (52) 257.
92. Brolley et al., Phys. Rev. 120 (60) 905.
93. Allred et al., Phys. Rev. 88 (52) 425.
94. Conner et al., Phys. Rev. 88 (52) 468.
95. Ref. 51
96. Davidenks et al., J. Nucl. Energy 2 (57) 258.
97. Balabanov et al., Atomnaya Energiya Suppl. 5 (57) 43.
98. Argo et al., Phys. REv. 87 (52) 612.
99. Kobzev et al., Sov. J. Nucl. Phys. 3 (66) 774.
100. Bame and Perry, Phys. Rev. 107 (57) 1616.
101. Allen and Jarmie, Phys. Rev. 111 (58) 1129.
102. Hemmendinger and Argo, Phys. Rev. 98 (55) 70.
103. Galonsky and Johnson, Phys. Rev. 104 (56) 421.
104. Stewart et al., Phys. Rev. 119 (60) 1649.
105. Brill et al., Atomnaya Energiya 16 (64) 141.
106. Stratton and Freir, Phys. Rev. 88 (52) 261.
107. Goldberg et al., Phys. Rev. 122 (61) 164.
108. Simmons and Malanigy, Bull. Am. Phys. Soc. 13 (68) 564.
109. Bretscher and French, Phys. Rev. 75 (49) 1154.
110. Allen and Poole, Proc. Roy. Soc. (London) A204 (50) 500.
111. Brolley et al., Phys. Rev. 82 (51) 502.
112. Paulsen and Liskien, Nucl. Phys. 56 (64) 394.
113. Brown et al., Phys. Rev. 96 (54) 80.
114. Tombrello et al., Phys. Rev. 154 (67) 935.
115. King and Smythe, Nucl. Phys. A183 (72) 657.
116. Baker et al., Nucl. Phys. A184 (72) 97.
117. Jarmie et al., LA-2014 (57).
118. Carlton, Thesis, U. of Georgia (70) Phys. Abst. 67885 (71).
119. Gruebler et al., Nucl. Phys. A176 (71) 631.
120. Stewart et al., Phys. Rev. 119 (60) 1649.

121. Kunz, Phys. Rev. 97 (55) 456.
122. Bonner er al., Phys. Rev. 88 (52) 473.
123. Frier and Halmgren, Phys. Rev. 93 (54) 825.
124. Yarnel et al., Phys. Rev. 90 (53) 292.
125. Jarmie and Jett, Phys. Rev. C10 (74) 145.
126. Hutson et al., Phys. Rev. C4 (71) 17.
127. Vanetsian and Fedchenko, Soviet J. of Atomic Energy 2 (57) 141.
128. Lovberg, Phys. Rev. 103 (56) 1393.
129. Igo and Leland, Phys. Rev. 154 (67) 950.
130. Brolley and Fowler, Fast Neutron Physics (60).
131. Rosen, Nuclear Forces and the Few Nuclear Problem (Pergamon 60) p. 481.
132. Brolley er al., Phys. Rev. 117 (60) 1307.
133. Sweetman, Phil. Mag. 46 (55) 358.
134. Artemov et al., JETP 10 (60) 474.
135. Clegg et al., Nucl. Phys. 50 (64) 621.
136. McDonald et al., Phys. Rev. 133 (64) B1178.
137. Tombrello et al., Nucl. Phys. 39 (62) 541.
138. Drigo et al., Nuovo Cim. 42B (66) 363.
139. Famularo et al., Phys. Rev. 93 (54) 928.
140. Kavanagh and Parker, Phys. Rev. 143 (66) 779.
141. Holm and Argo, Phys. Rev. 101 (56) 1772.
142. Frank and Grammel, Phys. Rev. 100 (55) 973A.
143. Agnew et al., Phys. Rev. 84 (51) 862.
144. Jarmie et al., Los Alamos Report 2014 (57).
145. Jarmie and Allen, Phys. Rev. 111 (58) 1121.
146. Strelenikov et al., Izv. Akad. Nauk USSR (Ser. Fiz.) 35 (71) 165.
147. Ivanovich et al., Nucl. Phys. A110 (68) 441.
148. Bacher et al., Nucl. Phys. A119 (68) 360.
149. Kuhn and Schlenk, Nucl. Phys. 48 (63) 353.
150. Moak, Phys. Rev. 92 (53) 383.
151. Youn et al., JETP 12 (61) 163.
152. Smith et al., Phys. Rev. 129 (63) 785.
153. Leland er al., Bull. Am. Phys. Soc. 10 (65) 51.
154. Kuhn and Schlenk, Joint Inst. Nucl. Res. USSR Report No. P1197 (63).
155. Ref. 147 & Ref. 148
156. Tombrello and Bacher, Phys. Rev. 130 (63) 1108.
157. Jenkin et al., Phys. Rev. C1 (70) 1622.
158. Bacher er al., Bull. Am. Phys. Soc. 13 (68) 1366.
159. Dwarakanath, Phys. Rev. C9 (74) 805.
160. Dwarakanath and Winkler, Phys. Rev. C4 (71) 1532.

161. Dwarakanath, Thesis, Caltech (69) Phys. Abstr. 39101 (70).
162. Slobodrian et al., Nucl. Phys. A194 (72) 577.
163. Good et al., Phys. Rev. 94 (54) 87.
164. Lauritsen et al., Phys. Rev. 92 (53) 1501.
165. Guggenheimer et al., Proc. Roy. Soc. A190 (47) 196.
166. Burge et al., Proc Roy Soc. A210 (51) 534.
167. Galonsky et al., Phys. Rev. 98 (55) 586.
168. Alfred et al., Phys. Rev. 82 (51) 786.
169. Freemantle et al., Phil. Mag. 45 (54) 1090.
170. Artemov and Vlasov, JETP 12 (61) 1124.
171. Stewart et al., Phys. Rev. 128 (62) 707.
172. Rothe et al., Bull. Am. Phys. Soc. 8 (63) 537.
173. Ohlsen and Young, Nucl. Phys. 52 (64) 134.
174. Senhouse and Tombrello, Nucl. Phys. 57 (64) 624.
175. Matons and Browne, Phys. Rev. 136. (64) B399.
176. Fukunaga et al., J. Phys. Soc. Japan 22 (67) 28.
177. Mani and Tarratts, Nucl. Phys. A107 (68) 624.
178. Jett et al., Phys. Rev. C3 (71) 1769.
179. Hemmendinger, Bull. Am. Phys. Soc. 1 (56) 96.
180. Allen and Jarmie, Phys. Rev. 111 (58) 1129.
181. Brolley et al., Nuclear Forces and the Few Nuclear Problem Vol. II, p. 455.
182. Tombrello and Phillips, Phys. Rev. 122 (61) 224.
183. Miller and Phillips, Phys. Rev. 112 (58) 2048.
184. Barnard et al., Nucl. Phys. 50 (64) 629.
185. Tombrello and Parker, Phys. Rev. 130 (63) 1112.
186. Spiger and Tombrello, Bull. Am. Phys. Soc. 9 (64) 703.
187. Chuang, Nucl. Phys. A174 (71) 399.
188. Spiger and Tombrello, Phys. Rev. 163 (67) 964.
189. Dunnil et al., Nucl. Phys. A93 (67) 201.
190. Ivanovich et al., Nucl. Phys. A110 (68) 441.
191. Harrison, Nucl. Phys. A92 (67) 253 and 260.
192. Harrison and Whitehead, Phys. Rev. 132 (63) 2607.
193. Fasoli et al., Nuovo Cim. 34 (64) 1832.
194. Merchez et al., J. Physique 29 (68) 969.
195. Bashkin and Richards, Phys. Rev. 84 (51) 1124.
196. McCray, Phys. Rev. 130 (63) 2034.
197. Elwyn, Holland, Davids et al., accepted by Phys. Rev. C, to be published.
198. Gould et al., Nucl. Cross Section and Tech. NPP 425, 697.
199. Spinka et al., Nucl. Phys. A164 (71) 1.
200. Bowersox, Phys. Rev. 55 (39) 323.

201. Marion et al., Phys. Rev. 104 (56) 1402.
202. Field and Kunze, Nucl. Phys. A96 (67) 513.
203. Beavmevielle, CEA-R-2624 (64).
204. Hub et al., Z. Phys. 252 (72) 332.
205. Varnagy et al., Nucl. Int. Methods 119 (74) 451.
206. Hooton and Ivanovich, AERE-R7761 (74).
207. Johnston and Sargood, Nucl. Phys. A224 (74) 349.
208. Jeronymo et al., Nucl. Phys. 43 (63) 424.
209. Kibler, Phys. Rev. 152 (56) 932.
210. Gemeinhardt et al., Zeit, fur Physik 197 (66) 58.
211. Paul and Lieb, Nucl. Phys. 53 (64) 465.
212. Bruno et al., J. Physique C1 (66) 85.
213. Black et al., Phys. Lett. 30B (69) 100.
214. Elwyn et al., Phys. Rev. C16 (77) 1744.
215. Risler et al., Nucl. Phys. A286 (77) 115.
216. Schier, et al., Nucl. Phys. 88 (66) 373.
217. McClenahan and Segal, Phys. Rev. C11 (75) 370.
218. Ruby et al., Nucl. Sci. Eng. 71 (79) 280.
219. Baggett et al., Phys. Rev. 85 (52).
220. Slattery et al., Phys. Rev. 108 (57) 809.
221. Bertrand et al., Saclay Report CEA-R-3428.
222. Whaling et al., Phys. Rev. 75 (49) 688.
223. Sawyer and Phillips, LA-1578.
224. Hirst et al., Phil. Mag. 45 (54) 762.
225. Elwyn et al., Phys. Rev. C19 (79) 592.
226. Pepper et al., Phys. Rev. 85 (52) 155.
227. Serov, et al., Soviet J. At. En. 12 (62) 1.
228. Valter, et al., Soviet J. At. En. 10 (61) 574.
229. Abramovich et al., Izv. Akad. Nauk SSSR (Ser. Fiz) 37 (73) 1967.
230. Ciric et al., Fizika (Yugoslavia) 4 (72) 40 and 193.
231. Ludecke et al., Nucl. Phys. A109 (68) 676.
232. Holmgren, Nuclear Research with Low Energy Accelerators, p. 213.
233. Mazari er al., Proc. 2nd Int. Conf. on Nuclidic Masses (63).
234. Reimann et al., Phys. Rev. Lett. 18 (67) 246.
235. Baker et al., Nucl. Phys. A184 (72) 97.
236. Reinmann et al., Can. J. Phys. 46 (68) 2241.
237. Treado et al., Bull. Am. Phys. Soc. 16 (71) 1186.
238. Gagne et al., Bull. Am. Phys. Soc. 15 (70) 1695.
239. Vignon et al., J. Physique 30 (69) 913.
240. Tompson and Tripard, Phys. Rev. C5)72) 1174.

241. Livesev and Piluso, Can. J. Phys. 52 (74) 1167.
242. Guichard et al., Nature 272, No. 5649 (78) 155.
243. Ref. 231 and Ref. 217
244. McClenahan, Thesis, Northweatern U. (74).
245. Gould and Boyce, Nucl. Sci. and Eng. 60 (76) 477.
246. Dearnaley et al., Nucl. Phys. 36 (62) 71.
247. Barnes et al., Bull. Am. Phys. Soc. 7 (62) 111.
248. Singh and Gemmell, Bull. Am. Phys. Soc. 10 (65) 538.
249. Meyer et al., Nucl. Phys. A101 (67) 114.
250. Balakrishnan et al., Nuovo Cim 1A (71) 205.
251. Warren et al., Phys. Rev. 91 (53) 917.
252. Malmberg, Phys. Rev. 101 (56) 114.
253. Kinsey and Stone, Phys. Rev. 103 (56) 972.
254. Gogny and Jean, Compt. Rend. 260 (65) 510.
255. Heydrenburg et al., Phys. Rev. 74 (48) 405.
256. Conrad et al., Nature 45 (58) 204.
257. Carallaro et al., Nucl. Phys. 36 (62) 597.
258. Maxson, Phys. Rev. 128 (62) 1321.
259. Miller et al., Nucl. Phys. 54 (64) 155.
260. Madsen and Vedelsby, Nucl. Phys. 55 (64) 477.
261. Johnson et al., Phys. Rev. 77 (51) 413.
262. Taschek and Hemmendinger, Phys. Rev. 74 (48) 373.
263. Willard and Perston, Phys. Rev. 81 (51) 480.
264. Cranberg, LA-1654 (54).
265. Batchelor, Proc. Phys. Soc. A68 (55) 452.
266. Batchelor and Morrison, Proc. Phys. Soc. A68 (55) 1081.
267. Marion et al., Phys. Rev. 100 (55) 91.
268. Macklin and Gibbons, Phys. Rev. 109 (58) 105.
269. Newson et al., Phys. Rev. 108 (57) 1294.
270. Jarmie and Seagrave, LA-2014 (56).
271. Bogdanov et al., Soviet J. At. En. 3 (59) 907.
272. Gibbons and Macklin, Phys. Rev. 114 (59) 571.
273. Hisatake et al., J. Phys. Soc. Japan 15 (60) 741.'
274. Bevington et al., Phys. Rev. 121 (61) 871.
275. Nilsson, Ark. Fys. 19 (61) 289.
276. Borchers and Poppe, Phys. Rev. 129 (63) 2679.
277. Bair et al., Nucl. Phys. 53 (64) 209.
278. Buccino et al., Nucl. Phys. 53 (64) 375.
279. Austin, Bull. Am. Phys. Soc. 7 (62) 269.
280. Bergstroem et al., Ark. Fys. 34 (67) 153.

281. Lefevre and Din, Austr. J. Phys. 22 (69) 669.
282. Peetermans, Thesis, U. of Liege.
283. Elbakr et al., Nucl. Inst. Meth. 105 (72) 519.
284. Meadows and Smith, ANL-7938 (72).
285. Presser and Bass, Nucl. Phys. A182 (72) 321.
286. Ford, Phys. Rev. 136 (64) B953.
287. Sellschop, Phys. Rev. 119 (60) 251.
288. Chase et al., Phys. Rev. 127 (62) 859.
289. Schilling et al., Nucl. Phys. A263 (76) 389.
290. Kavanagh, Nucl. Phys. 15 (60) 411.
291. Bagget et al., Phys. Rev. 85 (52) 434.
292. McClenahan et al., Phys. Rev. C11 (75) 370.
293. Parker, Phys. Rev. 150 (66) 851.
294. Bashkin, Phys. Rev. 95 (54) 1012.
295. Valkovic et al., Nucl. Phys. A96 (67) 241.
296. Garnir et al., Bull. Soc. R. Sci., Leige (Belgium) 42 (73) 195.
297. Crews, Phys. Rev. 82 (51) 100.
298. Serov et al., Soviet J. At. En. 12 (62) 1.
299. Valter et al., Soviet J. At. En. 10 (61) 574.
300. Arnold, In Proceeding, Cluster, Winnipeg (78) B8.
301. Valter et al., Soviet J. At. En. 10 (61) 577.
302. Seltz and Magnac-Valette, Compt. Rend. 251 (60) 2006.
303. Serov and Guzhovskii, Atomnaya Energiay 12 (62) 5.
304. Ciric et al., Fizika (Yugoslavia) 7, Suppl. 1 (77) 39.
305. Subbotic et al., Fizika (Yugoslavia) 9, Suppl. 1 (77) 44.
306. Fowler, Caughlan and Zimmerman, Ann. Rev. Astro. & Astrophys. 13 (75) 69.
307. Middlton and Pullen, Nucl. Phys. 51 (64) 50.
308. Hunchen et al., Nucl. Phys. 58 (64) 417.
309. Jelley et al., Phys. Rev. C11 (75) 2049.
310. Hardekopf, Bull. Am. Phys. Soc. 21 (76) 551.
311. Scheklinski et al., Nucl. Phys. A153 (70) 97.
312. Paul et al., Phys. Rev. 137 (65) B493.
313. Ling, et al., Nucl. Phys. A108 (68) 221.
314. Ling and Blatt, Nucl. Phys. A174 (71) 375.
315. Lin and Chin, J. Phys. (Taiwan) 10 (72) 76.
316. Cocke, Nucl. Phys. A110 (68) 321.
317. Din and Weil, Nucl. Phys. 86 (66) 509.
318. Dixon and Edge, Nucl. Phys. A156 (70) 33.
319. Dixon, Thesis, U. South Carolina (70).
320. Duggan et al., Nucl. Phys. 46 (63) 336.

321. Serov and Guzhovskii, Atomnaya Energiay 12 (62) 5.
322. Stanojevic et al., Fizika 3 (71) 99.
323. Sanada et al., J. Phys. Soc. Japan 26 (69) 853.
324. Wolicki and Meyer, Bull. Am. Phys. Soc. 6 (61) 415.
325. Orihara et al., Nucl. Phys. A139 (69) 226.
326. Cusson, Nucl. Phys. 86 (66) 481.
327. Bingham, Thesis, Florida State U. (70).
328. Bingham et al., Nucl. Phys. A175 (71) 374.
329. Bohler et al., Nucl. Phys. A179 (72) 504.
330. Kelleter et al., Nucl. Phys. A210 (73) 502.
331. Spear, Australian J. Phys. 12 (59) 99.
332. Kavanagh, Nucl. Phys. 18 (60) 492.
333. Mashkarov et al., Izv, Akad. Naul SSSR (Ser. Fiz.) 37 (73) 1729.
334. Kiss, et al., Nucl. Phys. A282 (77) 44.
335. Kild and Crinean, Australian J. Phys. 27 (74) 663.
336. Yasue et al., J. Phys. Soc. Japan 36 (74) 1254.
337. Dearnaley, Phil. Mag. 1 (56) 821.
338. Mozer, Phys. Rev. 104 (56) 1386.
339. Mo and Hornyak, Phys. Rev. 187 (69) 1220.
340. Rohrer and Brown, Nucl. Phys. A210 (73) 465.
341. Bertrand et al., Comm. A L'energie Atomique, RPT. CEA 3575 (68).
342. Montague et al., Nucl. Phys. a199 (73) 457.
343. Sierk and Tombrello, Nucl. Phys. A210 (73) 341.
344. Tu and Hornyak, Bull. Am. Phys. Soc. 14 (69) 489.
345. Votava, Thesis, U. North Carolina (72).
346. Djaloeis et al., Nucl. Phys. 15 (72) 266.
347. Powell et al., Nucl. Phys. A147 (70) 65.
348. Lombard and Friedland, Z. Phys. 249 (72) 349.
349. Machali et al., Nucl. Phys. A112 (68) 654.
350. Renken, Phys. Rev. 132 (63) 2627.
351. Ralph and Dunnam, Phys. Rev. 120 (60) 249A.
352. Bardes and Owen, Phys. Rev. 120 (60) 1369.
353. Evans et al., Phys. Rev. 75 (49) 1161.
354. Kotlay, Acta. Phys. Acad. Sci. Hung. 16 (63) 93.
355. Siemssen et al., Nucl. Phys. 69 (65) 209.
356. Canavan, Phys. Rev. 87 (52) 136.
357. Biggerstaff et al., Nucl. Phys. 36 (62) 631.
358. De Jong et al., Physica 18 (52) 676.
359. Dolinov and Melikov, Vest. Mosk. Univ. Fiz. Astron., P116 (66).
360. Ambrossino et al., J. Physique C1 (66) 62.

361. Farouk et al., Z. F. Phys. 201 (67) 52.
362. Huric, Phys. Rev. 98 (55) 85.
363. McCrary et al., Phys. Rev. 108 (57) 392.
364. Read and Calvert, Proc. Phys. Soc. 77 (61) 65.
365. Read et al., Nucl. Phys. 23 (61) 386.
366. Bondouk et al., Ann. Der. Phys. 32 (75) 255.
367. Friedland et al., Z. Phys. 267 (74) 97.
368. Sledzinska et al., Acta. Phys. Polonica 88 (77) 277.
369. Tanaka, J. Phys. Soc. Japan 44 (78) 1405.
370. Zwieglinski et al., Nucl. Phys. A250 (75) 93.
371. Cohen and Herling, Nucl. Phys. A141 (70) 595.
372. Nam and Osetinskii, Soviet J. Nucl. Phys. 9 (69) 279.
373. Earwaker, Nucl. Phys. A90 (67) 56.
374. Bondouk et al., Rev. Roumaine Phys. 19 (74) 653.
375. McEver et al., Nucl. Phys. A178 (72) 529.
376. Taylor et al., Nucl. Phys. 15 (72) 31.
377. Artemov et al., Yadernaya Fiz. 1 (65) 1019.
378. Dorenbusch and Browne, Phys. Rev. 131 (63) 1212.
379. Ehlers, Thesis, Washington State U. (70).
380. Moazed and Holmgren, Phys. Rev. 166 (68) 977.
381. Goss, Thesis, Ohio State U. (70).
382. Goss et al., Phys. Rev. C7 (73) 1837.
383. Taylor et al., Nucl. Phys. 65 (65) 318.
384. Saleh, et al., Ann. Der Physik 31 (74) 76.
385. Overley, Thesis, Caltech (60).
386. Overley and Wahling, Phys. Rev. 128 (62) 315.
387. Boerli et al., Fizika (Yugolsavia) 2 (70) 19.
388. Jenkin et al., Nucl. Phys. 50 (64) 516.
389. Segel et al., Phys. Rev. 145 (66) 736.
390. Szabo et al., Nucl. Phys. A195 (72) 527.
391. Stocker and Browne, Phys. Rev. C9 (74) 102.
392. Lombaard, et al., Z. Phys. 219 (69) 124.
393. Busch et al., Nucl. Phys. A223 (74) 183.
394. Comsan et al., Atomkernergie 13 (68) 415.
395. Assimakopoulos and Gangas, Nucl. Phys. A108 (68) 497.
396. Black et al., Phys. Rev. Lett. 25 (70) 877.
397. Friedland and Berleger, Z. Phys. 211 (68) 373.
398. Rendic et al., Bull. Am. Phys. Soc. 16 (71) 1153.
399. Roy et al., Nuovo Cim. 6 (73) 374.
400. Becker, Phys. Rev. 119 (60) 1076.

401. Breuer, A. Phys. 178 (64) 268.
402. Marion and Weber, Phys. Rev. 103 (56) 1408.
403. Longequeue et al., Compt. Tend. 264 A/B (67) 1032.
404. Legge, Nucl. Phys. 26 (61) 608.
405. Purser and Wildenthal, Nucl. Phys. 44 (63) 22.
406. Paris et al., Physica 20 (54) 573.
407. Poore et al., Nucl. Phys. A92 (67) 97.
408. Burke et al., Phys. Rev. 93 (54) 188.
409. Croissiaux, Ann.der Phys. 5 (60) 409.
410. Endt, et al., Physica 18 (52) 423.
411. Harrison et al., Phys. Rev. 117 (60) 532.
412. Lee and Siemssen, Bull. Am. Phys. Soc. 10 (65) 510.
413. Ahmad et al., 4th AINSE Nucl. Phys. Conf., Sydney (72) p.76.
414. Arena et al., Lett. Nuovo Cim. 5 (72) 879.
415. Black et al., Phys. Rev. Lett. 25 (70) 877.
416. Holmgren et al., Nucl. Phys. 48 (63) 1.
417. Gerardin et al., Nucl. Phys. A169 (71) 521.
418. Herling et al., Phys. Rev. 178 (69) 1551.
419. Duggan et al., Nucl. Phys. A151 (70) 107.
420. Buffa and Brussel, Nucl. Phys. A195 (72) 545.
421. Nusslin and Braun-Munzinger, Z. Phys. 240 (70) 217.
422. Patterson et al., Proc. Phys. Soc. 90 (67) 577.
423. Squier et al., Nucl. Phys. A119 (68) 369.
424. Bell et al., Nucl. Phys. A179 (72) 408.
425. Kuan et al., Nucl. Phys. 60 (64) 509.
426. Bell et al., Nucl. Phys. A193 (72) 385.
427. Patterson et al., Proc. Phys. Soc. 85 (65) 1085.
428. Schiffer et al., Phys. Rev. 104 (56) 1064.
429. Patterson et al., Proc. Phys. Soc. 88 (66) 641.
430. Singh, Nucl. Phys. A155 (70) 453.
431. Gallmann et al., Nucl. Phys. A123 (69) 27.
432. David et al., Nucl. Phys. A182 (72) 234.
433. Mo and Weller, Phys. Rev. C8 (73) 972.
434. Davidson et al., Caltech Report LAP-165 (78).
435. Weaver et al., UCRL-74938 (73).
436. Anderson et al., Nucl. Phys. A223 (74) 286.
437. Fowler et al., Ann. Rev. Astron. Astrophys. 5 (67) 525.
438. Segel et al., Phys. Rev. B139 (65) 818.
439. Symons et al., Nucl. Phys. 46 (63) 93.
440. Dehnhard, Rev. Mod. Phys. 37 (65) 450.

441. Chase et al., Phys. Rev. 166 (68) 997.
442. Williams et al., Phys. Rev. 144 (66) 801.
443. Olness and Warburton, Phys. Rev. 166 (68) 1004.
444. Buechner et al., Phys. Rev. 79 (50) 262.
445. Elkin, Phys. Rev. 92 (53) 127.
446. Fortune and Vincent, Phys. Rev. 185 (69) 1401.
447. Friendland and Verleger, Z. Phys. 222 (69) 138.
448. Briuer, Z. Phys. 178 (64) 268.
449. Kavanagh and Barnes, Phys. Rev. 112 (58) 503.
450. Weller and Blue, Nucl. Phys. A211 (73) 221.
451. Din et al., Nucl. Phys. A93 (67) 190.
452. Almond and Risser, Nucl. Phys. 72 (65) 436.
453. Thornton et al., Nucl. Phys. A198 (72) 397.
454. Silverstein and Herling, Phys. Rev. 181 (69) 1512.
455. Ciric et al., Fizika (Yugoslavia) 9, Suppl. 1 (77) 39.
456. Black et al., Nucl. Phys. A153 (70) 233.
457. Holmgren et al., Phys. Rev. 114 (59) 1281.
458. Hahn and Ricci, Nucl. Phys. A101 (67) 353.
459. Mante et al., Paper 8B6, Asilomar (73).
460. Brill, Soviet J. Nucl. Phys. 1 (65) 37.
461. Liskien and Paulsen, Report EANDC (E) -143 "L" (72).
462. Liskien and Paulsen, Report EANDC (E) - 152 "L" (72).
463. Liskien and Paulsen, Report EANDC (E) - 144 "L" (72).
464. G. M. Hale and D. C. Dodder, "R-Matrix Analysis of Light Element Reactions for Fusion Applications", Presented at the International Conference on Nuclear Cross Sections for Technology, Knoxville, TN, Oct. 79.
465. A. Elwyn et al., Private communication.
466. Imai et al., Nucl. Phys. 246 (75) 76.
467. Rourina, Phys. Rev. 81 (51) 593.
468. Mather, Phys. Rev. 82 (51) 133.
469. Allred et al., Phys. Rev. 88 (52) 433.
470. Worthington et al., Phys. Rev. 90 (53) 899.
471. Yntema and White, Phys. Rev. 95 (54) 1226.
472. Zimmerman et al., Phys. Rev. 96 (54) 1322.
473. Herb et al., Phys. Rev. 55 (39) 998.
474. Cork and Hartsough, UCRL-2373 (53).
475. Faris and Wright, Phys. Rev. 79 (50) 577.
476. Wilson et al.,Phys. Rev. 72 (47) 1131.
477. Kikuchi et al., J. Phys. Soc. Japan 15 (60) 9.
478. Knecht et al., Phys. Rev. 148 (66) 1031.
479. Jarmie et al., Phys. Rev. C3 (71) 10.
480. Johnston and Young, Phys. Rev. 116 (59) 989.

481. Sloeodrian et al., Phys. Rev. 174 (68) 1122.
482. Wassmer and Muhry, Helv. Phys. Acta 46 (73) 626.
483. Putnam, Phys. Rev. 87 (52) 932.
484. Kreger et al., Phys. Rev. 93 (54) 837.
485. Williams and Rasmussen, Phys. Rev. 98 (55) 56.
486. Freier et al., Phys. Rev. 75 (49) 1345.
487. Mcdonald et al., Phys. Rev. 133 (64) B1178.
488. Garreta et al., Nucl. Phys. 132 (69) 204.
489. Brockman, Phys. Rev. 102 (56) 391.
490. Brockman, Phys. Rev. 108 (57) 1000.
491. Bacher et al., Phys. Rev. C5 (72) 1147.
492. Sanada, J. Phys. Soc. Japan 14 (59) 1463.
493 Phillips, Phys. Rev. 112 (58) 2043.
494. Dodder et al., Phys. Rev. C15 (77) 518.
495. Kraus and Linck, Nucl. Phys. 224 (74) 45.
496. Chien and Brown, Phys. Rev. C10 (74) 1767.
497. Briggs et al., Phys. Rev. 91 (53) 438.
498. Steigest and Sampson, Phys. Rev. 92 (53) 660.
499. Lauritsen et al., Phys. Rev. 92 (53) 1501.
500. Phillips et al., Phys. Rev. 100 (55) 960.

CHAPTER III

FUSION REACTION KINETICS

CHAPTER III

FUSION REACTION KINETICS

III-1. Kinetic Equations for a Fusion Reacting Plasma

The time dependent velocity distribution function of a species k in a volume element dV of a fusion reacting plasma can be described by a set of coupled Boltzmann equations, which can be denoted as follows:

$$\frac{\partial f_k(v_1)}{\partial t} + \vec{v}_1 \cdot \nabla_r f_k(v_1) + \frac{\vec{F}}{m_k} \cdot \nabla_v f_k(v_1) \equiv \sum_{\ell} \left(\frac{\partial f_k(v_1)}{\partial t}\right)_{\ell}$$

$\equiv$ Production rate of particle k of velocity v_1 by various fusion reaction channels.

$-$ Consumption rate due to various fusion reactions which involve particle k of velocity v_1.

$+$ Particle k of different velocity v_k suffering a scattering collision (radiation, Coulomb, nuclear elastic, nuclear inelastic and interferences) in dV that changes v_k into v_1 of interest.

$-$ Particle k with velocity v_1 in dV suffering a collision.

$$= \sum_{i,j,\ell} \iint f_i(v_i)\, f_j(v_j)\, u_{ij}\, \sigma^{\ell}_{kij}(u_{ij};\, v_1)\, d^3v_i\, d^3v_j$$

$$- \sum_{i,\ell} \int f_k(v_1)\, f_i(v_i)\, u_{1i}\, \sigma^{\ell}_{ik}(u_{1i})\, d^3v_i$$

$$+ \sum_{i} \iint f_k(v_k)\, f_i(v_i)\, u_{ik}\, \sigma_{ik}(u_{ik};\, v_1)\, d^3v_i\, d^3v_k$$

$$- \sum_{i} \int f_k(v_1)\, f_i(v_i)\, u_{1i}\, \sigma_{ik}(u_{1i})\, d^3v_i \qquad \text{(III-1)}$$

,where

$$u_{ij} = |\, \vec{v}_i - \vec{v}_j \,| \qquad \text{(III-2)}$$

$$u_{1i} = |\, \vec{v}_1 - \vec{v}_i \,| \qquad \text{(III-3)}$$

$\sigma^{\ell}_{kij}(u_{ij};\, v_1) \equiv$ Reaction cross section of particles i and j with relative velocity u_{ij} react via reaction channel ℓ to produce particle k of velocity v_1.

$\sigma^{\ell}_{ik}(u_{1i}) \equiv$ Reaction cross section of particle k and i with relative velocity u_{1i} react via reaction channel ℓ.

$\sigma_{ik}(u_{ik};\, v_1) \equiv$ Scattering (radiation, Coulomb, Nuclear elastic, nuclear inelastic and interferences) cross section of particle i and k with relative velocity u_{ik} which changes v_k into v_1 of interest.

$\sigma_{ik}(u_{1i}) \equiv$ Scattering cross section of particle k of velocity v_1 and particle i of velocity v_i.

$f_i(v_m) \equiv$ Value of distribution function of particle i of velocity v_m.

The indexes i, j and k represent species in the plasma, such as electrons, p, d, t, ^3He, α, ^6Li, ^7Li, ^7Be, ^9Be, ^{10}B, ^{11}B, ^{11}C, ^{12}C and neutron. There are many reaction channels that are of interest.

III-2. Simplified Model Used in This Analysis

The proper determination of the potential of an advanced fuel cycle requires a study of fusion reaction kinetics, including subtle effects like fast fusion, nuclear elastic and inelastic scattering, Doppler broadening of the energy distribution of reaction products, radiations and the partition of slowing down energy between ions and electrons. The description of all of these aspects of fusion reaction kinetics requires many coupled, non-linear, time dependent, differential-integral Boltzmann equations. Analytic solutions of these equations can only be obtained for specialized and greatly simplified situations. To follow the time evolution of the distribution function requires numerical solution of these equations using large high speed computers, and the computing cost could be prohibitively expensive. However, a linear approximation, the multigroup energy technique, will provide an inexpensive solution for the reaction kinetics study.(1) It is assumed that the velocity distribution function is made up of a

Maxwellian bulk with a small tail of energetic particles and can be expressed as:

$$f_\ell(v,t) = f_\ell^M(v,t) + f_\ell^*(v,t) \qquad \text{(III-4)}$$

where f_ℓ, f_ℓ^M and f_ℓ^* refer to the distribution function, the Maxwellian distribution function and the distribution function representing the tail of energetic particles. The discrete nature of large energy transfer events such as nuclear elastic scattering, large angle coulomb scattering, nuclear inelastic scattering and fast fusion reaction can also be fit into this scheme conveniently.

III-3. Slowing Down Theory

A typical fusion plasma temperature is in the tens to hundreds of keV range, while the reaction products are in the MeV to tens of MeV range. To treat the relaxation of the reaction products, the rate of energy loss of a charged particle by coulomb scattering has been calculated numerous times with varying degrees of sophistication.[2-5] It is necessary to take into account, for light elements, the nuclear-force contribution to scattering. This has also been noted by Devanly and Stein.[6] However, these previous studies[2-8] assumed that charged particle slowing down can be described by a continuous theory. This approximation is valid only if the particle energy transfer per collision is small. However, nuclear elastic scattering, large angle coulomb scattering, nuclear inelastic scattering and fast fusion reactions will transfer large amounts of energy which cannot be properly described by the continuous slowing down theory. A better treatment of the process[1] is to use a continuous theory for the small energy transfer range and a discrete theory for the large energy transfer range.

The small energy transfer collisions due to coulomb scattering are typically several orders of magnitude larger than other nuclear reaction cross sections at small angle. However, in some cases, nuclear-coulomb interference could be on the same order. It is assumed that coulomb scattering and nuclear-coulomb interference are the only sources of small energy transfer collisions. With adjustments which will be described later, coulomb scattering interactions can properly describe the slowing down time based on small energy transfer collisions.

The average instantaneous rate of coulomb energy loss for a particle, k, slowing down in a plasma consisting of several kinds of particles j, can be expressed by the following two equations:[3,7]

$$-\left(\frac{\delta E_k}{\delta t}\right)_e^c = \left(\frac{4\pi e^4}{m_e}\right)\left(\frac{Z_k^2}{v_k}\right) n_i \, L_e \, F\left(\frac{v_k}{u_e}\right) \bar{Z} \qquad \text{(III-5)}$$

$$-\left(\frac{\delta E_k}{\delta t}\right)_i^c = \left(\frac{4\pi e^4}{m_e}\right)\left(\frac{Z_k^2}{v_k}\right) n_i \sum_\ell \frac{Z_\ell^2 \, \beta_\ell \, L_\ell \, F(v_k/u_\ell)}{m_\ell / m_e} \qquad \text{(III-6)}$$

where the superscript c refers to coulomb scattering and the subscripts e, k and ℓ refer to electron, particle k and ion species ℓ. Further, Z refers to charge number, m to mass of the species, n_i to total ion density, β to the atomic fraction of ions in the plasma and u to the speed of the thermal particle. The subscript j refers to either electron or ions and $x_j \equiv v_k/u_j$.

$$F(x_j) \equiv \mathrm{erf}(x_j) - (1 - m_j/m_k)\ x_j\ e^{-x_j^2} \qquad \text{(III-7)}$$

The coulomb logarithm, L_j, is written as

$$L_j = \frac{1}{2}\ \ell n(1 + \Lambda_j^2)\quad , \qquad \text{(III-8)}$$

where the arguments are given by the following ratio:

$$\Lambda_j = \ell_D/b_{oj} \qquad \text{classical} \qquad \text{(III-9)}$$

$$= \ell_D/\lambda_j \qquad \text{quantum} \qquad \text{(III-10)}$$

with ℓ_D, b_{oj} and λ_j being the total Debye shielding length, the cutoff impact parameter and the center of mass wavelength in two body scattering, respectively.

By adjusting the cutoff impact parameter b_{oj} so that only small energy transfer collisions can occur and by adding a weighting factor to take the nuclear-coulomb interference contribution into account, the continuous slowing down theory can be described by:

$$-\left(\frac{\delta E_k}{\delta t}\right)_e^S = \left(\frac{4\pi e^4}{m_e}\right)\left(\frac{Z_k}{v_k}\right) n_i\ L_e\ F(v_k/u_e)\ \bar{Z} \qquad \text{(III-11)}$$

$$-\left(\frac{\delta E_k}{\delta t}\right)_i^S = \left(\frac{4\pi e^4}{m_e}\right)\left(\frac{Z_k}{v_k}\right) n_i \quad \sum_\ell \frac{Z_\ell^2\ \beta_\ell\ L_\ell^*\ W_\ell F(v_k/u_\ell)}{m_\ell/\ m_e} \qquad \text{(III-12)}$$

where the superscript S refers to small energy transfer scattering, L_ℓ^* is the adjusted value of L_ℓ (called small energy transfer logarithm), and W refers to the weighting factor which takes the nuclear-coulomb interference contribution into account. Define

$$L_\ell^* = L_\ell \cdot \ell n \left(\frac{1-\cos\theta_c}{1-\cos\theta_b}\right) / \ell n\left(\frac{1-\cos\theta_b}{1-\cos\theta_d}\right) \tag{III-13}$$

$$W_\ell = \int_{\cos\theta_d}^{\cos\theta_c} \frac{d\sigma^S}{d\Omega}\, d\cos\theta \Big/ \int_{\cos\theta_d}^{\cos\theta_c} \frac{d\sigma^C}{d\Omega}\, d\cos\theta \tag{III-14}$$

where θ_d refers to the deflection angle (in C.M. system) corresponding to an impact parameter of ℓ_D, θ_b is the cutoff angle for traditional coulomb scattering, and θ_c is the deflection angle for maximum energy transfer in the small energy transfer range.

Summing the two contributions, i.e., Eqs. (III-11) and (III-12), and making the substitutions $E_k = \frac{1}{2} m_k v_k^2$, $ds = v_k\, dt$, the energy loss becomes related to the path length by:

$$- n_i\, ds = dv_k \{G(v_k,t)\}^{-1} \tag{III-15}$$

where:

$$G(v_k) = \left(\frac{4\pi e^4}{m_e}\right)\left(\frac{Z_k}{m_k v_k^3}\right) \left\{L_e\, F(v_k/u_e)\bar{Z} + \sum_\ell \frac{Z_\ell^2 \beta_\ell L_\ell^* W_\ell F(v_k/u_\ell)}{m_\ell / m_e}\right\} \tag{III-16}$$

Since the composition and the temperature may change with time, e.g., reactions are taking place in the plasma, the function G is time-dependent and denoted as G(v,t).

III-4. Reactions While Slowing Down

If a slowing down particle k can react with a background particle ℓ, with a cross section $\sigma^R_{k\ell}$, then the instantaneous probability per unit length that the reaction will take place during the slowing down process is given by:

$$\frac{dP^{*R}_{k\ell}(v_k,t)}{ds} = \frac{1}{v_k} \int d\vec{v}\ \sigma^R_{k\ell}(|\vec{v}_k-\vec{v}|)\ |\vec{v}_k-\vec{v}|\ f_\ell(v,t) \qquad \text{(III-17)}$$

where $f_\ell(v,t)$ is the distribution function of particle ℓ and the superscript (*) denotes an instantaneous quantity. The instantaneous reaction probability of a particle k about its velocity v_k can be expressed as

$$P^{*R}_{k\ell}(v_k,t)\ dv_k = \int d\vec{v}\ \frac{f_\ell(v,t)\ \sigma_{k\ell}(|\vec{v}_k-\vec{v}|)\ |\vec{v}_k-\vec{v}|}{v_k\ n_i\ G(v_k,t)}\ dv_k \qquad \text{(III-18)}$$

The integration over the slowing down path can be converted to an integration from the initial velocity v_k to the final velocity u_k, yielding:

$$P^R_{k\ell}(v_k \rightarrow u_k,t) = \int_{u_k}^{v_k} d\vec{V} \int d\vec{v}\ \frac{f_\ell(v,t)\ \sigma^R_{k\ell}(|\vec{V}-\vec{v}|)|\vec{V}-\vec{v}|}{V\ n_i\ G(V,t)} \qquad \text{(III-19)}$$

Since the particle k can react with one or more ions or react through several channels the total reaction probability is given as a sum over all reactions and channels. The instantaneous probability then becomes:

$$P^{*R}_{kT}(v_k,t)\,dv_k = \left\{ \sum_{\ell} \int d\vec{V}\, \frac{f_\ell(v,t)\{\Sigma_n \sigma^{Rn}_{k\ell}(|\vec{V}-\vec{v}|)\}\,|\vec{V}-\vec{v}|}{v_k\, n_i\, G(v_k,t)} \right\} dv_k \qquad \text{(III-20)}$$

and

$$P^{R}_{kT}(v_k \rightarrow u_k,t) = \sum_{\ell} \int_{u_k}^{v_k} d\vec{V} \int d\vec{v}\, \frac{f_\ell(v,t)\{\Sigma_n \sigma^{Rn}_{k\ell}(|\vec{V}-\vec{v}|)\}\,|\vec{V}-\vec{v}|}{V\, n_i\, G(V,t)} \qquad \text{(III-21)}$$

III-5. The Reactivity of a Propagating Reaction

The reactivity can be enhanced by the propagating effect[1,10,11] in the cycles such as p-^{6}Li. The p-^{6}Li cycle is particularly useful to demonstrate the procedure to derive the power density formula for a propagating reaction cycle.

In order to show the procedures for which the power density formula of a fully propagating reaction cycle is obtained, an overly simplified case is to consider the reactions

$$p + {}^6\text{Li} \rightarrow {}^3\bar{\bar{\text{He}}} + \alpha \qquad \text{(III-22)}$$

$$^3\text{He} + {}^6\text{Li} \rightarrow \bar{\bar{p}} + 2\alpha \qquad \text{(III-23)}$$

The Maxwellian fusion reaction rates in this case are

$$a_{16} = n_1 n_6 \langle\sigma v\rangle_{16} \qquad \text{(III-24)}$$

$$a_{36} = n_3 n_6 \langle\sigma v\rangle_{36} \qquad \text{(III-25)}$$

where n_1, n_3 and n_6 are the densities of protons, ^{3}He, and ^{6}Li respectively, and $\langle\sigma v\rangle$'s are the reaction rate parameters. Let $\bar{\bar{\Gamma}}_{36}$, $\bar{\bar{\Gamma}}_{16}$ be the probabilities that fast ^{3}He and fast protons produced by reactions (III-22) and (III-23) will fuse with ^{6}Li prior to slowing down. Then the total production rate of ^{3}He is

$$P_3 = \frac{a_{16} + a_{36}\,\bar{\bar{\Gamma}}_{16}}{1 - \bar{\bar{\Gamma}}_{36}\bar{\bar{\Gamma}}_{16}} \qquad \text{(III-26)}$$

The power output in this branch is P_3Q_{16}. The consumption rate of ^{3}He is

$$C_3 = \frac{a_{36} + a_{16}\bar{\bar{\Gamma}}_{36}}{1 - \bar{\bar{\Gamma}}_{36}\bar{\bar{\Gamma}}_{16}} \qquad \text{(III-27)}$$

The power output in this branch is C_3Q_{36}, where Q_{16} and Q_{36} are the nuclear reaction Q values for reactions (III-22) and (III-23)

The equilibrium ^{3}He content is found by setting $P_3 = C_3$ and gives

$$n_3 = n_1\frac{\langle\sigma v\rangle_{16}}{\langle\sigma v\rangle_{36}}\,\frac{(1-\bar{\bar{\Gamma}}_{36})}{(1-\bar{\bar{\Gamma}}_{16})} \qquad \text{(III-28)}$$

By substituting n_3 into the sum of the power output of the two branches, one has the total fusion power density:

$$P_F = a_{16}\,\frac{(Q_{16}+Q_{36})}{1 - \bar{\bar{\Gamma}}_{16}} \qquad \text{(III-29)}$$

The fusion power density formula in this case is composed of two parts. The numerator is the power density formula of the conventional catalyzed p-^{6}Li cycle. The denominator expresses the propagating effect.

The power density formula for the more general case with reactions

$$
\begin{aligned}
&p + {}^{6}Li \rightarrow {}^{3}\bar{\bar{He}}\ (2.3\ \text{MeV}) + \alpha \\
&{}^{3}He + {}^{6}Li \rightarrow \bar{\bar{p}}\ (11.2\ \text{MeV}) + 2\alpha \\
&d + {}^{3}He \rightarrow \bar{\bar{\bar{p}}}\ (14.6\ \text{MeV}) + \alpha \\
&d + d \rightarrow n + {}^{3}\bar{He}\ (.9\ \text{MeV}) \\
&d + d \rightarrow \bar{p}\ (3\ \text{MeV}) + t \\
&{}^{3}He + {}^{3}He \rightarrow 2\bar{p}\ (3.1\ \text{MeV}) + \alpha
\end{aligned}
\qquad \text{(III-30)}
$$

is complicated. To distinguish fast protons, we have used different numbers of overbars as in eqn. (III-30). The following notation is used in the power density formula to follow. The probability of fast particles, $\bar{a}$, $\bar{\bar{a}}$, etc. reacting with a thermal particle b is expressed as $\bar{\Gamma}_{ab}$, $\bar{\bar{\Gamma}}_{ab}$, etc. respectively. The Maxwellian reaction rate is expressed as $a_{\ell bc}$, where ℓ denotes the branch the reaction takes. $Q_{\ell bc}$ is the reaction Q value. The fusion power density is

$$
P_F = \frac{a_{16} + a_{T22}\bar{\Gamma}_{16} + 2(a_{33}+a_{322}\bar{\bar{\Gamma}}_{33})\bar{\Gamma}_{16} + (a_{36}+a_{322}\bar{\bar{\Gamma}}_{36})\bar{\bar{\bar{\Gamma}}}_{16} + a_{23}\bar{\bar{\Gamma}}_{16}}{1 - (\bar{\Gamma}_{33}\bar{\Gamma}_{16}+\bar{\Gamma}_{36}\bar{\bar{\Gamma}}_{16}+\bar{\Gamma}_{32}\bar{\bar{\bar{\Gamma}}}_{16})} Q_{16}
$$

$$
+ \frac{a_{36} + a_{16}\bar{\Gamma}_{36} + a_{322}\bar{\bar{\Gamma}}_{36}}{1-(\bar{\Gamma}_{33}\bar{\Gamma}_{16}+\bar{\Gamma}_{36}\bar{\bar{\Gamma}}_{16}+\bar{\Gamma}_{32}\bar{\bar{\bar{\Gamma}}}_{16})} Q_{36} + \frac{a_{33} + a_{16}\bar{\Gamma}_{33} + a_{322}\bar{\bar{\Gamma}}_{33}}{1-(\bar{\Gamma}_{33}\bar{\Gamma}_{16}+\bar{\Gamma}_{36}\bar{\bar{\Gamma}}_{16}+\bar{\Gamma}_{32}\bar{\bar{\bar{\Gamma}}}_{16})} Q_{33}
$$

$$
+ \frac{a_{23} + a_{16}\bar{\Gamma}_{32} + a_{322}\bar{\bar{\Gamma}}_{32}}{1-(\bar{\Gamma}_{33}\bar{\Gamma}_{16}+\bar{\Gamma}_{36}\bar{\bar{\Gamma}}_{16}+\bar{\Gamma}_{32}\bar{\bar{\bar{\Gamma}}}_{16})} Q_{23} + a_{322}Q_{322} + a_{T22}Q_{T22}. \qquad \text{(III-31)}
$$

The density of ^{3}He and of D, as well as the fast fusion probabilities, must be calculated in a self-consistent way.

The power density formula for the actual p-^{6}Li cycle is much more complicated. The numerical calculations for the equilibrium content of the various species, the fast fusion reactivities, and the electron temperature T_e are cumbersome. A detailed description of the problems involved and the method developed is expressed in Chapter IV.

III-6. Doppler Broadening and Energy Distribution of Products from Nuclear Reactions

The spread in energy of the fusion reaction products results from the spread in energy of the colliding particles in the center of mass frame and the motion of the center of mass of the colliding ion pair.[1] Let the velocity relative to the laboratory frame of two species be $\vec{V}_1$ and $\vec{V}_2$. The total momentum $\vec{P}$ in the laboratory frame is

$$P = m_1\vec{V}_1 + m_2\vec{V}_2 = (m_1 + m_2)\vec{V}_c = (m_3 + m_4)\vec{V}_c \qquad \text{(III-32)}$$

where species 3 and 4 are products of the reaction. $\vec{V}_c$ is the velocity of the center of mass of the reacting pair. Any radiation given off during the collision or during the compound nucleus state is neglected for the time being.

The energy of the daughter particles (species 3 and 4) in the center of mass frame are related to the energy of initial particles by:

$$E_3^c + E_4^c = E_1^c + E_2^c + Q \equiv E^c + Q = \frac{1}{2}\frac{m_1 m_2}{m_1+m_2}(\vec{V} - \vec{V}_2)^2 + Q \qquad \text{(III-33)}$$

where E_j^c is kinetic energy of particle j in the center of mass and Q is the reaction energy. The energies of the fusion products in the center of mass frame are related by the requirement that:

$$P_3^c + P_4^c = 0 = m_3\vec{U}_3 + m_4\vec{U}_4 \qquad \text{(III-34)}$$

$$E_3^c = \frac{1}{2} m_3 U_3^2 = \frac{1}{2} m_3 (- \frac{m_4}{m_3} \vec{U}_4)^2 \qquad \text{(III-35)}$$

$$= \frac{m_4}{m_3} E_4^c \qquad \text{(III-35)}$$

Hence the center of mass energy equation gives

$$E_3^c + E_4^c = (1 + \frac{m_3}{m_4}) E_3^c = E^c + Q \qquad \text{(III-36)}$$

or

$$E_3^c = \frac{m_4}{m_3+m_4} (E^c + Q) \qquad \text{(III-37)}$$

Since the energy of particle 3 in the center of mass frame is

$$E_3 = \frac{1}{2} m_3 U_3^2 = \frac{m_4}{m_3+m_4} (E_c + Q) \qquad \text{(III-38)}$$

one has

$$U_3 = \{\frac{2}{m_3} \cdot \frac{m_4}{m_3+m_4} (E^c + Q)\}^{1/2} \qquad \text{(III-39)}$$

Hence, the energy of particle 3 in the laboratory frame will be

$$E_3 = \frac{1}{2} m_3 V_3^2 = \frac{1}{2} m_3 (\vec{V}_c + \vec{U}_3)^2$$

$$= \frac{1}{2} m_3 (U_3^2 + V_c^2 + 2V_c U_3 \cos\theta) \ldots \qquad \text{(III-40)}$$

where θ is the angle between $\vec{V}_c$ and $\vec{U}_3$.

The angular distribution of a reaction in the energy range of interest could be isotropic in the center of mass frame (such as for the D-T reaction), or anisotropic (such as for the p-^{6}Li reaction. See Fig. III-1).

We can rewrite equation (III-40) in terms of the initial state and the final emission angle θ as

$$\begin{aligned} E_3 &= \frac{1}{2} m_3(U_3^2 + V_c^2 + 2V_cU_3\cos\theta) \\ &= \frac{1}{2} m_3U_3 + \frac{1}{2} m_3\left(\frac{m_1\vec{V}_1 + m_2\vec{V}_2}{m_1 + m_2}\right)^2 + m_3\left|\frac{m_1\vec{V}_1 + m_2\vec{V}_2}{m_1 + m_2}\right| U_3\cos\theta \\ &= \frac{m_4}{m_3+m_4} (E^C+Q) + \frac{m_3}{(m_1+m_2)^2} \{m_1E_1 + m_2E_2 + 2(m_1m_2E_1E_2)^{1/2}\cos\xi\} \\ &\quad + \frac{2}{m_1+m_2} \{m_1E_1 + m_2E_2 + 2(m_1m_2E_1E_2)^{1/2}\cos\xi\}^{1/2} \\ &\qquad \left\{ \frac{m_3m_4}{m_3+m_4} (E^C + Q) \right\}^{1/2} \cos\theta \qquad \text{(III-41)} \end{aligned}$$

where ξ is the angle between the velocities $\vec{V}_1$ and $\vec{V}_2$.

The term $(m_4/(m_3+m_4))E^C$ in equation (III-41) represents an additive contribution that is typically on the order of a few tens of keV's for d-t Maxwellian reactions. It can be on the order of hundreds of keV's for p-^{6}Li Maxellian reactions. In addition, the variation of E^C is roughly equal to the width of the reaction cross section. The contribution from the motion of the center of mass,

$$\frac{m_3}{(m_1+m_2)^2} \{m_1E_1 + m_2E_2 + 2(m_1m_2E_1E_2)^{1/2} \cos\xi\} \qquad \text{(III-42)}$$

ranges from a few keV to a few hundred keV. The major spread in energy comes from the term

$$\frac{2}{m_1+m_2}\{m_1E_1+m_2E_2+2(m_1m_2E_1E_2)^{\frac{1}{2}}\cos\xi\}^{\frac{1}{2}}\ \{\frac{m_3m_4}{m_3+m_4}\ (E^C+Q)\}^{\frac{1}{2}}\ \cos\theta \qquad \text{(III-43)}$$

since this term is proportional to the product of the relative velocity of the reaction products and the translational velocity of the center of mass.

If there is radiation given off during the collision or during the compound nucleus state, the energy of particle 3 in the laboratory frame can be expressed as in equation (III-41) provided that E^C+Q is replaced by $E^C + Q - E_\gamma$, where E_γ is the radiation energy given off.

In order to derive the energy distribution function of the reaction products, let us consider the ion species 1 with number density n_1 and velocity distribution $\hat{f}_1(\vec{V}_1)$ reacting with ion species 2 with number density n_2 and velocity distribution function $\hat{f}_2(\vec{V}_2)$. The reaction rate per unit volume for a process with reaction cross section $\sigma(|\vec{V}_1-\vec{V}_2|)$ is

$$R = n_1n_2 \int d^3\vec{V}_1d^3\vec{V}_2\ \hat{f}_1(\vec{V}_1)\hat{f}_2(\vec{V}_2)|\vec{V}_1-\vec{V}_2|\sigma(|\vec{V}_1-\vec{V}_2|) \qquad \text{(III-44)}$$

The energy distribution of the reaction products with mass m_3 and energy E_3 can be expressed as

$$\frac{dR}{dE_3} = n_1 n_2 \int d^3\vec{V}_1 d^3\vec{V}_2 f_1(\vec{V}_1) f_2(\vec{V}_2) \; |\vec{V}_1 - \vec{V}_2| \frac{d\sigma}{dE_3} \qquad \text{(III-45a)}$$

Using the relation of E_3 and the final emission angle θ and integrating over the azimuthal angle, eqn.(III-45a) can be written as:

$$= 2\pi n_1 n_2 \int d^3\vec{V}_1 d^3\vec{V}_2 f_1(\vec{V}_1) f_2(\vec{V}_2) |\vec{V}_1 - \vec{V}_2| \frac{d\sigma}{d\Omega} \cdot \left(-\frac{d(\cos\theta)}{dE_3}\right) \qquad \text{(III-45b)}$$

The term $\frac{d}{dE_3}(\cos\theta)$ can be found from equation (III-41) and therefore $\frac{dR}{dE_3}$ can be calculated, provided $\frac{d\sigma}{d\Omega}$ is given. Equation (III-45) can also be used for both elastic and inelastic scattering processes.

III-7. Power Balance Calculations

The model used in the power balance calculation for an advanced fusion fuel cycle is described in Fig. III-2. The energetic fusion products, knock-on ions and injections give their energy to the electrons and ions, which in turn rethermalize among themselves. The plasma loses energy via ash removal, transport and bremsstrahlung radiation.

The ion temperature and electron temperature in an advanced fuel cycle fusion plasma may reach 500 keV. The relativistically corrected bremsstrahlung and electron-ion rethermalization formulae must be used in the energy balance equations.

Bremsstrahlung radiative power is given(8, 9) by:

$$P_x = 2.94\times10^{-15}\, n_e^2\, Z_{eff}\, T_e^{1/2}(1+\eta)(\text{keV/cm}^3\text{-s}) \qquad \text{(III-46)}$$

where

$$Z_{eff} = \sum_j n_j\, Z_j^2/n_e\ , \qquad \text{(III-47)}$$

and the sum extends over all ion species. The relativistic correction factor η is

$$\eta = \frac{2T_e}{m_o c^2} + \frac{2}{Z_{eff}}\left(1 - \frac{1}{\left(1 + \frac{T_e}{m_o c^2}\right)^2}\right) \qquad \text{(III-48)}$$

where m_oc^2 is the rest mass energy of the electron.

The electron-ion rethermalization power is given by

$$P_{ie} = \frac{3x10^{-12} n_e}{T_e^{3/2}} \left(\sum_j \frac{n_j Z_j^2}{A_j}\right) (T_i - T_e)\delta \qquad \text{(III-49)}$$

where δ is a relativistic correction factor given by

$$\delta = 1 - 0.3 \frac{T_e}{m_o c^2} \quad . \qquad \text{(III-50)}$$

With the relativistically corrected bremsstrahlung radiation P_x and electron-ion rethermalization, P_{ie}, the power balance equations can be written as:

$$\xi i \; P_{inj} + U_i P_F^* = P_{ie} + 1.5 \; a_i \;\; T_i \qquad \text{(III-51)}$$

$$(1 - \xi_i) \; P_{inj} + (1 - U_i) P_F^* + P_{ie} = P_x + 1.5 \; a_e \;\; T_e \qquad \text{(III-52)}$$

Where

P_{inj} = injection power (if any),

P_F^* = fusion power in charged fusion products,

ξ_i = fraction of the injection power to heat ions,

U_i = fraction of fusion power deposited in ion,

a_i = ash removing rate for ions,

and

a_e = number of electrons associated with removing ion ash.

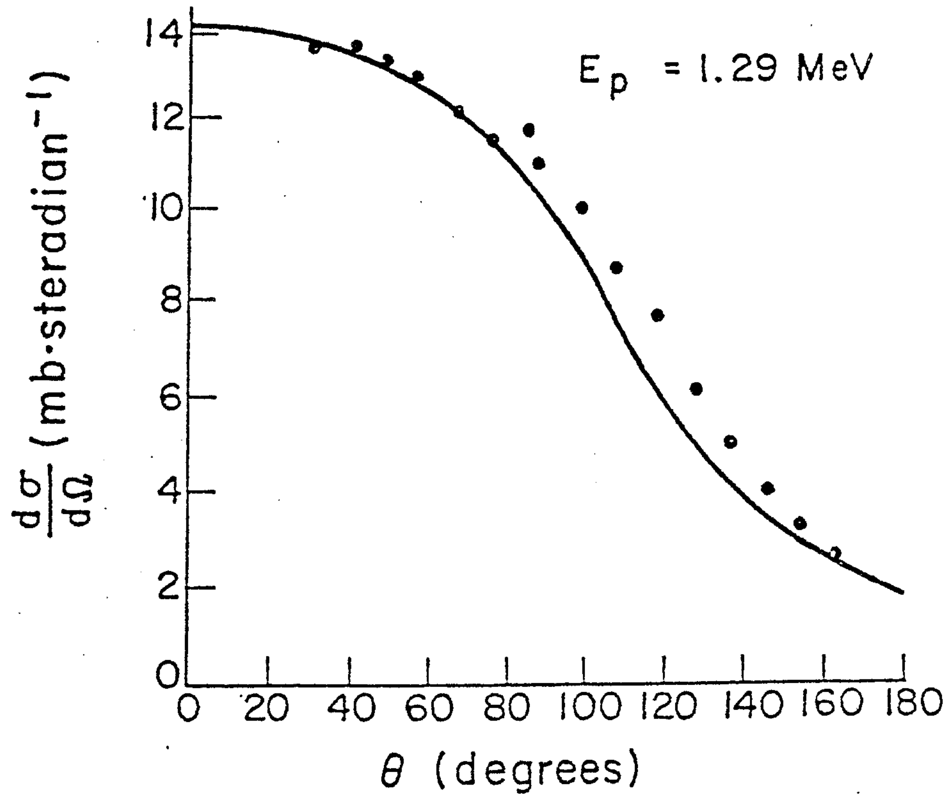

Fig. III-1. Angular distribution of the p-^{6}Li reaction cross section.

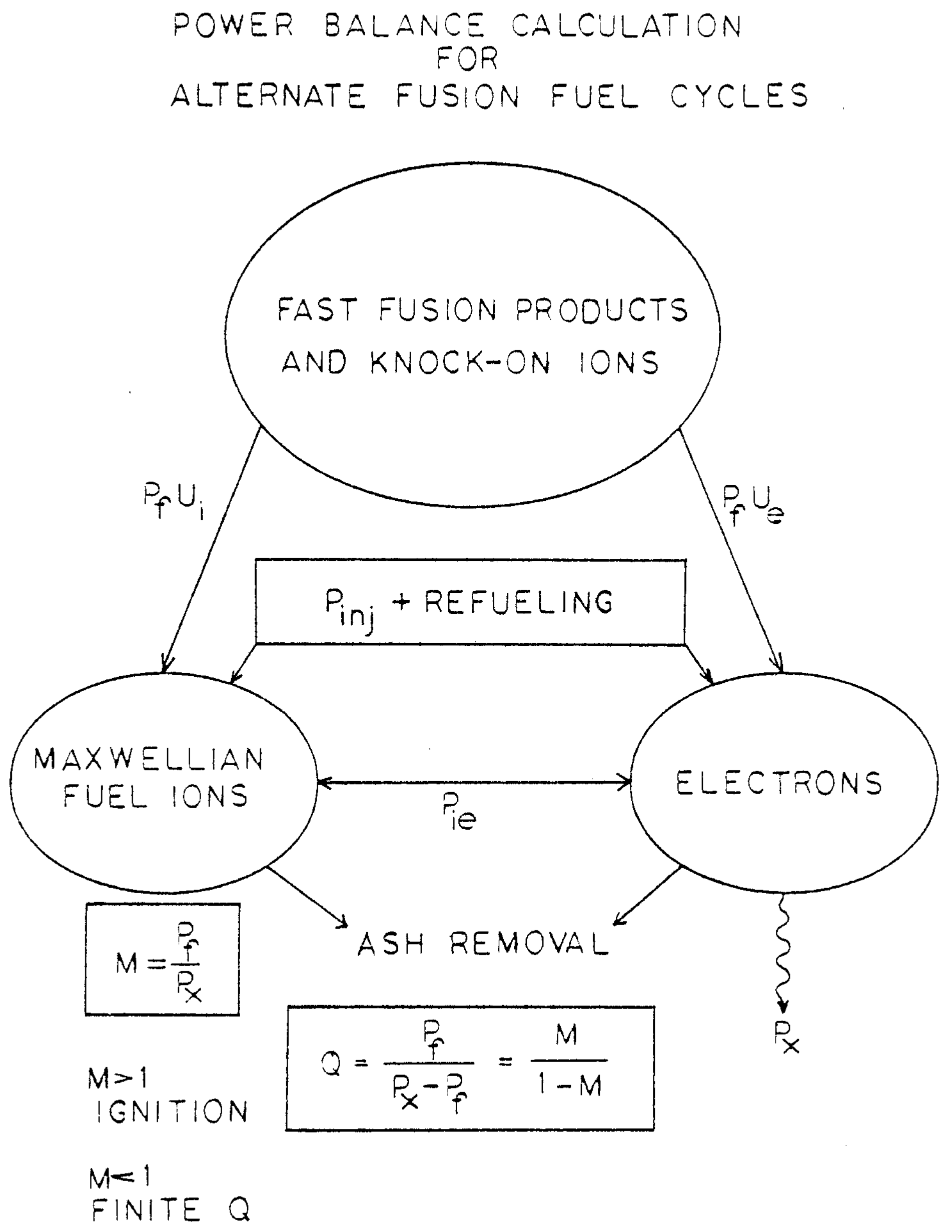

Fig. III-2. Power balance calculation for advanced fusion fuel cycles.

CHAPTER III

REFERENCES

1. Geoffrey W. Shuy, Advanced Fusion Fuel Cycles and Fusion Reaction Kinetics (Preliminary Proposal), UWFDM-335. Dec. ('79).
2. L. Longmire, Elementary Plasma Physics, Interscience Publishers, New York ('63).
3. I. P. Shkarofsky, R. W. Johnson and M. P. Bachynski, The Particle Kinetics of Plasma, Addison-Wesley Publishing Co., Inc. Reading, Massachusetts ('66).
4. S. T. Butler and M. J. Buckingham, Phys. Rev. 126 ('62) 1.
5. D. J. Sigmar and G. Joyce, Nucl. Fusion 11 ('71) 447.
6. J. J. Devanly and M. L. Stein, Nucl. Sci and Eng. 46 ('71) 323.
7. W. A. Houlberg, UWFDM-103 ('74).
8. J. M. Dawson, UCLA Plasma Group Report PPG-273 ('76).
9. J. G. Cordey, Lecture 2. Course on Theory of Magnetically Confined Plasma (Varenna, Italy) Sept. 1977.
10. G. W. Shuy and R. W. Conn, The p-^{6}Li Propagating Reaction Cycle, Transcation, ANS Winter Conference, San Francisco, Oct. ('79).
11. R. W. Conn and G. W. Shuy, Advanced Fuel Cycles and Propagating p-^{6}Li Cycle, UWFDM-262, Sept. ('78).

CHAPTER IV

THE STEADY STATE SIMULATION CODE
FOR
ADVANCED FUSION FUEL CYCLE BURN KINETICS

CHAPTER IV

THE STEADY STATE SIMULATION CODE FOR ADVANCED FUSION FUEL CYCLE BURN KINETICS

The potential of an advanced fusion fuel cycle can, as the first step of the analysis, be identified if the distribution of the equilibrium content of various species is properly determined. This requires one to solve the fusion reaction kinetic equations, including the effects like fast fusion, nuclear elastic and inelastic scattering, Doppler broadening of the energy distribution of reaction products and the tail-tail interaction of slowing down energy between ions and electrons. The description of these physical aspects of a steady state fuel burn process, as detailed in Chapter III, requires many coupled, nonlinear differential and algebraic equations. Analytical solution of these equations can be obtained for specialized and greatly simplified situations. To evaluate the distribution among species at steady state with all of these physical aspects requires numerical solution of these equations using large high speed computers, proveide that all the interaction cross sections are known. It is assumed that the interaction cross sections are known for the time being.

Since there is no existing computer code to perform such calculations, several have been developed which are of different levels of sophistication.

From the particle balance equations, which take into account all the reactions involved, one can solve for the equilibrium density ratio of species in a fuel cycle. In addition, the energy balance equations, the fast fusion probabilities, the slowing down time of the energetic particles and the large energy transfer collisions are needed if the fast reaction events are included. The p-^{6}Li fuel cycle is chosen to illustrate the problems involved and the method developed.

The particle balance equations are cumbersome and it is convenient to use the following notations.

$S_{cab} \equiv \langle cab \rangle \equiv \langle \sigma v \rangle_{ab}^{c}$ (in cm^3/sec)

= Reaction parameter for reaction $a + b \rightarrow c + d$ where c is a reaction product chosen to characterize the reaction branch (channel)

$S_{ab} \equiv \langle ab \rangle \equiv \sum_i \langle c_i ab \rangle$ includes all of the branches

$G_a \equiv \gamma_a = n_a/n_s$ = the ratio of the number density of specie a to the reference specie s.

$GS_{cab} \equiv (abcab) = \gamma_a \gamma_b \, 2^{-\delta_{ab}} \langle cab \rangle$

where δ_{ab} is the Kronecker delta.

$GS_{ab} \equiv (ab\ ab) = \gamma_a \gamma_b \, 2^{-\delta_{ab}} \sum_i \langle c_i ab \rangle$

$GFS_{cab} \equiv (\overline{abcab}) = GS_{cab}$ + all of the fast reactions due to the energetic a or b produced in the reactions involved prior to slowing down.

$\equiv GS_{cab} + FS_{cab}$

$GFS_{ab} \equiv (\overline{ab\ ab}) = \sum_i (\overline{abc_i ab})$

$EP_a \equiv (\overline{a\ P\ a})$ = Promotion rate of particle a due to large energy transfer interaction.

For p-^{6}Li, the proton is chosen as the reference specie and define the density ratios as $\gamma_1 = n_p/n_p = 1$, $\gamma_2 = n_d/n_p$, $\gamma_3 = n_3/n_p$, $\gamma_t = n_t/n_p$, $\gamma_6 = n_6/n_p$, $\gamma_L = n_{7_{Li}}/n_p$, $\gamma_7 = n_{7_{Be}}/n_p$. The ion temperature T_i and γ_6 will be specified in each run. The reaction rates of the major reactions considered are denoted by:

$(\overline{26726})$, $(\overline{26L26})$, $(\overline{26t26})$, $(\overline{26326})$, $(\overline{26A26})$, $(\overline{22322})$, $(\overline{22t22})$, $(\overline{16316})$, $(\overline{23p23})$, $(\overline{36236})$, $(\overline{36p36})$, $(\overline{33p33})$, $(\overline{37p37})$, $(\overline{t7pt7})$, $(\overline{27p27})$, $(\overline{ttAtt})$, $(\overline{2tA2t})$, $(\overline{2Ln2L})$, $(\overline{t32t3})$, $(\overline{t31t3})$, $(\overline{t3pt3})$, $(\overline{tLntL})$, $(\overline{3Lp3L})$, $(\overline{1L71L})$, $(\overline{1LA1L})$, and $(\overline{1t31t})$.

The particle balance equations can be described as follows:

for ^{3}He:
$$(\overline{26326}) + (\overline{22322}) + (\overline{16316}) + (\overline{1t31t}) = (\overline{23\ 23}) + (\overline{36\ 36}) + 2(\overline{33\ 33}) + (\overline{t3\ t3}) + (\overline{37\ 37}) + (\overline{3L\ 3L}) + (\overline{3\ P\ 3}) \quad \text{(IV-1)}$$

$$\text{for d:}\quad (\overline{36236}) + (\overline{t32t3}) = (\overline{26\ 26}) + 2(\overline{22\ 22}) + (\overline{23\ 23}) + (\overline{27\ 27}) + (\overline{2t\ 2t}) + (\overline{2L\ 2L}) + (\overline{2\ P\ 2}) \qquad \text{(IV-2)}$$

$$\text{for } {}^{7}\text{Be:}\quad (\overline{26726}) + (\overline{36236}) + (\overline{1L71L}) = (\overline{27\ 27}) + (\overline{37\ 37}) + (\overline{t7\ t7}) + (\overline{7\ P\ 7}) \qquad \text{(IV-3)}$$

$$\text{for t:}\quad (\overline{26t26}) + (\overline{22t22}) = (\overline{t7\ t7}) + 2(\overline{tt\ tt}) + (\overline{2t\ 2t}) + (\overline{t3\ t3}) + (\overline{tL\ tL}) + (\overline{1t\ 1t}) + (\overline{t\ P\ t}) \qquad \text{(IV-4)}$$

$$\text{for } {}^{7}\text{Li:}\quad (\overline{26L26}) = (\overline{2L\ 2L}) + (\overline{tL\ tL}) + (\overline{3L\ 3L}) + (\overline{1L\ 1L}) + (\overline{L\ P\ L}) \qquad \text{(IV-5)}$$

although equations (IV-1), (IV-2), (IV-3), (IV-4) and (IV-5) are coupled, the five unknowns (γ_3, γ_2, γ_t, γ_7 and γ_L) can be obtained from the five equations for any T_i provided that the fast reaction rates are known. To calculate the fast reaction probabilities, it is necessary to know all γ values and the electron temperature. To calculate T_e, one must have all γ values, all fast reaction rates, and T_e itself. A self-consistent iteration method is developed to hancle the task.

The self-consistent iteration method is a numerical approach to solve for various γ values, all fast reaction rates, and T_e self-consistently. It consists of 2 inner iteration loops inside a master iteration loop. The calculation is described briefly in the block diagram in Fig. IV-1.

The character of the energy transfer insures the convergence of the iteration loop which yields T_e and the fast fusion probabilities. However, knowledge of reaction kinetics is required to insure the convergence of other inner iteration loops and the master loop. Usually, several sets of second order simultaneous equations and more than one iteration loop for the equilibrium species density ratio are constructed to avoid numerical instabilities.

In order to handle the fast particle balance equations and hence the fast fusion reaction rates correctly and efficiently, a multigroup energy technique is employed. It is expressed as follows:

$0 = dn_j/dt$ = slowing down rate from fast adjacent group
+ production rate from nuclear reactions
- slowing down rate to next adjacent group
- consumption rate in nuclear reactions. (IV-6)

where $j = 1, 2, 3, \ldots$ represent, for example, e^-, p, d, t ^3He, ^4He, ^6Li, ^7Li, ^7Be, etc. In this multigroup approach the particle balance is affected by the energy balance. The fusion production and consumption rates also must be averaged over the energy populations of the other reactants.

Based on the approximate Fokker-Planck equation of Rosenbluth, MacDonald and Judd[1] which can be written as equation (IV-7), the energy balance correctly includes the tail-tail interactions which affect the particle balances and reactivities.

$$\frac{1}{n_0\gamma}\frac{\partial f_k(v_1)}{\partial t} = -\nabla_v \cdot \{f_k(v_1)\ \nabla_v(\frac{m_k+m_e}{m_e} \int d^3v\ \frac{f_e}{u_e} + \sum_i \frac{m_k+m_i}{m_i} \int d^3v_i\ \frac{f_i(v_i)}{u_i})\}$$

$$+ \frac{1}{2}\frac{\partial^2}{\partial\vec{v}\partial\vec{v}} : \{f_k(v_1)\ \frac{\partial^2}{\partial\vec{v}\partial\vec{v}} (\int dv_e u_e f_e + \sum_i \int dv_i u_i f_i)\} \qquad \text{(IV-7)}$$

where $u_i = |\vec{v}_1-\vec{v}_i|$, $u_e = |\vec{v}_1-\vec{v}_e|$, $\gamma = (4\pi e^4 Z_k^2 \bar{Z}^2/m_k^2)\ \ln\Lambda$, (IV-8)

$\bar{Z}$ is the effective Z of the plasma, n_0 is the number density of electrons and m's are masses.

By design, only a few specific physical parameters are inputs. For example, T_i and γ_6 are the only inputs required for the p-^{6}Li case. The code first prepares all values of S_{cab} for a given T_i, sets all of the fast reaction probabilities and γ's (except $\gamma_1 = 1$ and γ_6) equal to zero and sets $T_e = .75\ T_i$. The remaining first generation γ's are then calculated based on the above values. The calculations continue according to the procedure outlined and yield consistent values of the equilibrium species content ratios, fast reaction probabilities, and the electron temperature.

The code successfully gives the equilibrium contents of the fuel, calculates the relative power density, neutron production, average neutron energy and so on. It can then searchs for the self consistent electron temperature, given T_i, to determine a solution consistent with electron drag, ash removal energy loss and bremsstrahlung losses to calculate the ratio of fusion power to power losses. A number greater than one implies ignition at infinite $n\tau$. The energy amplification factor can then be determined as a function of $n\tau_E$ in equilibrium.

K. A. Brueckner and H. Brysk[2] have calculated the d-t fast fusion probabilities due to large energy transfer collisions of an α particle from the d+t reaction in an inertial d-t plasma, using the first five reactions of eqn. (IV-9). A similar situation has been reconstructed, and simulated with the BAFSS (the burn advanced fuel in steady state) code, and the results are compared in Table IV-1. P_B is the fast d-t fusion reaction probability as read from the graph in the Brueckner-Brysk paper. The quantities P_{S1} include the five reactions simulated by Brueckner and Brysk, and are close to the P_B values. When the reaction channels denoted in eqn. (IV-9) are open, the fast fusion probabilities become P_{S2}. Finally, when a full version of BAFSS code is activated, adding reactions of eqn. (IV-10) including tail-tail interactions and computing T_e self consistently, the fast fusion reaction probabilities become P_{S3}.

$$
\begin{aligned}
d + t &\rightarrow n + \bar{\alpha} \\
\bar{\alpha} + d &\rightarrow \bar{d} + \alpha \\
\bar{\alpha} + t &\rightarrow \bar{t} + \alpha \qquad \text{(IV-9)} \\
\bar{d} + t &\rightarrow n + \bar{\alpha} \\
\bar{t} + d &\rightarrow n + \bar{\alpha}
\end{aligned}
$$

$$
\begin{aligned}
&d + d \rightarrow n + {}^3\bar{He} \\
&d + d \rightarrow \bar{p} + \bar{t} \\
&\bar{p} + d \rightarrow \bar{d} + p \\
&\bar{p} + t \rightarrow \bar{t} + p \qquad \text{(IV-9)} \\
&d + {}^3He \rightarrow \bar{\bar{p}} + \bar{\alpha} \\
&\bar{\bar{p}} + d \rightarrow \bar{d} + p \\
&\bar{\bar{p}} + t \rightarrow \bar{t} + p
\end{aligned}
$$

$$
\left.
\begin{aligned}
&{}^3He + {}^3He \rightarrow 2\bar{p} + \bar{\alpha} \\
&t + {}^3He \rightarrow p + n + \bar{\alpha} \\
&t + {}^3He \rightarrow \bar{d} + \bar{\alpha} \\
&d + {}^3\bar{He} \rightarrow \bar{p} + \bar{\alpha}
\end{aligned}
\right\} \qquad \text{(IV-10)}
$$

T_i	20keV	40keV	60keV	$T_i=T_e$
P_B	.00874	.172	.206	yes
P_{S1}	.00872	.176	.214	yes
P_{S2}	.00887	.192	.251	yes
P_{S3}	.01303	.247	.331	no

TABLE IV-1

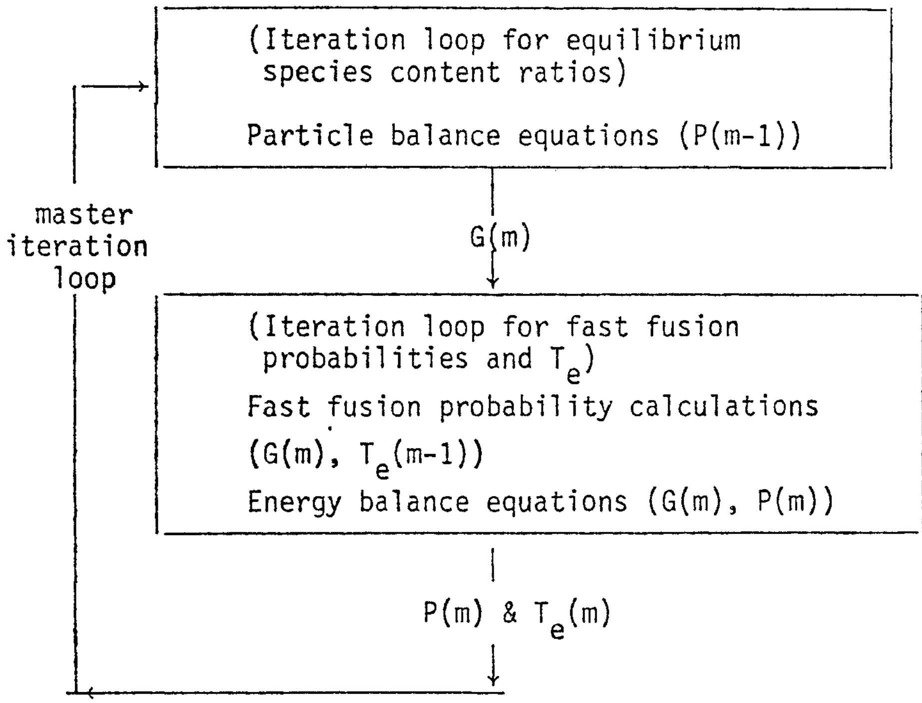

1. Use the fast fusion probabilities of the previous generation (denoted as P(m-1)) in the particle balance equations, iterate and obtain a new generation equilibrium species content ratio (denoted as G(m)).

2. Use G(m) and T_e of the previous generation (denoted as $T_e(m-1)$) to calculate the fast fusion probabilities. Use G(m) and the fast fusion probabilities in the energy balance equations to calculate T_e. The iteration will yield a new generation value of P(m) and $T_e(m)$.

3. Continue (1) and (2) until G, P, and T_e converge to the degree specified.

Fig. IV-1

CHAPTER IV

REFERENCES

1. M. Rosenbluth, W. M. MacDonald and D. L. Judd, Phys. Rev., 107 (57) 1.
2. Keith A. Brueckner and Henry Brysk, J. Plasma Phys. 10 (73) 141.

CHAPTER V

THE TIME DEPENDENT SIMULATION CODE
FOR
ADVANCED FUSION FUEL CYCLE BURN KINETICS

CHAPTER V

THE TIME DEPENDENT SIMULATION CODE FOR ADVANCED FUSION FUEL CYCLE BURN KINETICS

V-1. Computer Code Survey

Other burn codes developed to date for problems as described in this thesis have all been specialized to answer specific questions about the burn dynamics under rather simple burn conditions.

(1) The University of Illinois

Some six diffenert burn codes developed at the University of Illinois are focused[1] on fuels containing d, t and ^3He. Most of these codes are designed for the analysis of conventional steady-state burns. Start-up scenarios can be examined using the "start-up code" but here again the scope of reactants is very restricted.

(2) The ECF Code

The ECF Code at Oak Ridge[2] is now capable of handling over 30 different fusion reactions. It handles fusion power multiplication from fast ions and nuclear elastic scattering as linear processes. The relaxation of fast particles by Coulomb or nuclear elastic collisions is treated assuming the background thermal plasma to be stationary during slowing-down of the fast particles. This is not appropriate in those situations in which the evolution of the plasma parameters is faster than the relaxation times of fast particles. The code is however adequate for establishing the conditions of a mild steady-state thermonuclear burn.

(3) The FOKN Code

The FOKN Code[3,4] developed at LLL, is the only fully non-linear burn code. This code solves for the time-evolution of the full velocity distribution function of the various reactants. The linear approximation, i.e., the assumption that the velocity distribution function is made up of a Maxwellian bulk with a small tail of energetic particles is dispensed with. The full details of the time-evolution of this distribution are also available which makes possible the exploration of intense thermonuclear burns and rapid start-up scenarios. This code also includes the details of the effects of nuclear elastic collisions, synchroton radiation and bremsstrahlung on the shapes of the distribution functions. The major drawbacks of this code are:

The level of its detail makes it very expensive to run.

The reactions associated with lithium and beryllium have not yet been included.

V-2. Physics Features and Subtle Issues

The advanced fusion fuel cycle analysis requires a time dependent burn kinetics code to follow the many reactions that can be involved, including subtle effects like two component fusions, nuclear elastic and inelastic scattering, Doppler broadening of the energy distribution of reaction products, and the fraction of slowing down energy given seperately to the ions and electrons.

In addition, advanced fuel cycles are likely to operate at ion temperatures approaching 300 keV and electron temperatures in excess of 100 keV. As such, a careful calculation of relativistic bremsstrahlung losses and of synchrotron radiation is required. With so many coupled non-linear processes involved, it is difficult to analyze advanced fusion fuel cycles in detail, such as startup scenarios, ash removal, refueling and heating power requirements, without such a tool. A time dependent 0-dimension burn advanced fuel kinetics code (BAFCO) has been written to serve this purpose. A block diagram describing the physics features of the code is shown in Fig. V-1.

Conservation of particles and conservation of energy are strictly followed for the transport and slowing down schemes used by the code.

To illustrate why various features of the BAFCO code are required, the p-^{6}Li cycle will be used as an example.

Primary Reactions:

$$p + {}^6Li \rightarrow {}^3He\ (2.3\ MeV) + {}^4He\ (1.7\ MeV) \qquad (V\text{-}1)$$

$${}^3He + {}^6Li \rightarrow p\ (11.3\ MeV) + 2\ {}^4He\ (2.81\ MeV) \qquad (V\text{-}2)$$

$$\rightarrow d\ (0.4\ MeV) + {}^7Be\ (0.1\ MeV) \qquad (V\text{-}3)$$

$$\rightarrow p + n + {}^7Be \qquad (V\text{-}4)$$

<u>Secondary and Tertiary Reactions:</u>

$$d + {}^6Li \rightarrow n + {}^7Be\ (.42\ MeV)$$

$$\rightarrow p\ (4.4\ MeV) + {}^7Li\ (.63\ MeV)$$

$$\rightarrow p\ (1.6\ MeV) + t + {}^4He \qquad (V\text{-}5)$$

$$\rightarrow n + {}^3He + {}^4He$$

$$\rightarrow 2\ {}^4He\ (11.2\ MeV)$$

$$d + {}^3He \rightarrow p\ (14.6\ MeV) + {}^3He\ (4.7\ MeV) \qquad (V\text{-}6)$$

$$d + d \rightarrow n + {}^3He\ (.82\ MeV)$$

$$(V\text{-}7)$$

$$\rightarrow p\ (3\ MeV) + t\ (1\ MeV)$$

$$d + {}^7Be \rightarrow p\ (11.2\ MeV) + 2\ {}^4He\ (2.8\ MeV) \qquad (V\text{-}8)$$

$$d + t \rightarrow n + {}^4He\ (3.5\ MeV) \qquad (V\text{-}9)$$

$$t + {}^3He \rightarrow d\ (9.6\ MeV) + {}^4He\ (4.8\ MeV)$$

$$(V\text{-}10)$$

$$\rightarrow p + n + {}^4He$$

$${}^3He + {}^3He \rightarrow 2p\ (5.7\ MeV) + {}^4He\ (1.4\ MeV) \qquad (V\text{-}11)$$

$${}^3He + {}^7Be \rightarrow 2p\ (4.5\ MeV) + 2\ {}^4He\ (1.1\ MeV) \qquad (V\text{-}12)$$

$$t + {}^7Be \rightarrow p\ (4.2\ MeV) + n + 2\ {}^4He\ (1.1\ MeV) \qquad (V\text{-}13)$$

$$d + {}^7Li \rightarrow n + 2\ {}^4He\ (2.521\ MeV) \qquad (V\text{-}14)$$

In addition there are at least thirteen $^6Li+^6Li$ exothermic reactions which produce all elements from H to ^{12}C and produce neutrons. Many of the fusion reaction products are energetic and may react with elements in the background plasma prior to complete slowing down (fast fusion or two-component fusion events). Including these fast fusion events is crucial, particularly for cycles that are either propagating or chain events. Some important fast fusion reactions in the p-^{6}Li cycle (the fast particle has a bar over the element's designation) include:

$$\left\{\begin{array}{l} \bar{p} + {}^6Li \rightarrow {}^3\bar{He} + \alpha \\ {}^3\bar{He} + {}^6Li \rightarrow \bar{p} + 2\alpha \\ \bar{p} + {}^6Li \rightarrow {}^3\bar{He} + \alpha \\ \vdots \end{array}\right\} \quad (V\text{-}15) \qquad \left\{\begin{array}{l} \bar{p} + {}^6Li \rightarrow {}^3\bar{He} + \alpha \\ {}^3\bar{He} + d \rightarrow \bar{p} + \alpha \\ \bar{p} + {}^6Li \rightarrow {}^3\bar{He} + \alpha \\ \vdots \end{array}\right\} \quad (V\text{-}16)$$

$$\left\{\begin{array}{l} \bar{p} + {}^6Li \rightarrow {}^3\bar{He} + \alpha \\ {}^3\bar{He} + {}^6Li \rightarrow d + {}^7Be \\ d + {}^6Li \rightarrow \bar{p} + {}^7Li \\ \bar{p} + {}^6Li \rightarrow {}^3\bar{He} + \alpha \\ \vdots \end{array}\right\} \quad (V\text{-}17) \qquad \left\{\begin{array}{l} \bar{p} + {}^6Li \rightarrow {}^3\bar{He} + \alpha \\ {}^3\bar{He} + {}^6Li \rightarrow d + {}^7Be \\ d + {}^7Be \rightarrow \bar{p} + 2\alpha \\ \bar{p} + {}^6Li \rightarrow {}^3\bar{He} + \alpha \\ \vdots \end{array}\right\} \quad (V\text{-}18)$$

and there are many others. As such, there is a high premium placed on the very efficient numerical approach to the treatment of slowing down of fast fusion products. Such an efficient procedure have been developed for implementation in the code.

With so many reactions involved, other subtle issues arise which should be point out. In general, it is difficult, a priori, to establish a criterion for the inclusion or rejection of a particular reaction channel. First, while the values for $<\sigma v>$ and Q are known, the density of each specie in the plasma is not known. Thus, the fusion reaction rates are unknown. Second, the temperature may vary widely during a burn, so that almost all reactions may at some time be influential. For an initially self-consistent model, all reactions with comparable $<\sigma v>$ or $<\sigma v>Q$ values should be incorporated. Only parameter studies at a later time will determine whether specific reactions are important in the simulation process. At that point, those which do not affect the results in a significant way will be eliminated.

Another issue involves the techniques used to handle a problem with so many reaction channels and associated time constants. Two standard approaches are:

(A) Write many small codes, each of which solves a specific, limited problem. This is inconvenient since there may be many combinations of reactions of interest. This approach makes it difficult to perform parametric studies which are required since the inclusion or deletion of a particular reaction channel requires that a new code be written. The University of Illinois burn code has been of this type.

(B) Write one large code incorporating all possible reaction channels in such a way as to be selective with respect to which reactions are included for a particular case. This approach poses a severe problem with respect to execution speed because the straightforward approach is to set switches in the code to include or ignore certain selected reactions. This is usually accomplished by means of costly "if" statements. Since $\gtrsim 10^6$ evaluations may be required per run, the time spent trying to speed-up the code by selecting reactions may actually make running time longer. Because of the execution time associated with "if" statements, the two codes which currently incorporate "all" possible reactions (namely the ECF code at Oak Ridge and the FOKN Code at LLL) calculate each reaction channel without any selection scheme. The execution time of these codes can be excessive and they do not easily lend themselves to parametric studies.

A solution being pursued in the BAFCO code involves the use of certain compiler characteristics to replace "if" statements. This can lead to a fast flexible code which can be used for both simple problems and the most complex. Using these features of "intelligent compilers", the simulation code is made very general in scope and fast in speed. In addition, the same compiler characteristics facilitate the required parametric studies.

V-3. Basic Equations of the BAFCO Code

The basic equations are the particle balance, the energy balance, the fusion reactions induced by energetic particles, the slowing down of fast particles by Coulomb and nuclear elastic collisions and Doppler broadening effects. Since particles are present with energies from thermal to the initial energy of production, the most efficient approach to handling the dynamics is to employ a multigroup energy technique.

(1) Particle Balance

The evolution of the density of a given specie j is

$\frac{dn_j}{dt}$ = beam source (if any)

+ slowing down rate from fast adjacent group
+ production rate from nuclear reactions
- slowing down rate to next adjacent group
- consumption rate in nuclear reactions
- confinement loss (V-19)

where j = 1, 2, 3, . . . represent, for example, e^-, p, d, t, ^{3}He, ^{4}He, ^{6}Li, ^{7}Li, ^{7}Be. etc. In this multigroup approach the particle balance is affected by the energy balance detailed next. The fusion production and consumption rates also must be averaged over the energy populations of the other reactants.

(2) Energy Balance

The dominant slowing-down process is by Coulomb scattering and the energy loss rate is given by

$$\frac{dE}{dt} = -(8\pi)^{\frac{1}{2}} \left(\frac{Ze^2}{4\pi\varepsilon_0}\right)^2 \sum_j \frac{Z_j^2 N_j \ell n \Lambda_j F(V/V_j)}{M_j V_j} \qquad \text{(V-20)}$$

$$F\left(\frac{V}{V_j}\right) = \frac{V_j}{V}\left(\int_0^{V/V_j} e^{-t^2}\, dt\right) - (1 - M_j/M)\, e^{-V^2/V_j^2} \qquad \text{(V-21)}$$

E, M, A, and V are the energy, mass, atomic number, and speed of the fast particle whereas n_j, T_j, M_j, Z_j and V_j are the density, temperature, mass, atomic number and speed, respectively, of the background plasma specie. Nuclear elastic and inelastic scattering reactions are also important and are included in the multigroup approach as

$$\left.\frac{dn_k}{dt}\right|_{\text{nuclear}} = \text{gain through scattering} - \text{loss through scattering}$$

$$= \sum_j \int_0^{t_j} dt \int_{E_{K_0}}^{E_k} dE_f \int_{E_{j_0}}^{E_j} n_j V_{kj} \sigma_{kj}\, (E_j, E_f) dE_i f(E_i)$$

$$- \sum_\ell \int_0^{t_\ell} dt \int_{\alpha E_{k\ell}}^{E_{k\ell}} f(E_f) dE_f \int n_k V_{k\ell} \sigma_{kj} (E_i, E_f)\, dE_i \qquad \text{(V-22)}$$

As is done in the FOKN code, these scattering terms include multi-dimensional integrals which can be evaluated <u>once</u> as transfer matrices prior to a computational run and tabulated.

The evolution of the temperature of the thermal background is obtained from the equations

$$\frac{d}{dt} \sum_j \left(\frac{3}{2} n_j T_j\right) = \text{heating rate by fast particles (Coulomb and nuclear)} + \text{refueling and auxiliary heating} - \text{heat loss to electrons}$$

- ash removal losses

- confinement losses $\left(\frac{3}{2}\,\Sigma\frac{n_j T_j}{\tau_{Ej}}\right)$ (V-23)

$\frac{d}{dt}\left(\frac{3}{2}\,n_e T_e\right)$ = heating by fast ions

+ ion-electron rethermalization

+ refueling and auxiliary heating

- confinement losses $\left(\frac{3}{2}\,\frac{n_e T_e}{\tau_{Ee}}\right)$

- radiation losses

- ash removal losses (V-24)

At present, radiation losses from the electrons include the standard relativistically correct estimates for bremsstrahlung as well as a crude model of synchrotron radiation losses.

V-4. Time Step

A time step must be estimated in a simulation code that will allow the plasma to evolve to some new state that is not too different from its previous state. This time step usually is determined by the highest ratio of the time rate of change and the original value in each term of the equations. In a typical advanced fusion fuel burn simulation, this ratio for ion temperature, electron temperature and electron density is about 1 or less while the ratio for the ion densities could be 10^{12} time larger. To enforce time steps that adequately resolve the large changes in any variable would end up being prohibitively expensive.

The method used in the BAFCO code is to treat the slower varying functions as semi-adiabatic values which are calculated over a longer time step and used as a constant in the short time steps. Careful study shows that a fast-changing term in the calculation could be composed of a product of a slow-changing function and a fast-changing function. Each term of the equations involved in the simulation code has been thoroughly examined and decomposed prior to the construction of the code. Criteria have been established to control the time steps used to recalculate the semi-adiabatic values.

The treatment of the fast fusion events in BAFCO code is particularly useful in elaborating this subject.

The fast charged particles undergo coulomb collisions with the background plasma. The energy of the particle is lost to the cooler target and the expression for the rate of energy loss is given in eqn. (V-20). Let $\sigma(|\vec{V} - \vec{V}_j|)$ be the reaction cross section for a fast charged particle of velocity $\vec{V}$, on a background plasma specie j of velocity $\vec{V}_j$. Assuming that the background plasma specie j has a velocity distribution $\hat{f}(\vec{V}_j)$ and that $\int \hat{f}(\vec{V}_j) d^3\vec{V}_j = 1$, the probability of a fast particle slowing down from $E_{\ell+1}$ to E_ℓ and reacting with plasma specie j is given by:

$$\int_{E_{\ell+1}}^{E_\ell} n_j \int |\vec{V}-\vec{V}_j| \, \sigma(|\vec{V}-\vec{V}_j|) \, \hat{f}(\vec{V}_j) \, d^3\vec{V}_j \, \frac{dt}{dE_f} \, dE_f \, \ldots \qquad \text{(V-25)}$$

where $E_f = \frac{1}{2} MV^2$ and dE_f/dt is the total rate of energy loss of the charged particle via coulomb collisions. The integration of the reaction probability involves the evaluation of dE_f/dt which depends on E_f, n_j, T_i and T_e (especially E_f, n_e and T_e). Therefore, it must be performed at each time step (of the calculation of the density energy balance equations).

A fast particle can undergo any of a large number of different reactions; e.g. $\bar{d} + d \rightarrow n + {}^3He$, $\bar{d} + d \rightarrow p + t$, $\bar{d} + t \rightarrow n + \alpha$, $\bar{d} + {}^3He \rightarrow p + \alpha$, $\bar{d} + {}^6Li \rightarrow 2\alpha$, $\bar{d} + {}^6Li \rightarrow p + t + \alpha$, $\bar{d} + {}^6Li \rightarrow n + {}^3He + \alpha$, $\bar{d} + {}^6Li \rightarrow n + {}^3He + \alpha$, $\bar{d} + {}^6Li \rightarrow p + {}^7Li$, $\bar{d} + {}^6Li \rightarrow n + {}^7Be$, $\bar{d} + {}^7Li$, $\bar{d} + {}^7Be$, etc. Including the fast events is crucial, particularly for cycles that are either propagating or chain events.

For these reasons, it had been thought that an advanced fuel cycle burn code would be prohibitively expensive if one calculates fast fusion probabilities to the required accuracy.

The reaction probability is

Reaction probability for particle slowing down from $E_{\ell+1} \rightarrow E_\ell$

$$= \int_{E_{\ell+1}}^{E_\ell} n_j \int |\vec{V}-\vec{V}_j| \; \sigma(|\vec{V}-\vec{V}_j|) \; \hat{f}(\vec{V}_j) \; d^3\vec{V}_j \; \frac{dt}{dE_f} \cdot dE_f$$

$$\simeq n_j \sum_{k=1}^{K} \{\int |\vec{V}_k-\vec{V}_j| \sigma(|\vec{V}_k-\vec{V}_j|) \; \hat{f}(\vec{V}_j) d^3\vec{V}_j\} \cdot \left.\frac{dt}{dE_f}\right|_{E_f=E_k} \cdot \Delta E \qquad \text{(V-26)}$$

where $E = (E_{\ell+1} - E_\ell)/k$, $E_k = E_\ell + k\,\Delta E = \frac{1}{2} M V_k^2$.

After tedious algebra, it can be shown that if $\hat{f}(\vec{V}_j)$ is the Maxwellian distribution, then

$$SVB(E_k) \equiv \langle\sigma v\rangle_b \equiv \int |\vec{V}_k - \vec{V}_j|)\hat{f}(\vec{V}_j)\ d^3\vec{V}_j$$

$$\equiv \frac{2W_j e^{-u^2}}{\sqrt{\pi}\ u} \int_0^\infty x^2 \exp(-x^2)\sinh(2ux)\sigma(xW_j)\ dx \quad \text{(V-27)}$$

where $u = V_k/W_j$, $x = |\vec{V}_k - \vec{V}_j|/W_j$, $W_j = \sqrt{2KT_j/M_j}$. (V-28)

It is clear that $\langle\sigma v\rangle_b$ is a function of E_k and T_i only. Fortunately, it is relatively insensitive to T_i. We can also define

$$\Delta t(E_k,\ n_e.\ T_e) = - \left.\frac{\Delta E/dE_f}{dt}\right|_{E_f = E_k} . \quad \text{(V-29)}$$

This function is very sensitive to E_k, n_e and T_e, but is not sensitive to the ion temperature, or density. In normal operation, n_e and T_e are relatively constant in time. Using these expressions, eqn. (V-26) becomes

$$n_j \sum_{k=1}^{K} SVB(E_k)\ \Delta t(E_k,\ T_e,\ n_e) \quad \text{(V-30)}$$

with $E_k = E_\ell + k\Delta E$, $E = (E_{\ell+1} - E_\ell)/K$.

From the preceding discussion, it can be seen that there are two independent quantities to calculate: (1) n_j, which is given by the particle balance equation at each short time step; and (2)

$\Sigma SVB(E_k)\Delta t$, which is relatively constant in time and can thus be calculated once for many short time steps.

V-5. Nuclear Inelastic Scattering

No nuclear inelastic scattering is included in the current version. Provisions have been made to add this calculation at a later time.

V-6. Energy Distribution from Nuclear Reaction Products

Assuming isotopy of reaction cross sections and neglecting the velocity of the background species, a simplified treatment has been implemented for the two-component reaction products in the TRW upgrade version of the BAFCO code. Since the major contribution of the two-component reactions comes from the lower energy group, where the velocity of the background species is comparable to that of the fast species, a correct treatment has to be developed. Provisions have been made to develop that at a later date.

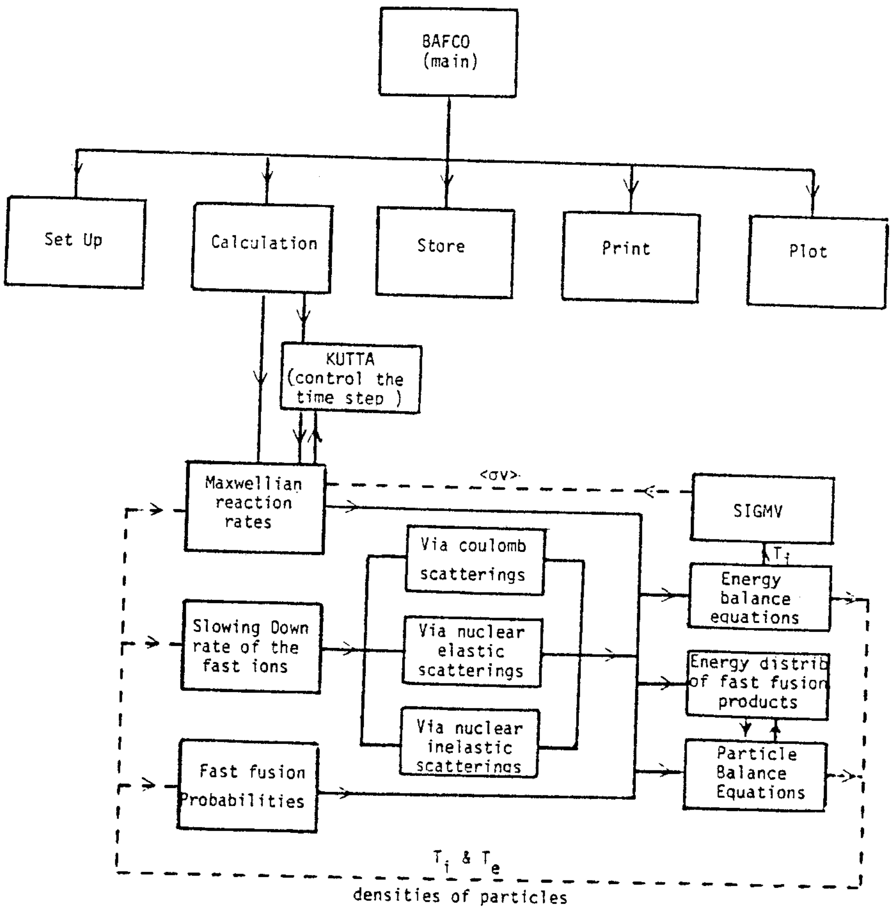

Fig. V-1. Block diagram showing physics feafures of the BAFCO computer code.

CHAPTER V

REFERENCES

1. G. H. Miley, et al., Private communication
2. R. D. Sharp and J. Rand McNally, Jr., ORNL-TM-5013, Sept., 1975
3. UCID-17196, Documented by Terry Chu, July, 1976
4. G. Lee, et al., UCRL-74192, Nov., 1972
5. R. Conn and G. Shuy, UWFDM 262, 1978 and private communication

CHAPTER VI

ADVANCED FUSION FUEL CYCLE ANALYSES

CHAPTER VI

ADVANCED FUSION FUEL CYCLE ANALYSES

VI-1. New Effects Investigated

There are three new effects in the analysis of advanced fuel cycles which have been investigated and found to increase the reactivity of the cycles, to alter energy balance calculations and to affect predicted Q values or ignition conditions. The first effect is the propagation in the cycles such as p-^{6}Li. ^{3}He, the energetic p+^{6}Li reaction product, reacts with ^{6}Li and produces an energetic proton before solowing down; these protons can undergo fast fusion again and propagate the reaction further. The second effect is the enhanced fast fusion reactivity due to nuclear elastic scattering. Nuclear elastic scattering of the energetic fusion products with the background fuel ions produces additional energetic particles which can undergo fast fusion and further propagate the reaction. The third effect is the enhanced fast fusion reactivity due to tail-tail interactions which make the tail fast fuel ions stay longer in the more reactive energy region; resulting in higher reaction probabilities.

Including the tail-tail interacion, the stripped proton distribution (where the Maxwellian portion has been substracted out) in a reacting p-^{11}B plasma with γ_B=0.1 is shown as the solid curve in Fig. VI-1 as a function of proton energy. The stripped distribution is defined by eqn. (III-4), γ_B is the density ratio of ^{11}B to p and the ion temperature of the plasma is 300 keV. The dashed curve is the proton-stripped distribution function in the same plasma while the tail-tail interactions are neglected. It is clearly shown that the slowing down process is altered by tail-tail interactions.

A pronounced resonance occurs at $E_p \simeq 600$ keV with $\Gamma \simeq 300$ keV in the p-^{11}B reaction cross section. Comparing the stripped proton distribution functions calculated in both cases, it can be seen that the tail-tail interactions which alter the slowing down have the effect of making the tail fast fuel ion distribution larger in the most reactive energy region, thereby enhancing the reactivity.

The energy transferred to electrons by a 14.5 MeV proton is shown in Fig. VI-2 as a function of electron temperature. The background plasma in this case is that of a steady state, catalysed d-d plasma. The dashed curve is the fraction of the initial energy received by electrons when only the coulomb interaction is assumed. The solid curve gives the result when the effects of coulomb and nuclear elastic scattering and the subsequent slowing down of the fast ion produced by the large energy transfer collisions are included. Finally, the dash-dot curve properly includes the tail-tail interactions. Accounting for nuclear elastic scattering, subsequent slowing down and the tail-tail interaction, a 14.5 MeV proton in a 75 keV ion temperature steady state catalysed d-d plasma will transfer 71% of its energy to 50 keV electrons compared to 78% when the tail-tail interactions are neglected and 94% when only coulomb scattering is assumed. At an electron temperature of 100 keV, the percentage of energy transferred to the electrons decreases to 38% compared to 51% when the tail-tail interactions are neglected and 85% with coulomb interactions only. The effect is clearly important in a plasma energy balance calculation.

Including these new effects, the analyses for the steady state catalysed d-d, d-^{3}He and p-^{11}B have been carried out. It is found that the reactivity is enhanced, the energy deposition of the fusion products to the plasma ions is increased, and the ignition condition required for these fuel cycles is relaxed.

V-2. The d-^{3}He Cycle

The primary reactions of this cycle are:

$$d + {}^3He \rightarrow p\ (14.68\ MeV) + {}^4He\ (3.67\ MeV) \qquad (VI-1)$$

$$d + d \rightarrow p\ (3.02\ MeV) + t\ (1.01\ MeV) \qquad (VI-2)$$

$$d + d \rightarrow n\ (2.45\ MeV) + {}^3He\ (.82\ MeV) \qquad (VI-3)$$

$${}^3He + {}^3He \rightarrow 2p\ (5.72\ MeV) + {}^4He\ (1.43\ MeV) \qquad (VI-4)$$

Secondary and tertiary reactions included:

$$d + t \rightarrow n\ (14.07\ MeV) + {}^4He\ (3.52\ MeV) \qquad (VI-5)$$

$$t + t \rightarrow 2n\ (5.03\ MeV) + {}^4He\ (1.26\ MeV) \qquad (VI-6)$$

$$t + {}^{3}He \rightarrow p\ (10.08\ MeV) + n\ (1.61\ MeV) + {}^{4}He\ (.4\ MeV)$$

or (5.37 MeV) or (5.37 MeV) or (1.34 MeV) (VI-7)

$$t + {}^{3}He \rightarrow d\ (9.55\ MeV) + {}^{4}He\ (4.77\ MeV) \qquad (VI-8)$$

$$p + d \rightarrow n + 2p \quad Q = -2.225\ MeV \qquad (VI-9)$$

$$p + t \rightarrow n + {}^{3}He \quad Q = -.764\ MeV \qquad (VI-10)$$

Propagating fusion reaction sequences in the d-^{3}He cycle (the fast particle has a bar over the element's designation) are:

$$\left\{\begin{array}{l} d + {}^{3}He \rightarrow \bar{p} + {}^{4}\bar{He} \\ \bar{p} + d \rightarrow \bar{d} + p \\ \bar{d} + {}^{3}He \rightarrow \bar{p} + {}^{4}\bar{He} \end{array}\right\} \quad (VI-11) \quad \left\{\begin{array}{l} {}^{3}He + d \rightarrow \bar{p} + {}^{4}\bar{He} \\ \bar{p} + {}^{3}He \rightarrow {}^{3}\bar{He} + p \\ {}^{3}\bar{He} + d \rightarrow \bar{p} + {}^{4}\bar{He} \end{array}\right\} \quad (VI-14)$$

$$\vdots \qquad\qquad\qquad\qquad \vdots$$

$$\left\{\begin{array}{l} d + d \rightarrow {}^{3}\bar{He} + n \\ {}^{3}\bar{He} + d \rightarrow \bar{p} + {}^{4}\bar{He} \\ \bar{p} + d \rightarrow \bar{d} + p \\ \bar{d} + d \rightarrow {}^{3}\bar{He} + n \end{array}\right\} \quad (VI-13) \quad \left\{\begin{array}{l} d + d \rightarrow {}^{3}\bar{He} + n \\ {}^{3}\bar{He} + d \rightarrow {}^{4}\bar{He} + \bar{p} \\ {}^{4}\bar{He} + d \rightarrow \bar{d} + {}^{4}He \\ \bar{d} + d \rightarrow {}^{3}\bar{He} + n \end{array}\right\} \quad (VI-14)$$

$$\vdots \qquad\qquad\qquad\qquad \vdots$$

and there are other. See eqns. (VI-1) through (VI-10) for the energies of the reaction products.

Neutrons are produced only from side d-d reactions and the number can be made relatively small by burning lean in d, as shown in

Figs. VI-3 and VI-4. For reference, the d-t cycle produces 3.56×10^{11} neutrons per joule. At constant , however, the power density also decreases although not as rapidly. Also, burns that are too lean in d will not be reactive enough to maintain ignition or high Q. In Fig. VI-5 noted that ignition is not feasible if the ratio of ^{3}He to d in a mixture is greater than about 8 even if confinement is perfect.

The enhanced reactivity of a 50-50 d-^{3}He mixture at T_i = 100 keV for different electron temperatures are shown in Fig. VI-6. Curves of $n_e\tau_E$ required for ignition are shown if Fig. VI-7 as a function of ion temperature using both the standard Maxwellian averaged $\langle\sigma v\rangle$ and the properly enhanced $\langle\sigma v\rangle$ value. Clearly, the required $n\tau_E$ value at any temperature is decreased when the enhanced reactivity effect is included. At 100 keV, assuming $\tau_i = \infty$ the required $n_e\tau_E$ is as low as 2×10^{14} cm^{-3}-s, comparable to that required of the d-t cycle at 20 keV. The main drawback to d-^{3}He is the material source of ^{3}He itself.

VI-2. The Catalyzed d-d Cycle

The major reactions of this cycle are:

$$d + d \rightarrow p\ (3.02\ \text{MeV}) + t\ (1.01\ \text{MeV}) \qquad \text{(VI-15)}$$

$$d + d \rightarrow n\ (2.45\ \text{MeV}) + {}^{3}He\ (.817\ \text{MeV}) \qquad \text{(VI-16)}$$

$$d + t \rightarrow n\ (14.07\ \text{MeV}) + {}^{4}He\ (3.52\ \text{MeV}) \qquad \text{(VI-17)}$$

$$d + {}^{3}He \rightarrow p\ (14.68\ \text{MeV}) + {}^{4}He\ (3.67\ \text{MeV}) \qquad \text{(VI-18)}$$

The minor reactions included:

$$^3He + ^3He \rightarrow 2p\ (5.72\ MeV) + ^4He\ (1.43\ MeV) \qquad (VI-19)$$

$$t + t \rightarrow 2n\ (5.03\ MeV) + ^4He\ (1.26\ MeV) \qquad (VI-20)$$

$$t + ^3He \rightarrow p\ (10.08\ MeV) + n\ (1.61\ MeV) + ^4He\ (.4\ MeV)$$

$$\text{or} \qquad \text{or} \qquad \text{or}$$

$$(5.37\ MeV) \qquad (5.37\ MeV) \qquad (1.34\ MeV) \qquad (VI-21)$$

$$p + d \rightarrow n + 2p \quad Q = -2.225\ MeV \qquad (VI-22)$$

$$p + t \rightarrow n + ^3He \quad Q = -.764\ MeV \qquad (VI-23)$$

In addition to the propagating fusion reaction sequences given in eqn. (VI-11) through eqn. (VI-14), a few of the others are:

$$\left\{\begin{array}{l} d + d \rightarrow \bar{p} + \bar{t} \\ \bar{p} + d \rightarrow \bar{d} + p \\ \bar{d} + d \rightarrow \bar{p} + \bar{t} \\ \vdots \end{array}\right\} \qquad (VI-24) \qquad \left\{\begin{array}{l} d + d \rightarrow {}^3\bar{He} + n \\ {}^3\bar{He} + d \rightarrow \bar{\bar{p}} + \bar{\alpha} \\ \bar{\bar{p}} + d \rightarrow \bar{d} + p \\ \bar{d} + d \rightarrow {}^3\bar{He} + n \\ \vdots \end{array}\right\} \qquad (VI-25)$$

$$\left\{\begin{array}{l} d + d \rightarrow \bar{t} + \bar{p} \\ \bar{t} + d \rightarrow \bar{\alpha} + n \\ \bar{\alpha} + d \rightarrow \bar{d} + \alpha \\ \bar{d} + d \rightarrow \bar{t} + \bar{p} \\ \vdots \end{array}\right\} \qquad (VI-26) \qquad \left\{\begin{array}{l} d + d \rightarrow {}^3\bar{He} + n \\ {}^3\bar{He} + d \rightarrow \bar{\alpha} + \bar{\bar{p}} \\ \bar{\alpha} + d \rightarrow \bar{d} + \alpha \\ \bar{d} + d \rightarrow {}^3\bar{He} + n \\ \vdots \end{array}\right\} \qquad (VI-27)$$

The enhanced reactivities at T_i = 75 keV as a function of electron temperature are shown in Fig. VI-8. The ignition criterion for

$n\tau_E$ is relaxed as shown in Fig. VI-9.

VI-3. The p-^{11}B Cycle

The reactions in this cycle are

$$\rightarrow\ {}^4He + {}^8Be\ (g.s.) \qquad \text{(VI-28a)}$$
$$\qquad\qquad \lfloor\rightarrow\ 2\,{}^4He$$

$$p + {}^{11}B\ \rightarrow\ {}^4He + {}^8Be^*\ (2.94\ MeV) \qquad \text{(VI-28b)}$$
$$\qquad\qquad \lfloor\rightarrow\ 2\,{}^4He$$

$$\rightarrow\ 3\,{}^4He\ \ \text{(continuum breakup)} \qquad \text{(VI-28c)}$$

$$p + {}^{11}B\ \rightarrow\ n + {}^{11}C \qquad Q = -2.765\ MeV \qquad \text{(VI-29)}$$

The dominant reaction branch is eqn. (VI-28b). The endothermic neutron reaction branch is at least three orders of magnitude lower in reactivity. The propagation sequence is:

$$\left\{\begin{array}{ccccc} p & + & {}^{11}B & \rightarrow & 3\,{}^4\bar{He} \\ {}^4\bar{He} & + & p & \rightarrow & \bar{p} + {}^4He \\ \bar{p} & + & {}^{11}B & \rightarrow & 3\,{}^4\bar{He} \end{array}\right\} \qquad \text{(VI-30)}$$

The enhanced reactivity at T_i = 250 keV for different electron temperatures is shown in Fig. VI-10. The resulting increase in $\langle\sigma v\rangle$ relative to the Maxwellian averaged value is shown in Fig. VI-11. When this is included in an energy balance calculation, it is found that the p-^{11}B cycle can ignite if the losses are due solely to bremsstrahlung and ash removal (as opposed to previous studies[1-3] which showed the maximum Q is less than 3 but did not include reactivity enhancement effects). Using power balance equations (III-51) and (III-52), appropriate relativistic formulae for bremsstrahlung and electron-ion rethermalization, the results are summarized in Table VI-1. Thus, including propagation and large energy transfer collisions and the tail-tail interactions, have considerably brightened the prospects for viable minimum nertron production cycle.

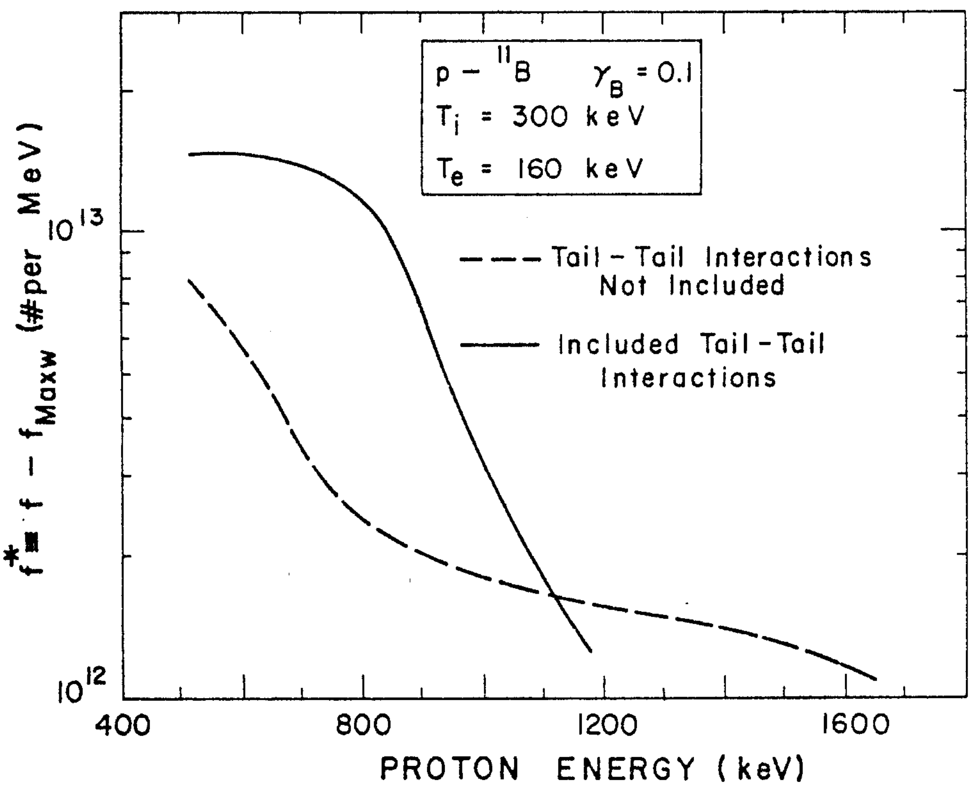

Fig. VI-1. Stripped distribution of protons as a function of energy for p-^{11}B reacting plasma.

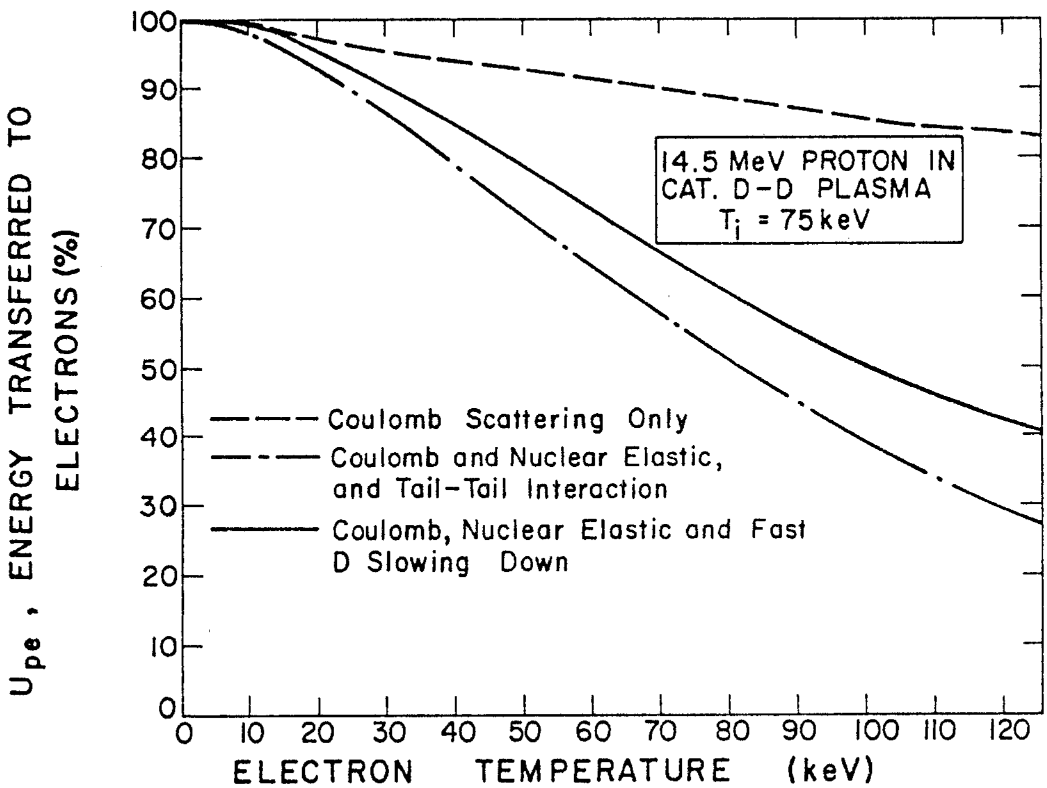

Fig. VI-2. Energy transferred to electrons by 14.5 MeV protons as a function of electron temperature in the catalyzed d-d reacting plasma.

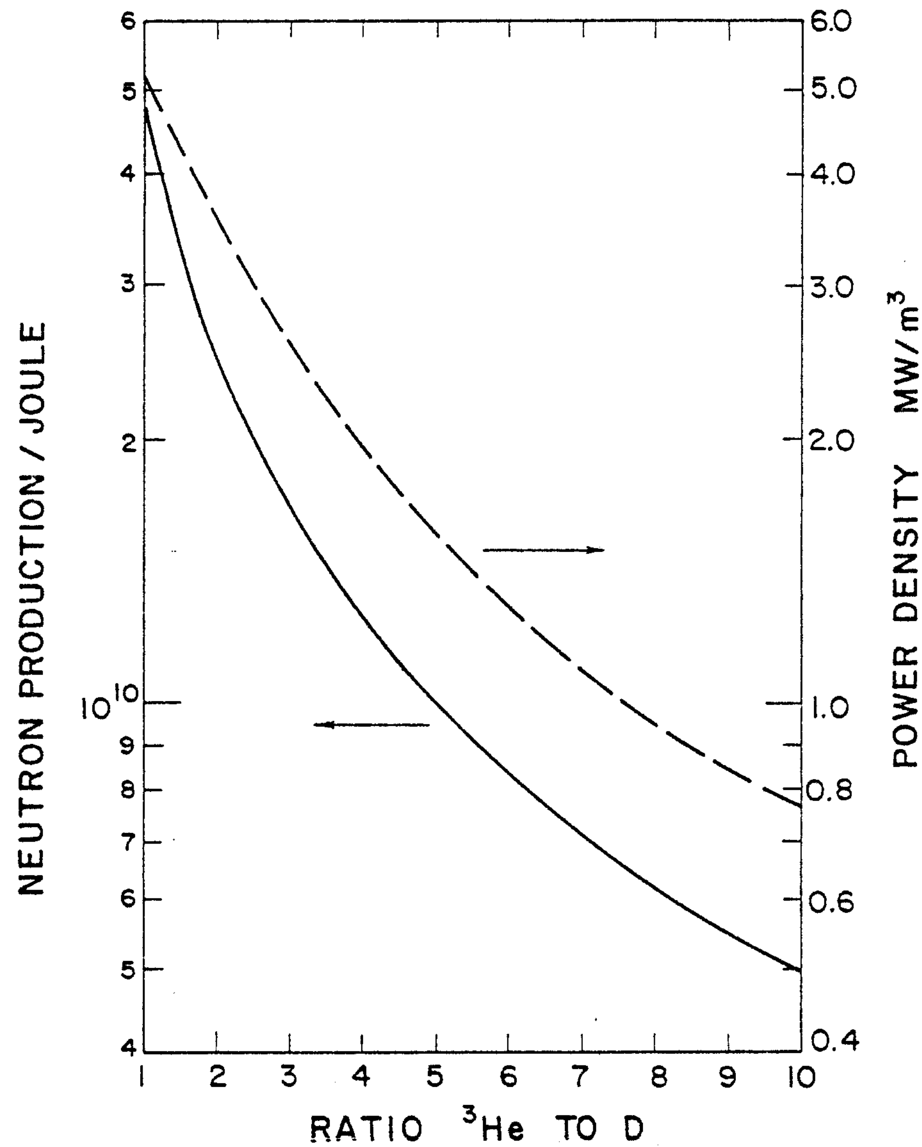

Fig. VI-3. Neutron production and power density for d-^{3}He fuel cycle as a function of ^{3}He/d density ratio.

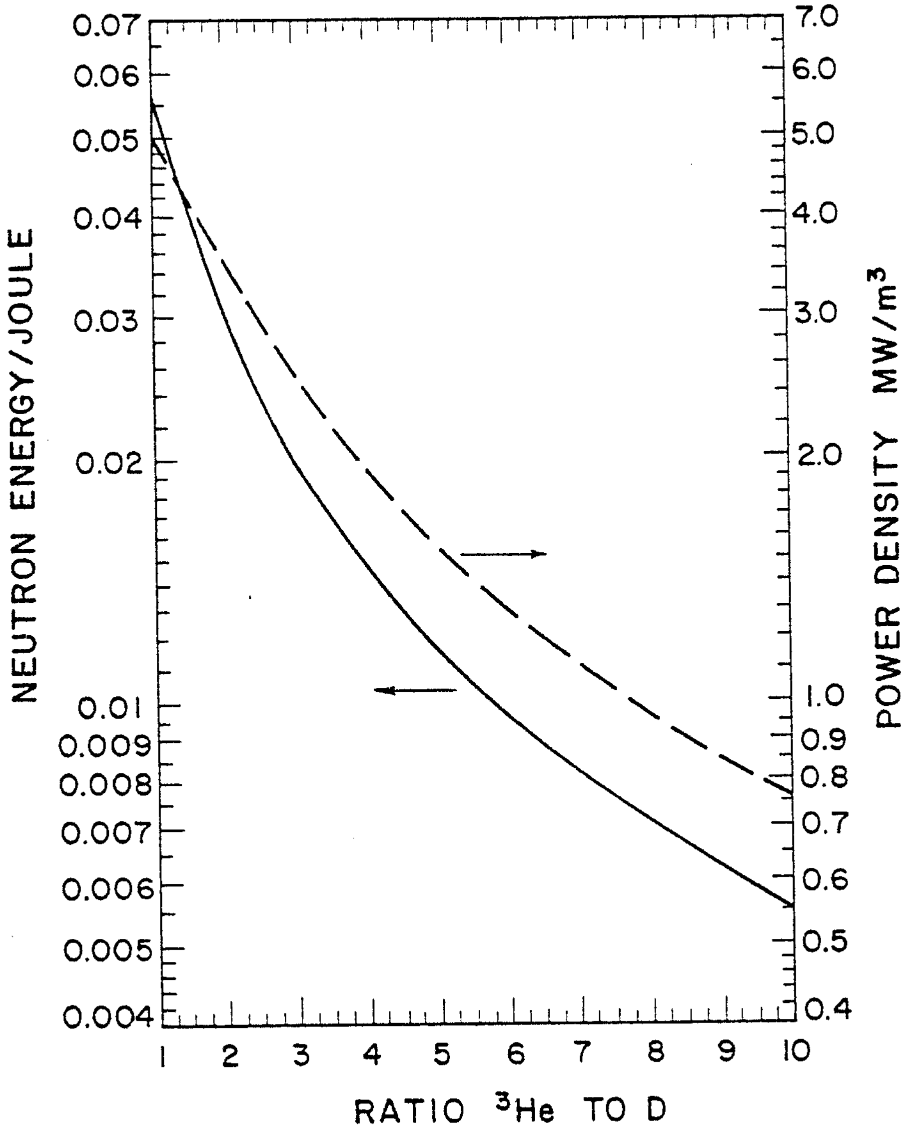

Fig. VI-4. Neutron energy and power density for d-^{3}He fuel cycle as a function of ^{3}He/d density ratio.

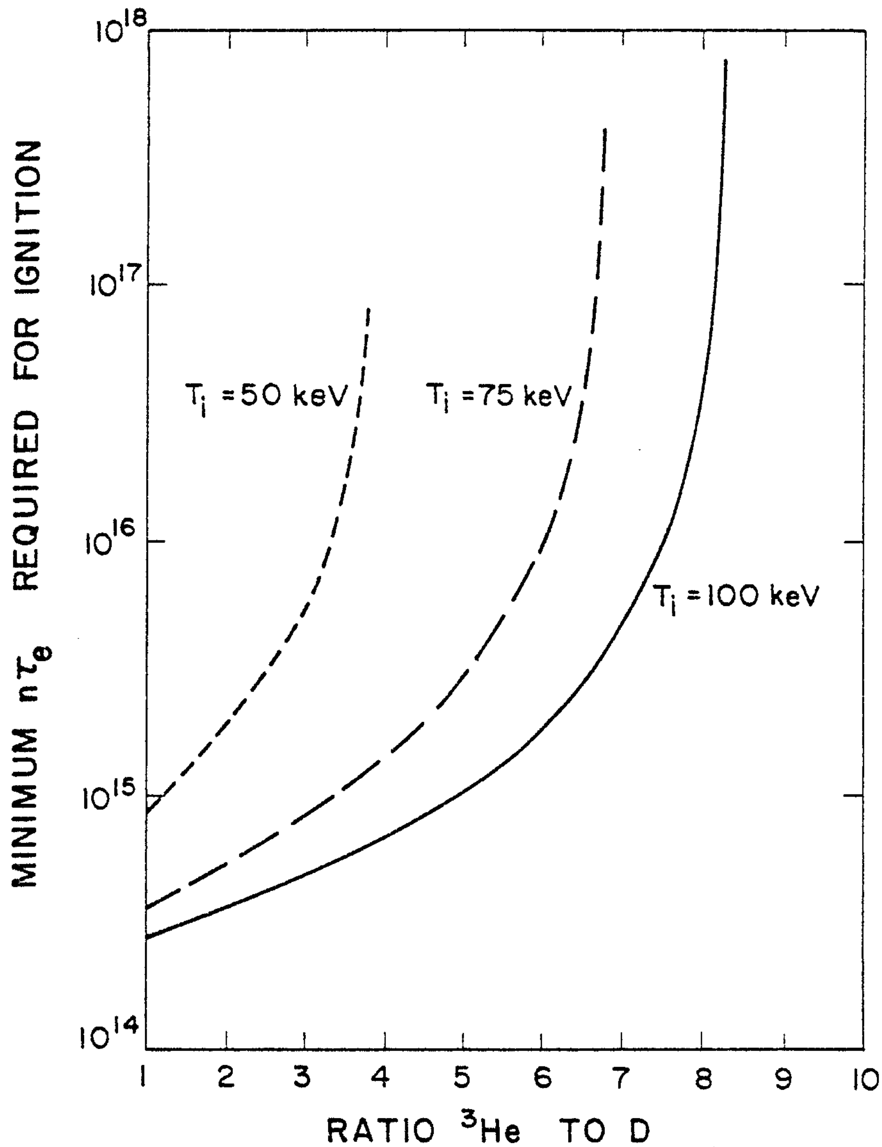

Fig. VI-5. Minimum $n\tau_E$ required for ignition, assuming perfect ion energy confinement, for d-^{3}He cycle, for different ion temperatures.

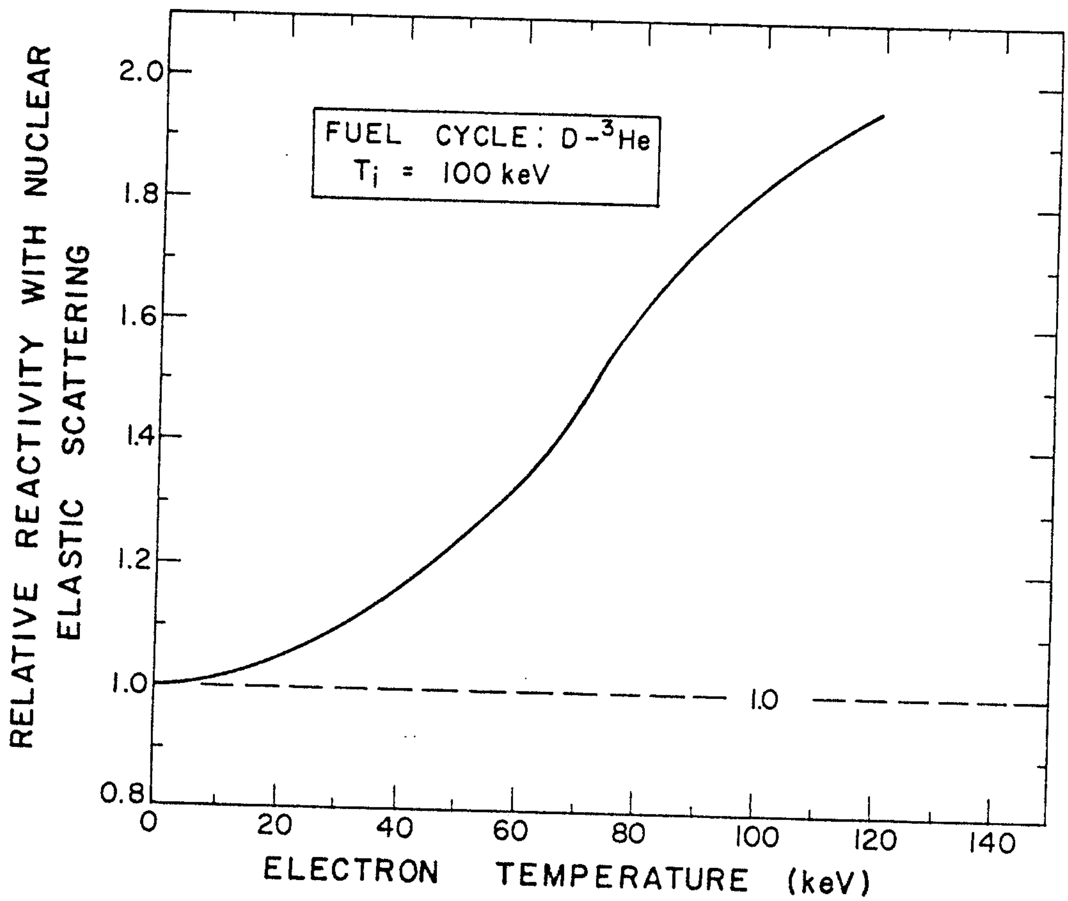

Fig. VI-6. Relative reactivity for d-^{3}He fuel cycle at different electron temperatures.

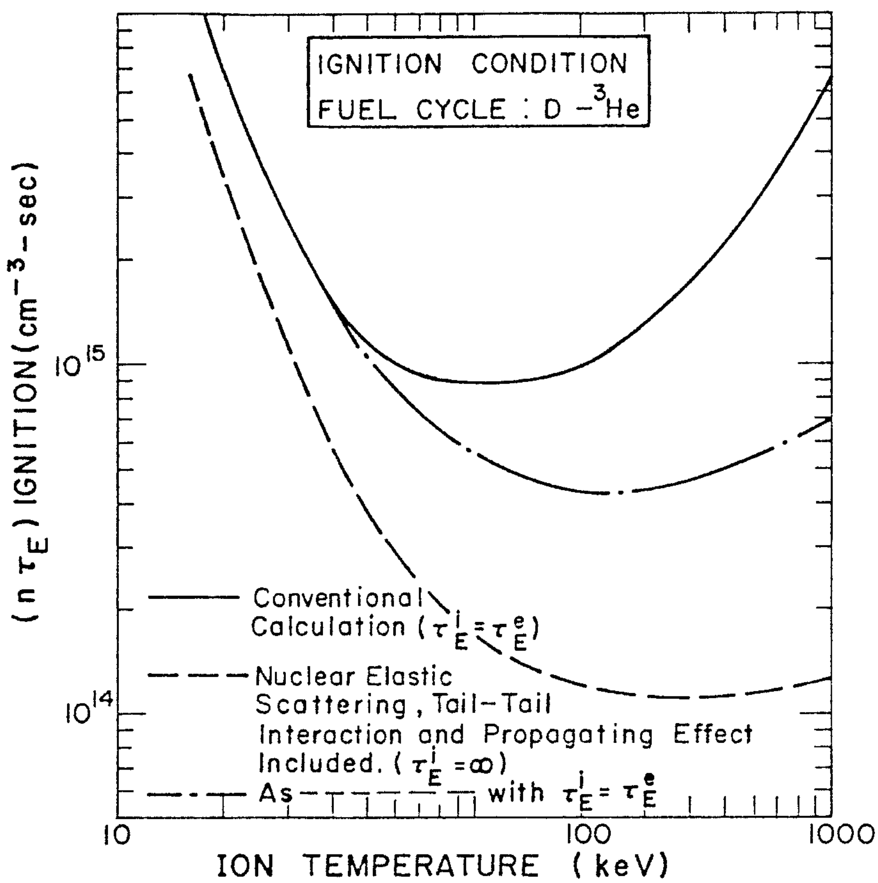

Fig. VI-7. Minimum required $n\tau_E$ for different ion temperatures for the d-^{3}He fuel cycle.

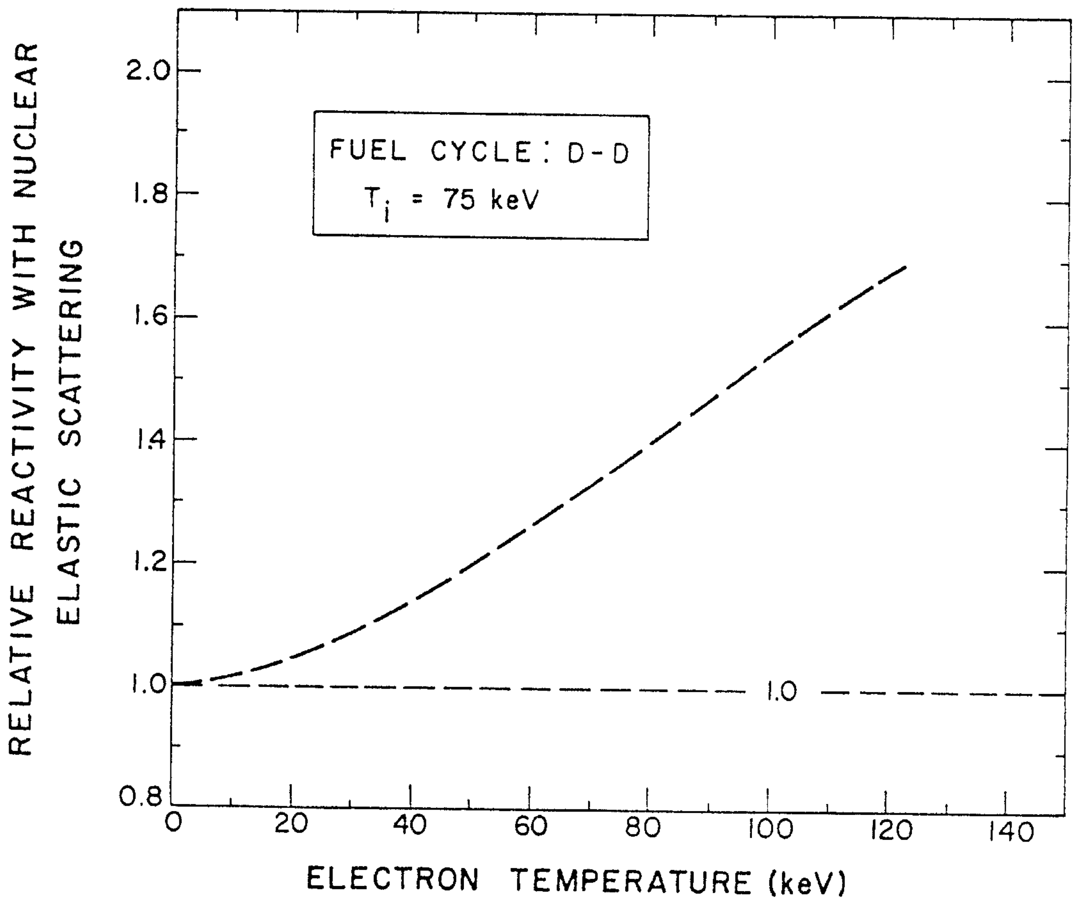

Fig. VI-8. Enhanced reactivity at T_i = 75 KeV for different electron temperatures, d-d fuel cycle.

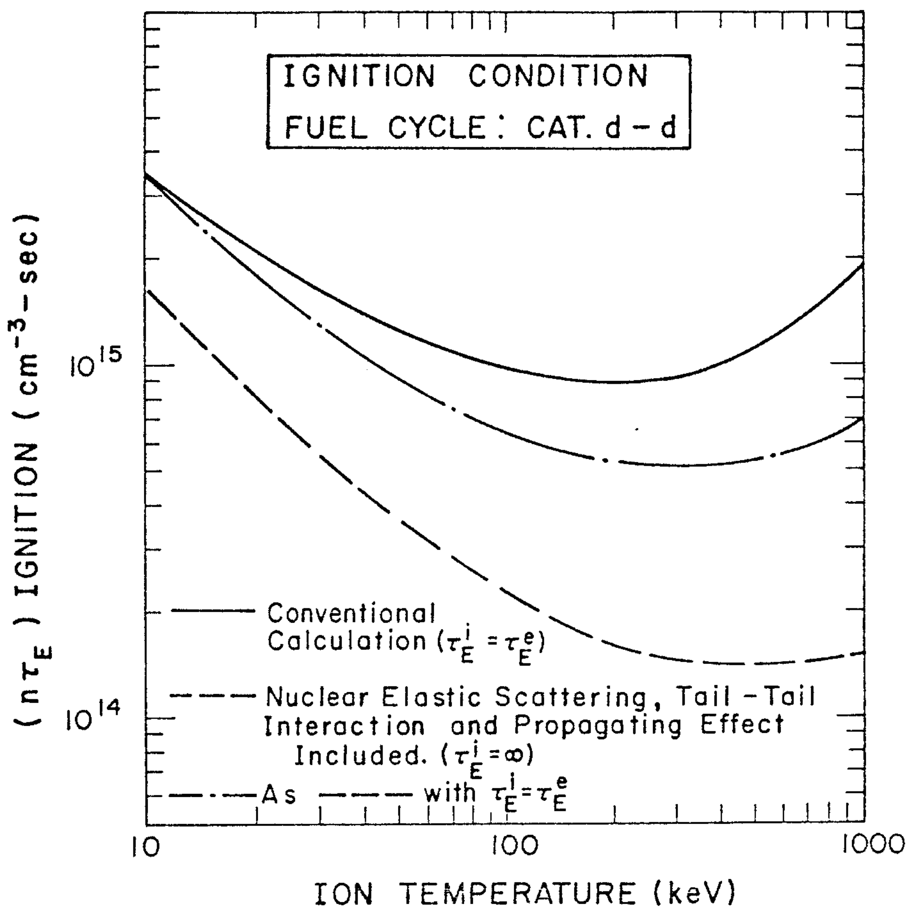

Fig. VI-9. Minimum required $n\tau_E$ for ignition for catalyzed d-d fuel cycle, as a function of ion temperature.

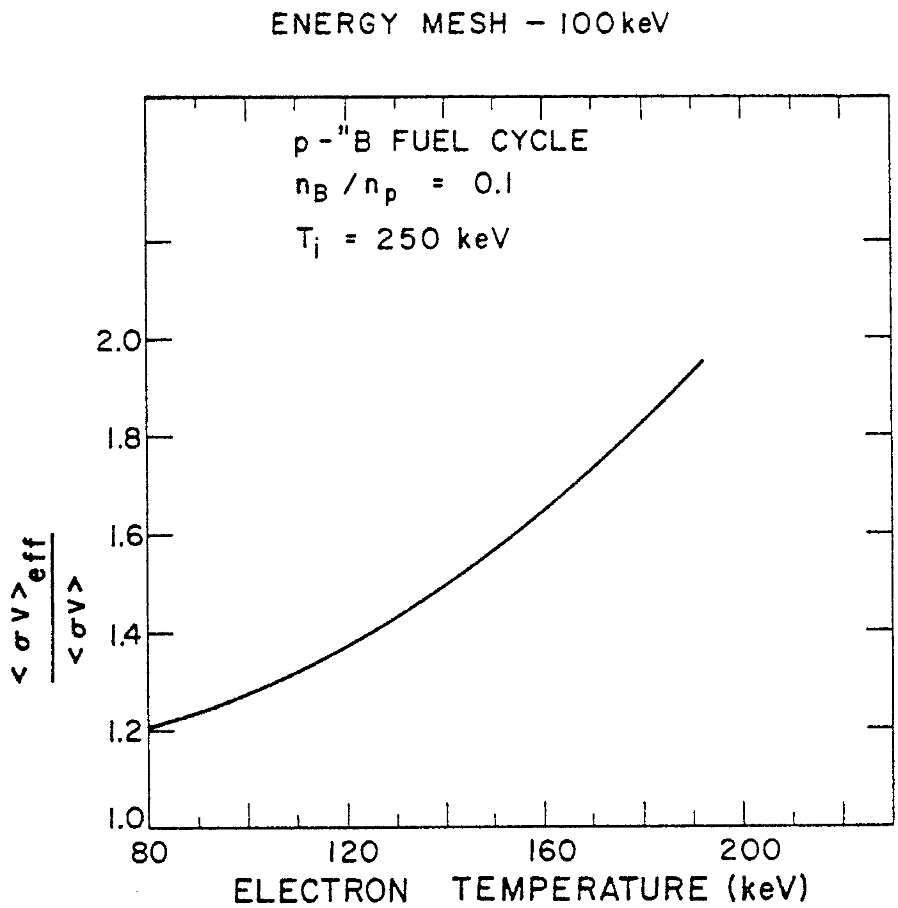

Fig. VI-10. Enhanced reactivity at different electron temperatures for the p-^{11}B fuel cycle.

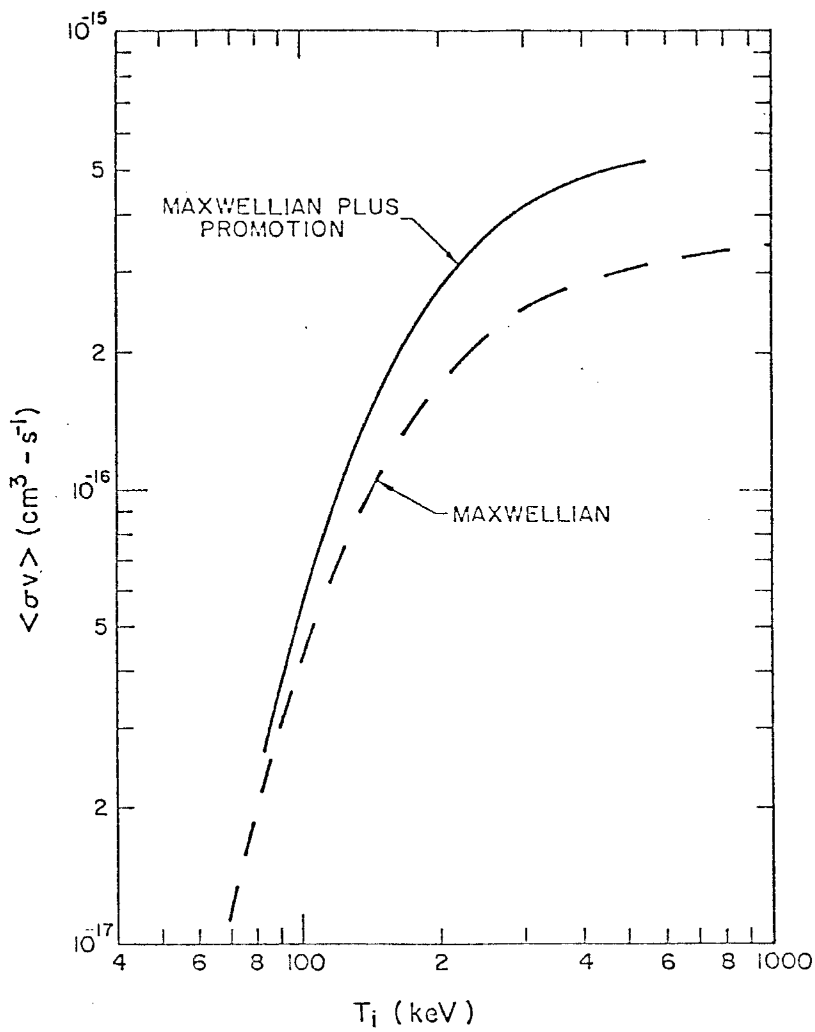

Fig. VI-11. Increase in <σv> relative to the Maxwellian averaged value for the p-^{11}B fuel cycle, as a function of ion temperature.

Table VI-1

Power Balance for p-^{11}B Cycle

T_i(keV)	T_e(keV)	$M = \frac{\text{Fusion Power}}{\text{Brem. Power}}$	$Q = \frac{\text{Fusion Power}}{\text{Input Power}}$	$(n\tau_E)_{minimum}$ required (For Q = 5)
200	140	.8	4.	---
250	155	.97	32.	$\simeq 2.4\times10^{15}$
300	160	1.08	∞ (Ignition)	$\simeq 1.36\times10^{15}$

References for Chapter VI

1. J. M. Dawson, UCLA Plasma Group Report, PPG-273 (Aug. 1976)
2. J. G. Cordey, lecture 2. Course on Theory of Magnetically Confined Plsmas (Varenna, Italy) Sept. 1977
3. R. W. Conn, et al., "Aspects of Octopoles as Advanced Cycle Fusion Reactors" in Fusion Reactor Design Problems, IAEA (Vienna) 1978

CHAPTER VII

SUMMARY AND FUTURE DIRECTION

CHAPTER VII

SUMMARY AND FUTURE DIRECTION

VII-1. Summary

Three new effects in advanced fusion fuel cycle analysis - proper inclusion of large energy transfer collisions, propagating enhancement, and tail-tail interactions - have been investigated and found to increase the reactivity of the cycle, to alter energy balance calculations, and to affect predicted Q values and ignition conditions. For example, with the inclusion of these effects, the reactivity of the catalyzed d-d plasma at T_i = 75 keV can be increased from 21% at T_e = 50 keV to 53% at 100 keV relative to the reactivity neglecting nuclear elastic scattering. The result is due to fusion events between fast deuterons produced by large energy transfer collisions of the energetic fusion products with the background ions. The fraction of energy given to the electrons is likewise influenced by nuclear elastic scattering and tail-tail interactions. The fraction of a 14.5 MeV proton's energy given to the electrons at 100 keV decreases from 85% when only coulomb scattering is assumed, to 51% when nuclear scattering is added to the calculation, and decreases further to 38% when coulomb plus nuclear scattering and tail-tail interactions are properly included.

Charged particle cross sections required for advanced fusion fuel cycle calculations have been discussed. Reactions important for the d-d, d-^{3}He, d-^{6}Li and p-^{11}B cycles have been described. The inclusion of nuclear elastic scattering is found to be essential.

Important fusion cross section and energy ranges where data is required have been identified.

Kinetic equations to describe the velocity distribution functions for a reacting fusion plasma have been studied, and a linearized model has been formulated. A slowing down theory to treat the small energy transfer range by a continuous theory and to treat the large energy transfer range by a discrete multigroup energy technique has been developed. Formulae for the power density in propagating reaction cycles, the fast fusion probability for an energetic particle reacting to the background ions, the energy distribution of reaction products, and the power balance equations including injecting power, ash removal and the relativistically corrected electron-ion rethermalization and Bremsstrahlung radiation have been derived.

Computer codes including the appropriate kinetic equations, the fast fusion reactions, and nuclear elastic scattering have been developed, implemented and are presented along with results. Steady state analyses on catalyzed d-d, d-^{3}He and p-^{11}B have been completed. It is found that the p-^{11}B cycle can ignite if the losses are due solely to Bremsstrahlung and ash removal. The reactivity for the catalyzed d-d cycle is enhanced by 20% - 40%. Assuming perfect ion energy confinement, the minimum electron $n\tau_E$ value required for ignition is decreased from 9×10^{14} to 1.5×10^{14} with the inclusion of these effects. The reactivity for the d-^{3}He cycle is enhanced by 35% - 75%. Assuming perfect ion energy confinement, the minimum electron $n\tau_E$ requirement for ignition is reduced from 9×10^{14} to 1.01×10^{14}.

VII-2. Discussions

(1) Energy Distribution of Products from Nuclear Reactions and Transfer Matrices for Slowing Down

The equations for the exact treatment of these subjects have been derived in Section III-5. In order to include them in the present model of advanced fusion fuel cycle analysis, further expansions and simplifications are made next.

Using $f_i(\vec{V}_i) = f_i^M(\vec{V}_i) + f_i^*(\vec{V}_i)$ which is defined in Section III-2, equation (III-4), and

$$\hat{f}_i(\vec{V}_i) = \frac{n_i^M}{n_i} \hat{f}_i^M (\vec{V}_i) + \frac{n_i^*}{n_i} f_i^* (\vec{V}_i), \qquad \text{(VII-1)}$$

equation (III-45) becomes

$$\frac{dR}{dE_3} = 2n_1^M n_2^M I (\hat{f}_1^M, \hat{f}_2^M) + 2n_1^M n_2^* I (\hat{f}_1^M, \hat{f}_2^*) + 2n_1^* n_2^M I (\hat{f}_1^*, \hat{f}_2^M) + 2n_1^* n_2^* I (\hat{f}_1^*, \hat{f}_2^*), \qquad \text{(VII-2)}$$

where superscripts M and * refer to the Maxwellian bulk and stripped portion of the velocity distribution function and subscripts 1 and 2 refer to the ion species considered; $\hat{f}$'s are normalized functions of the corresponding f, $n = n^M + n^*$ is the number density, and

$$I(\hat{f}_1^j, \hat{f}_2^k) \equiv \int d^3V_1 \, d^3V_2 \, \hat{f}_1^j(\vec{V}_1) \, \hat{f}_2^k(\vec{V}_2) \cdot$$

$$|\vec{V}_1 - \vec{V}_2| \, \frac{d\sigma}{d\Omega} \cdot (- \frac{d(\cos\theta)}{dE_3}); \qquad \text{(VII-3)}$$

the superscripts j and k refer to either superscript M or *; other notations are defined in Section III-5. The integral functions $I(\hat{f}_1^M, \hat{f}_2^M)$, $I(\hat{f}_1^M, \hat{f}_2^*)$ and $I(\hat{f}_1^*, \hat{f}_2^M)$ depend on ion temperature of the plasma, $d\sigma/d\Omega$ of the reaction, the reaction Q which will influence $d(\cos\theta)/dE_3$ calculated from equation(III-41). By assuming isotropy of the reaction cross sections and neglecting $I(\hat{f}_1^*, \hat{f}_2^*)$, an accurate energy distribution of the reaction products, expressed by equation (VII-2), has been included in the steady state (constant T_i) calculations. Nevertheless, to include these expression in any time dependent simulation code would be prohibitively expensive, even provided a large enough computer is available with sufficient memory storage for the differential cross sections needed to perform the integration defined in equation (VII-3). To overcome these difficulties, a new approach to solving the non-linear Boltzman equation is required. Such an approach has been developed but implementation is beyond the scope of this thesis (see the Appendix).
For the time being, a simplified treatment detailed next has been used to construct the transfer matrices for slowing down and thermalization which are implemented in the BAFCO code to handle the large energy transfer process. The same treatment has been developed and implemented in the version of BAFCO code used by the TRW company fusion

research group[1] (the TRW upgrade version) for the energy distribution products of two-component reactions.

Assuming isotropy of reaction cross sections and neglecting the velocity of one of the reactants, equations (III-41) and (III-45) can be rewritten as follows:

$$E_3 = (m_4/(m_3+m_4))Q + (m_1m_3+m_2m_4)/(m_3+m_4)^2\ E_1 + 2\ \{m_1^2m_3m_4\ (M_2E_1 + (m_3+m_4)Q)\}^{\frac{1}{2}} \cos\theta \qquad \text{(VII-4)}$$

$$\frac{dR}{dE_3} \equiv \Phi \cdot P(E_3)$$

$$= 2\pi n_1 n_2 \int d^3\vec{V}_1\ d^3\vec{V}_2\ \hat{f}_1(\vec{V}_1)\hat{f}_2(\vec{V}_2)|\vec{V}_1-\vec{V}_2|\ \frac{\sigma}{4\pi}\ (-\ \frac{d(\cos\theta)}{dE_3}\ )$$

$$= \begin{cases} \frac{1}{4}\Phi\ (m_3+m_4)^2/\{m_1^2m_3m_4\ (m_2E_1 + (m_3+m_4)Q)\}^{\frac{1}{2}} & \text{if } E_{min} \leq E_3 \leq E_{max} \\ 0 & \text{otherwise} \end{cases} \qquad \text{(VII-5)}$$

where Φ = reaction rate = $\int d^3\vec{V}_1 d^3\vec{V}_2\ f_1 f_2\ |\vec{V}_1-\vec{V}_2|\sigma$, (VII-6)

E_{max} and E_{min} are calculated from eqn. (VII-4) with $\theta = 0$ and $\theta = \pi$ respectively, $P(E_3)$ is the probability that the reaction product with mass m_3 will appear in an energy interval dE_3 about E_3, and other notations are defined in Section III-5. Therefore,

$$P(E_3) = \begin{cases} \frac{1}{4}(m_3+m_4)^2/\{m_1^2m_3m_4(m_2E_1 + (m_3+m_4)Q)\}^{\frac{1}{2}} & \text{if } E_{min} \leq E_3 \leq E_{max} \\ 0 & \text{otherwise} \end{cases} \qquad \text{(VII-7)}$$

Since the major contribution of the two-component reactions comes from the lower energy group, where the velocity of the background species is comparable to that of the fast species, this simplified model is only an appoximate. Nevertheless, the large energy transfer collisions are not dominated by the low energy groups, and so that the model is useful in constructing the transfer matrices for slowing down and thermalization, especially for high energy incident particles.

Even with this, the construction of matrices for slowing down is cumbersome. Both additional man power and funds are required to complete the calculation of the matrices needed to be fully implemented in BAFCO code.

(2) Change of the Energy Distribution Profile by the Consumption of Nuclear Reactants

The consumption rate per unit volume for ion species 1 with the velocity distribution $f_1(\vec{V}_1)$ which react with ion species 2 having a velocity distribution $f_2(\vec{V}_2)$ can be expressed as follows:

$$R_{C1}(\vec{V}_1) \equiv df_1(\vec{V}_1)/dt = f_1(\vec{V}_1) \int d^3\vec{V}_2\ f_2(\vec{V}_2)|\vec{V}_1-\vec{V}_2|\sigma(|\vec{V}_1-\vec{V}_2|) \tag{VII-8}$$

where subscipt C1 refer to consumption of ion species 1 and $\sigma(|\vec{V}_1-\vec{V}_2|)$ is the reaction cross section. The nuclear fusion reaction, in general, is a resonance reaction. The consumption rate of the reactants is not likely to be constant in energy. All of the analyses and simulation codes (ECF, FOKN, BAFCO) nevertheless have made this hidden assumption that the consumption rate of the velocity distribution of the reactants is constant in energy, when the reactant has a Maxwellian distribution. With this assumption of uniform consumption, the results produce an overestimate reactivity. To include this subject in advanced fusion fuel cycle analysis and in time dependent simulations is expected to be complecated.

VII-3. Future Direction

Obtaining the correct energy distribution profiles for various ion species and electrons in a reacting plasma from the appropriate kinetic equations incorporating the relevant physical processes is the key to an accurate fusion fuel cycle analysis. Techniques for solving nonlinear problem in fusion reaction kinetics such as the Monte-Carlo method employed for neutronics problems should be investigated. Another approach which appears to be promising is to expand each term of the Boltzmann equation in a complete set. This is elaborated on briefly in the appendix.

To evaluate the potential of advanced fusion fuel cycles the following investigations should be done in the near future:

1. Investigate how much these processes affect $n\tau$ requirements for Lawson and ignition conditions or the energy multiplication factor Q, using several models for energy containment time.

2. Utilize the time dependent advanced fusion fuel cycle burn kinetics code to investigate optimum fuel mixture, energy amplification factors, neutron yields, $n\tau_E$ requirements, startup scenarios, ash removal requirements and sensitivity of the burn dynamics to data uncertainty.

It may be important as the research progresses to have an elaborate space and time dependent simulation code.

CHAPTER VII

REFERENCE

1. The TRW, Inc. fusion research group, Private communication.

2. G. S. Bell and S. Glasstone, Nuclear Reactor Theory, Van Nostrand Reinhold Co. 1970.

3. Markushevich, Theory of Functions of a Complex Variable, Chelsea Publishing Co., New York, 1977.

APPENDIX

BRIEF ELABORATION ON THE EXPANSION OF THE BOLTZMANN EQUATION IN A COMPLETE SET

APPENDIX

BRIEF ELABORATION ON THE EXPANSION OF THE BOLTZMANN EQUATION IN A COMPLETE SET

To briefly illustrate the essential idea involved, let us assume that a non-orthonormal complete set $\begin{pmatrix} 1 \\ 1 \\ \vdots \\ 1 \end{pmatrix}$ exist, and expand some of the functions related to the Boltzmann equation in this complete set.

$$f_k(v_k) \equiv \begin{pmatrix} x_{1k} \\ x_{2k} \\ \vdots \\ x_{nk} \end{pmatrix} \tag{A-1}$$

$$\vec{v}_1 \cdot \nabla_r \begin{pmatrix} 1 \\ 0 \\ 0 \\ \vdots \\ 0 \end{pmatrix} = \begin{pmatrix} a_{11} & \cdots & a_{1n} \\ \vdots & & \vdots \\ a_{n1} & \cdots & a_{nn} \end{pmatrix} \begin{pmatrix} 1 \\ 1 \\ \vdots \\ 1 \end{pmatrix} \equiv A_1 \begin{pmatrix} 1 \\ 1 \\ \vdots \\ 1 \end{pmatrix} \tag{A-2a}$$

$$\vec{v}_1 \cdot \nabla_r \begin{pmatrix} 0 \\ 1 \\ 0 \\ \vdots \\ 0 \end{pmatrix} \equiv A_2 \begin{pmatrix} 1 \\ 1 \\ \vdots \\ 1 \end{pmatrix} \tag{A-2b}$$

$$\frac{\vec{F}}{m} \cdot \nabla_v \begin{pmatrix} 1 \\ 0 \\ 0 \\ \vdots \\ 0 \end{pmatrix} \equiv B_1 \begin{pmatrix} 1 \\ 1 \\ 1 \\ \vdots \\ 1 \end{pmatrix} \tag{A-3a}$$

$$\frac{\vec{F}}{m} \cdot \nabla_v \begin{pmatrix} 0 \\ 1 \\ 0 \\ \vdots \\ 0 \end{pmatrix} \equiv B_2 \begin{pmatrix} 1 \\ 1 \\ \vdots \\ 1 \end{pmatrix} \tag{A-3b}$$

$$\int \int \begin{pmatrix} 1 \\ 0 \\ 0 \\ \vdots \\ 0 \end{pmatrix} \begin{pmatrix} 1 \\ 0 \\ 0 \\ \vdots \\ 0 \end{pmatrix} u_{ij} \; \sigma^{\ell}_{kij}(u_{ij};\; v_1)\; d^3v_i\; d^3v_j$$

$$= \begin{pmatrix} c_{11} & \cdots & c_{1n} \\ \vdots & & \vdots \\ c_{n1} & \cdots & c_{nn} \end{pmatrix} \begin{pmatrix} 1 \\ 1 \\ \vdots \\ 1 \end{pmatrix} \equiv C^{ij\ell}_{11} \begin{pmatrix} 1 \\ 1 \\ \vdots \\ 1 \end{pmatrix} \qquad \text{(A-4a)}$$

$$\int \int \begin{pmatrix} 1 \\ 0 \\ 0 \\ \vdots \\ 0 \end{pmatrix} \begin{pmatrix} 0 \\ 1 \\ 0 \\ \vdots \\ 0 \end{pmatrix} u_{ij} \; \sigma^{\ell}_{kij}(u_{ij};v_1) d^3v_i d^3v_j \equiv C^{ij\ell}_{12} \begin{pmatrix} 1 \\ 1 \\ 1 \\ \vdots \\ 1 \end{pmatrix} \qquad \text{(A-4b)}$$

$$\int \begin{pmatrix} 1 \\ 0 \\ 0 \\ \vdots \\ 0 \end{pmatrix} \begin{pmatrix} 1 \\ 0 \\ 0 \\ \vdots \\ 0 \end{pmatrix} u_{1i}\, \sigma^{\ell}_{ik}(u_{1i})\; d^3v_i \equiv D^{i\ell}_{11} \begin{pmatrix} 1 \\ 1 \\ 1 \\ \vdots \\ 1 \end{pmatrix} \qquad \text{(A-5a)}$$

$$\int \begin{pmatrix} 1 \\ 0 \\ 0 \\ \vdots \\ 0 \end{pmatrix} \begin{pmatrix} 0 \\ 1 \\ 0 \\ \vdots \\ 0 \end{pmatrix} u_{1i}\, \sigma^{\ell}_{ik}(u_{1i})\; d^3v_i \equiv D^{i\ell}_{12} \begin{pmatrix} 1 \\ 1 \\ 1 \\ \vdots \\ 1 \end{pmatrix} \qquad \text{(A-5b)}$$

$$\int \int \begin{pmatrix} 1 \\ 0 \\ 0 \\ \vdots \\ 0 \end{pmatrix} \begin{pmatrix} 1 \\ 0 \\ 0 \\ \vdots \\ 0 \end{pmatrix} u_{ik}\, \sigma^{\ell}_{ik}(u_{ik};\; v_1) d^3v_i d^3v_k \equiv E^{i}_{11} \begin{pmatrix} 1 \\ 1 \\ 1 \\ \vdots \\ 1 \end{pmatrix} \qquad \text{(A-6a)}$$

$$\int \int \begin{pmatrix} 1 \\ 0 \\ 0 \\ \vdots \\ 0 \end{pmatrix} \begin{pmatrix} 0 \\ 1 \\ 0 \\ \vdots \\ 0 \end{pmatrix} u_{ik}\, \sigma^{\ell}_{ik}(u_{ik};\; v_1) d^3v_i d^3v_k \equiv E^{i}_{12} \begin{pmatrix} 1 \\ 1 \\ 1 \\ \vdots \\ 1 \end{pmatrix} \qquad \text{(A-6b)}$$

$$\int \begin{pmatrix}1\\0\\0\\ \vdots\\0\end{pmatrix} \begin{pmatrix}1\\0\\0\\ \vdots\\0\end{pmatrix} u_{1i}\, \sigma_{ik}(u_{1i}) d^3v_i \equiv F^i_{11} \begin{pmatrix}1\\1\\1\\ \vdots\\1\end{pmatrix} \tag{A-7a}$$

$$\int \begin{pmatrix}1\\0\\0\\ \vdots\\0\end{pmatrix} \begin{pmatrix}0\\1\\0\\ \vdots\\0\end{pmatrix} u_{1i}\, \sigma_{ik}(u_{1i}) d^3v_i \equiv F^i_{12} \begin{pmatrix}1\\1\\1\\ \vdots\\1\end{pmatrix} \tag{A-7b}$$

where the other notations are defined in Section III-1. Using equation (A-1) through (A-7) the Boltzman equation expressed in equation (III-1) can be written as

$$\frac{\partial}{\partial t}\begin{pmatrix}x_{1k}\\x_{2k}\\ \vdots\\x_{nk}\end{pmatrix} = \Big\{ \sum_{i,j,\ell} \sum_{p,q} X_{pi}\, X_{qj}\, C^{ij\ell}_{pq} - \sum_{i,\ell} \sum_{p,q} X_{pk} X_{qi} D^{i\ell}_{pq} + \sum_{i} \sum_{p,q} X_{pk} X_{qi}\, E^{i}_{pq} - \sum_{i} \sum_{p,q} X_{pk}\, X_{qi}\, F^{i}_{pq} - \sum_{p} X_{pk}\, A_p - \sum_{q} X_{qk} B_q \Big\} \begin{pmatrix}1\\1\\ \vdots\\1\end{pmatrix} \tag{A-8}$$

The advantage of this form is that as long as the complete set is chosen, the matrices A, B, C etc. can be constructed once only and the rest of the calculation becomes simple and easy.

The only question remaining is the existence of such a complete set, or a set of functions in which each term of the Boltzmann equation can be expanded. By applying Vitali's theorem[1], the existence of the Laplace transform and its inverse transform of $G(\tau)$

$$f(z) = \int_0^\infty d^{-Z\tau}\ G(\tau)\ d\tau \qquad \text{(A-9)}$$

if $G(\tau)<\alpha e^{C\tau}$ where α and τ are positive mumbers, can be mathematically proven. Mathematically the Laplace transform is known as the continuous analogue of the Dirichlet series $\sum_{n=1}^{\infty} a_n e^{-\lambda_n z}$. Therefore substituting $\tau = 1/T$, the reciprocal temperature, $z = v$, $z = v^2$ or $z = E$ whichever convenient, the complete set can be found.

APPENDIX

REFERENCE

1. Markushevich, Theory of Functions of a Complex Variable, Chelsea Publishing Co., New York, 1977.